



UNIVERSITÀ POLITECNICA DELLE MARCHE

FACOLTÀ DI INGEGNERIA

Corso di Laurea Magistrale in INGEGNERIA CIVILE

Dipartimento di Ingegneria Civile, Edile e Architettura (DICEA)

JUMPERS AND SPOOLS SUBMARINE PIPELINE CONNECTORS SUBJECT TO THE DYNAMIC LOADS INDUCED BY TWO-PHASE SLUG FLOW

*Sistemi di connessione per condotte sottomarine, Jumper e Spool,
soggetti a carichi dinamici indotti dal flusso bifase in regime di Slug*

Relatore:
Prof. Ing. Lando Mentrasti

Tesi di laurea di:
Vanda Barulli

Correlatore:
Ing. Mauro Pigliapoco, SAIPEM, Fano

ABSTRACT

Pipelines are the arteries of the oil and gas industry. They transport the hydrocarbons to and from both offshore and onshore facilities and connect the different subsea components.

In subsea oil or gas production system, a **subsea jumper** (or spool piece) is a short pipe connector used to transport production fluid between two subsea components like subsea piping, manifolds, Christmas trees, platforms. In a jumper, several pipeline sections are assembled in a variety of spatial configurations to adapt the plant sections to installation and operating tolerances. Furthermore, it withstands the loads and displacements caused by fluctuating flow, temperature, pressure and seismic event: they **uncouple**, from the structural point of view, the several segments of the plant. This flexibility makes the jumper sensitive to vibrations induced by multi-phase internal flow. In addition, under particular flow conditions, such as slug flow, these vibrations will be more significant.

Slug flow is an intermittent **multiphase** flow, characterised by an alternating segments of liquid slugs and gas pockets. It is one of the most undesired regimes, due to the associated instability, which imposes a major challenge to *flow assurance* in the oil and gas industry. This flow regime, on the one hand, can cause large changes in pressure and flow rate of the liquid; on the other hand, it induces significant mechanical loads for submarine structures, in particular jumpers and risers. This can generate sudden variations in mass distribution and pressure disturbances along the tube, which can induce large vibrations.

In practice, the slug regime is defined by flow assurance engineers through a fluidynamics analysis in which the pipeline is assumed to be *at rest*, a hypothesis as drastic as unrealistic, from a structural point of view. Namely, it is assumed that the eventual movement of the structure is not so wide as to modify also the slug regime. Therefore, in a first time, it was decided not to consider the effect that structure dynamics may have on the slug regime itself, by simulate the slug strain as a time variable massless forces (on the bends); in particular, choosing the time history with a frequency around the most significant natural frequency of the jumper.

These different slug trains generate two excitation mechanisms: the variation of weight along the straight sections, that is the gravitational loads (neglected in this analyses) and the impact forces on the curves generated by the centrifugal forces.

To assess this approach, it is also investigate the influence of the contribution of the mass pertinent to the “critical” slug train, on the structural response. In the same engineering spirit such a distributed and fixed mass has been added to the pipe system. The result show the great influence of the moving mass on this kind of dynamical regimes, with special regard to its relationship with the natural frequencies of the structure (derived by the modal analysis).

This work discusses the uncoupled interaction between a *jumper* and several train of massless slugs, flowing with different velocities and frequencies.



Finally, an approximated procedure is devised to take advantage of the information obtained from a specific designed *sequence* of modal analysis, correlated by *different* slug regimes, for the identification of the more severe loading conditions.

SINTESI

Le pipelines sono le arterie dell'industria del petrolio e del gas. Trasportano gli idrocarburi da e verso impianti offshore e onshore e collegano le diverse componenti sottomarine.

Nel sistema di produzione sottomarino di petrolio o gas, un **subsea jumper** (o spool) è un connettore utilizzato per trasportare il fluido di produzione tra due componenti sottomarine come tubazioni, manifolds, pozzi, piattaforme. Le sezioni delle tubazioni sono assemblate in una grande varietà di configurazioni spaziali per adattarsi meglio alle tolleranze di installazione e di funzionamento e per resistere ai carichi finali e agli spostamenti causati da flussi variabili, cambiamenti di temperatura e pressione, eventi sismici: essi disaccoppiano, dal punto di vista strutturale, i vari segmenti dell'impianto. Questa flessibilità, però, rende il jumper sensibile alle vibrazioni indotte dal flusso interno che è un flusso multifase. Inoltre, in particolari condizioni di flusso, come in regime di **slug flow**, queste vibrazioni risulteranno essere più significative.

Lo **slug flow** è un flusso intermittente, caratterizzato da un flusso alternato di porzioni di liquido e sacche di gas. Si tratta di uno dei regimi di flusso multifase più indesiderati che, a causa della relativa instabilità, impone una sfida importante per gli ingegneri della *flow assurance*. Questo regime di flusso, da una parte può causare grandi cambiamenti di pressione e portata del liquido; dall'altra parte induce carichi meccanici significativi per strutture sottomarine, in particolare jumpers and risers. Questo può generare repentine variazioni della distribuzione della massa e perturbazioni di pressione lungo il tubo, che possono indurre grandi vibrazioni.

Prima di studiare il comportamento della struttura sottoposta ai carichi generati dal regime di slug, è stata fatta un'**analisi modale** con la quale è stato possibile identificare le frequenze naturali elementari e il loro modo associato di vibrazione del sistema strutturale.

Nella pratica, il regime di slug è definito a priori dagli ingegneri della flow assurance attraverso un'analisi fluidodinamica in cui si presume che l'oleodotto sia a riposo, ipotesi tanto drastica quanto irrealistica, da un punto di vista strutturale. Si ipotizza che l'eventuale movimento della struttura non sia così ampio da modificare anche il regime di slug. Quindi, preliminarmente, si è deciso di non considerare l'effetto che la dinamica della struttura può avere sul regime stesso di slug, simulando il passaggio dei diversi treni di slug con delle forze variabili nel tempo (nelle curve) ma senza considerare la massa; in particolare, scegliendo la *time history* con una frequenza intorno alla frequenza naturale più significativa del jumper.

Questi diversi treni di slug generano due meccanismi di eccitazione: la variazione di peso lungo le sezioni rettilinee, cioè i *carichi gravitazionali* (trascurati in questa analisi) e le forze di impatto sulle curve dovute alle *forze centrifughe*.

Per valutare questo approccio, si studia anche l'influenza del contributo della massa pertinente al treno slug "critico", sulla risposta strutturale. Nello stesso spirito ingegneristico,



una appropriata massa distribuita e fissa è stata aggiunta al sistema. Il risultato mostra la grande influenza della massa mobile su questo tipo di regimi dinamici.

Questo lavoro discute l'interazione disaccoppiata tra un jumper e diversi treni di slug senza massa, che scorrono con velocità e frequenze diverse.

Infine, viene concepita una procedura approssimata per sfruttare le informazioni ottenute da una specifica sequenza progettata di analisi modale, correlata da diversi regimi di slug, per l'identificazione delle condizioni di carico più gravose.

CONTENTS

ABSTRACT.....	1
SINTESI.....	3
CHAPTER 1: <i>INTRODUCTION</i>	7
1.1. ABOUT THIS THESIS	7
1.2. THESIS ORGANIZATION	8
CHAPTER 2: <i>OFFSHORE FIELD OVERVIEW</i>	10
2.1. WHAT IS THE TRANSPORTATION SYSTEM?.....	10
2.1.1. SUBSEA WELLHEADS	12
2.1.2. SUBSEA TREES or X-MAS TREES.....	13
2.1.3. PIPELINE END TERMINATION	13
2.1.4. SUBSEA MANIFOLDS.....	14
2.1.5. UMBILICAL SYSTEMS.....	15
2.1.6. SUBSEA PRODUCTION RISERS	16
2.1.7. SUBSEA PIPELINES	20
2.1.8. SUBSEA JUMPERS AND SPOOLS.....	20
2.2. PIPE MATERIALS, COMPONENTS AND PARAMETERS.....	28
CHAPTER 3: <i>MULTIPHASE FLOW</i>	33
3.1. BACKGROUND.....	33
3.2. TWO-PHASE FLOW	35
3.2.1. GAS-LIQUID FLOW REGIMES IN HORIZONTAL PIPE.....	36
3.2.2. GAS-LIQUID FLOW REGIMES IN VERTICAL PIPE.....	38
3.2.3. BASIC FLOW PARAMETERS	41
3.3. SLUG FLOW	43
3.3.1. SLUG FLOW MECHANISMS.....	44
3.3.2. CLASSIFICATION OF SLUG FLOW.....	45
3.3.3. SLUG MITIGATION AND CATCH.....	48
3.3.4. PREDICTION OF SLUG FLOW	49
3.3.5. SLUG FLOW PARAMETERS.....	50
3.3.6. SLUG FLOW INPUT DATA	51
CHAPTER 4: <i>STRUCTURAL RESPONSE ANALYSIS</i>	53
4.1. LOADS DUE TO SLUG FLOW	53



4.1.1. GRAVITATIONAL LOADS.....	53
4.1.2. CENTRIFUGAL FORCE.....	53
4.1.3. OTHER CONTRIBUTORS.....	66
4.2. STRUCTURAL ANALYSIS.....	66
4.2.1. ANALYSIS CLASSIFICATION.....	66
CHAPTER 5: PIPES DYNAMICS WITH VARIABLE AND MOVING MASS.....	68
CHAPTER 6: CASE STUDY.....	72
6.1. METHODOLOGY.....	72
6.2. MODAL ANALYSIS.....	73
6.3. SLUG ANALYSIS.....	77
6.3.1. INPUT DATA.....	77
6.3.2. RESULTS.....	80
6.3.3. CRITICAL CASES IDENTIFICATION PROTOCOL.....	101
CHAPTER 7: CONCLUSIONS AND FUTURE STUDIES.....	104
APPENDIX A: ABAQUS™.....	106
A.1. BACKGROUND.....	106
PRE-PROCESSING.....	106
GEOMETRY.....	107
A.2. ABAQUS INPUT FILES.....	111
APPENDIX B: REACTION ON A CURVED PIPE DUE TO STEADY-STATE FLOW.....	117
BALANCE OF MOMENTUM.....	118
RESULTANT ON A FINITE PART OF THE BEND PIPE.....	119
CARTESIAN COMPONENT (to use in ABAQUS).....	120
Example 1. Generic bend, starting horizontally.....	121
Example 2. A quarter bend.....	121
Example 3. A half-quarter bend.....	122
List of FIGURE.....	123
List of TABLE.....	127
ACRONYMS.....	128
List of SYMBOLS.....	129
ACKNOWLEDGMENTS.....	138

CHAPTER 1: *INTRODUCTION*

1.1. ABOUT THIS THESIS

Pipelines are the arteries of the oil and gas industry. They transport the hydrocarbons to and from both offshore and onshore facilities and connect the different subsea components.

Around a pipeline, there is a formidable amount of issues, with their distinctive complications, often strictly coupled with each other. Among others, this is a prudential list of the involved subjects:

- *Fluid mechanics:*
 - *Multiphase fluid mechanics:* there are still many challenging theoretical problems that have not been solved so far, such as: *flow regime transition, flow instability, flow similarity, phase interaction* and so on.
 - *Bubble, slug, gas mixing:* they are undesired multiphase flow regimes, due to the associated instability, which imposes a major challenge to *flow assurance* in the oil and gas industry.
- *Heat exchange and transfer;*
- *Chemistry:* hydrate formation mitigation and removal;
- *Structural dynamics:*
 - *Large displacement analysis;*
 - *Moving mass:* is an essential aspect in this class of problems. The theoretical and numerical apparatus to face this formidable question is very complex.
 - *Fatigue and Fracture mechanics;*
- *Fluid-structure interaction:* the flow behaviour depends on the shape of the structure and, primarily, on its motion; on the other hand, the motion and deformation of the structure depend on the action the fluid exerts on the structure. Significant challenges associated with the FSI method include:
 - Computational, analysis and resource requirements;
 - Interface management and multi-discipline interaction;
 - Consistency of assumptions, input data and methodologies.
- *Flow Assurance;*
- *Construction:*
 - Plant design;
 - Organization;
- *Geotechnics;*
- *Ecology;*
- *Economics;*
- *Political economy.*

The studied problem

In subsea oil or gas production system, a **subsea jumper** (or spool piece) is a short pipe connector used to transport production fluid between two subsea components like subsea piping, manifolds, Christmas trees, platforms. Pipeline sections are assembled in a variety of spatial configurations to adapt to installation and operating tolerances and to withstand the final loads and displacements caused by fluctuating flow, temperature and pressure. Consequently, they provide some flexibility with respect to installation and operating conditions. This flexibility makes the jumper sensitive to vibrations induced by multi-phase internal flow. In addition, under particular flow conditions, such as slug flow, these vibrations will be more significant.

Slug flow is an intermittent flow, characterised by an alternating flow of liquid slugs and gas pockets. It is one of the most undesired multiphase flow regimes, due to the associated instability, which imposes a major challenge to *flow assurance* in the oil and gas industry. This flow regime can cause large pressure and liquid flowrate fluctuations inducing significant *mechanical loads* for subsea structures (jumper, riser). Thus, this intermittent flow can have an impact on production, on receiving equipment, on control systems and can be induced *dynamic mechanical loads*. Therefore, slug flow can generate rapid *variations* of the *mass distribution* and *pressure* perturbations along the pipe, which may induce large vibrations (FIV). Two excitation mechanisms can be identified: the *variation in weight* (gravitational loads) along the straight sections and the *impact loads* on the bends (centrifugal forces).

This work discusses the uncoupled interaction between a *jumper* and several train of massless slugs, flowing with different velocities and frequencies, regarded as time-dependent forces, ignoring the influence of the moving mass.

1.2. THESIS ORGANIZATION

The contents of this thesis are organized in five main chapters that are preceded with introduction (Chapter 1) and followed by a separate chapter for conclusions and future works (Chapter 7).

- **Chapter 1** (*Introduction*): introduction of the work and issues overview.
- **Chapter 2** (*Offshore Field Overview*): presentation of the offshore transportation system and detailed description of the pipeline components.
- **Chapter 3** (*Multiphase Flow*): consists of two main sections, the first part provide a general description of Multiphase Flow, in particular of Two-Phase Flow, and the second one presents a detailed review on slugging mechanisms, classifications, parameters and problems.
- **Chapter 4** (*Structural Response Analysis*): description of loads due to slug flow and the different structural analysis methods that can be used.



- **Chapter 5** (*Pipes Dynamics with Variable and Moving Mass*): general presentation of the dynamic problem with variable and moving mass.
- **Chapter 6** (*Case Study*): results from modal dynamic analysis and slug analysis. In this section are reported all the modes of vibration, the relative frequencies and the force-displacement graphs obtained from the different slug dynamic analysis.
- **Chapter 7** (*Conclusions and future works*): conclusions and recommendations for further studies.

CHAPTER 2: OFFSHORE FIELD OVERVIEW

2.1. WHAT IS THE TRANSPORTATION SYSTEM?

Pipelines are the arteries of the oil and gas industry (Palmer & King, 2008). They transport the hydrocarbons to and from both offshore and onshore facilities and connect the different subsea components. Pipeline can be classified in two categories:

- i. **Infield pipelines** transport fluids within the field (typical range of 4-12 in, i.e. 0.102-0.305 m). They are often called “flowlines” and may be made of flexible pipe or rigid pipe [see § 2.1.7].

Flowlines linking wells within a particular offshore facility or directly from the well to the process platform.

- ii. **Export pipelines** transport processed oil or gas from the platform to the coast (typical range 16-36 in, i.e. 0.406-0.914 m).

Export pipelines exporting the product from field to shore or to another facility far from the field. If the pipeline carries a mixture of oil and gas then it is a **multi-phase** pipeline. If the pipeline carries only oil or only gas, then it is a **single-phase** pipeline.

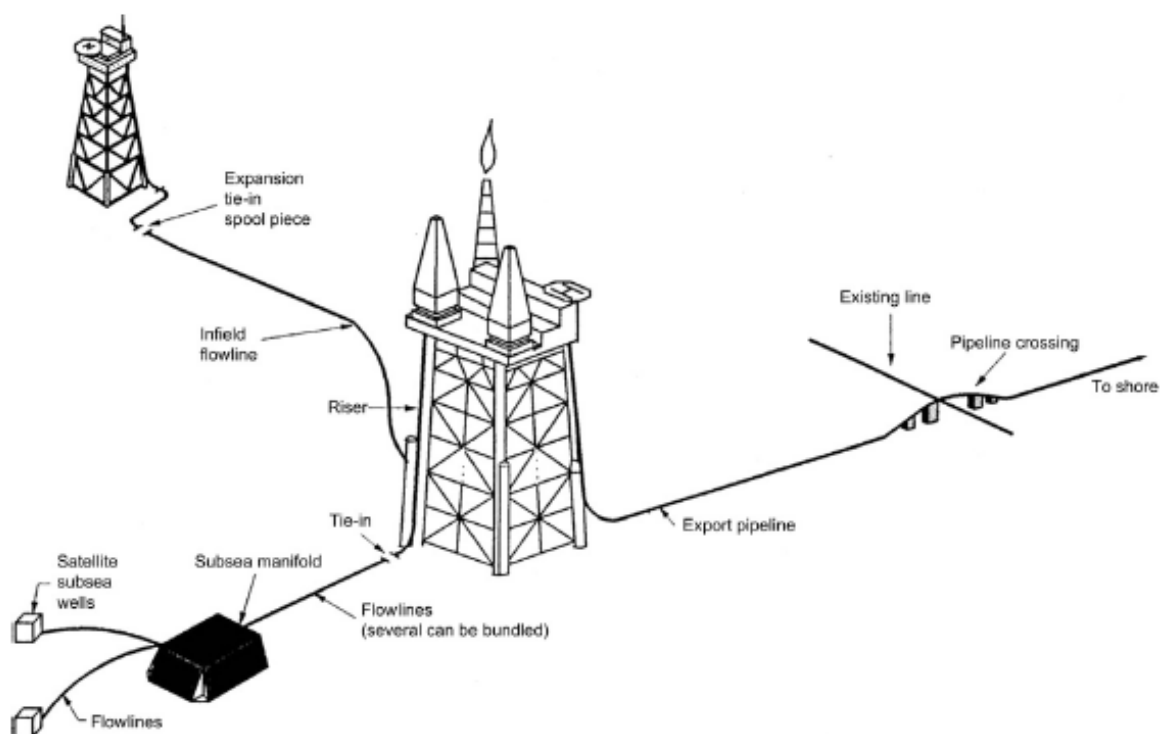


Figure 1 - Subsea Pipeline and Associated Infrastructure

New deep and ultra-deep hydrocarbon field developments see an increasing use of subsea production systems. A subsea production system consists of a subsea completed well, seabed

wellhead, subsea production tree, subsea tie-in to flowline system and subsea equipment and control facilities to operate the well (Bai & Bai, 2012).

This system consists of the following components:

- Subsea drilling systems;
- Subsea X-trees and wellhead systems;
- Umbilical and riser systems;
- Subsea manifolds and jumper systems;
- Tie-in and flowline systems;
- Control systems;
- Subsea installation.

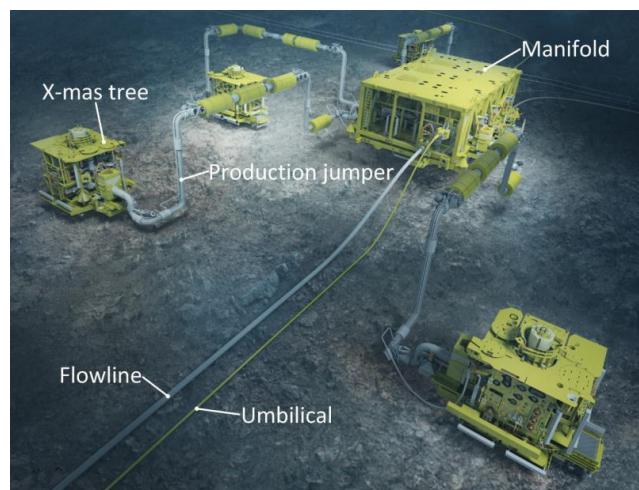
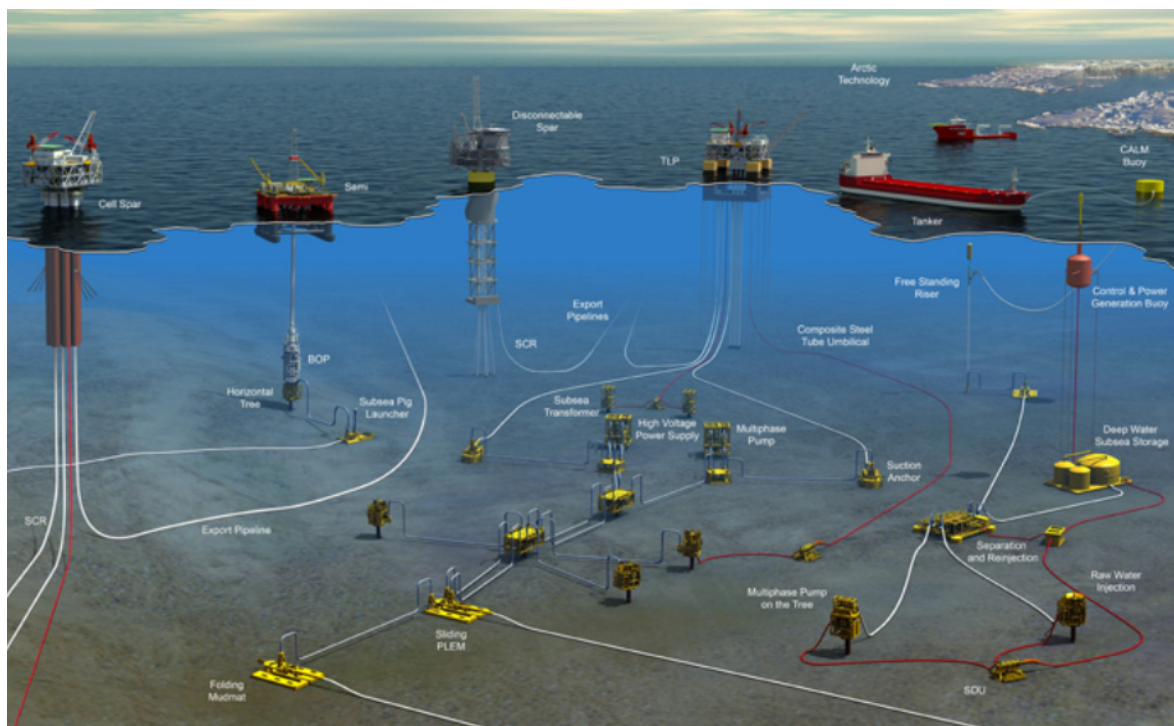


Figure 2 - Subsea Production System

The complete subsea production system comprises several subsystems necessary to produce hydrocarbons from one or more subsea wells and transfer them to a given processing facility located offshore (fixed, floating or subsea) or onshore, or to inject water/gas through subsea wells.

Subsea production systems can range in complexity from a single satellite well with a flowline linked to a fixed platform, to several wells on a template producing and transferring via subsea processing facilities to a fixed or floating facility, or directly to an onshore installation.

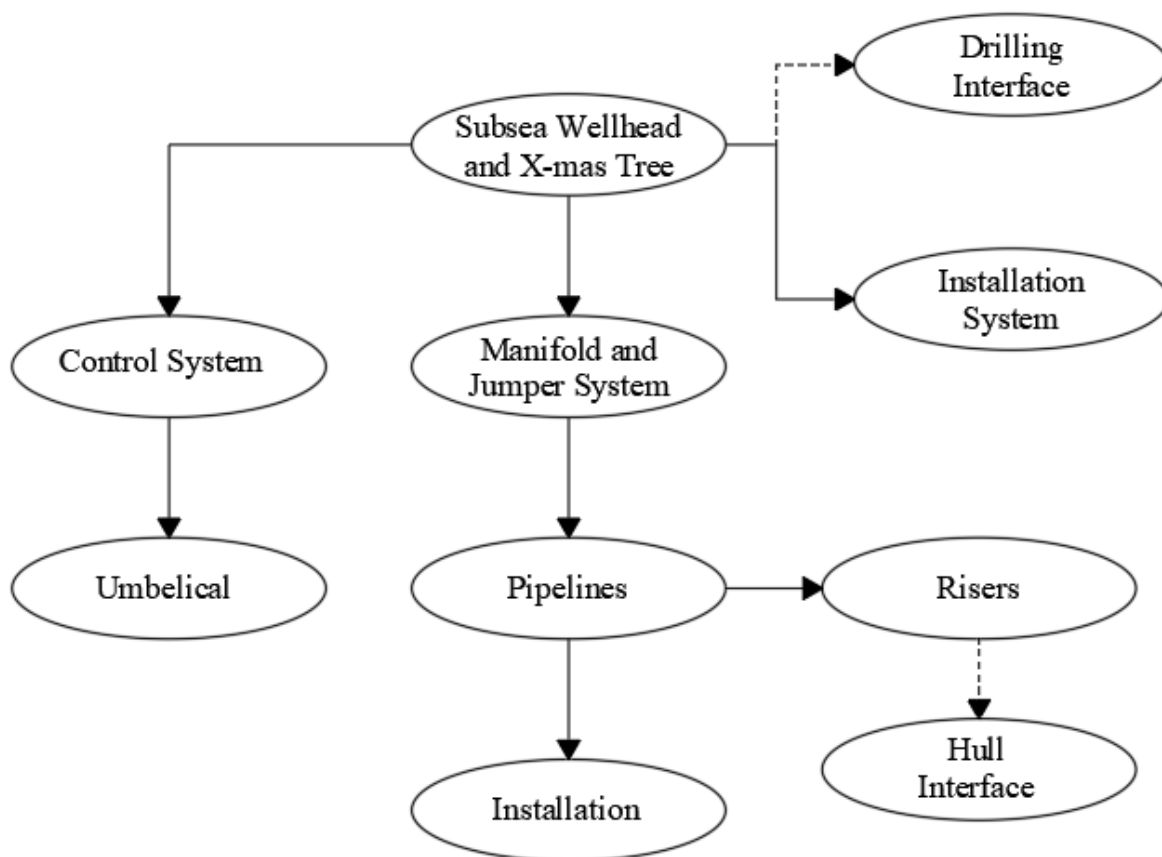


Figure 3 - Relationship among the major components of a Subsea Production Systems

The different mechanical structures involve in a subsea production system are:

2.1.1. SUBSEA WELLHEADS

Wellhead is a general term used to describe the pressure-containing component at the surface of an oil well that provides the interface for drilling, completion, and testing of all subsea operation phases (Bai & Bai, 2012).

2.1.2. SUBSEA TREES or X-MAS TREES

The **X-Tree** is an array of valves and valve blocks fitted to a wellhead to control and contain the well. It controls the flow of produced or injected fluids and interfaces with the wellhead, jumpers and manifold.

Subsea trees sit on top of the well at the sea floor.

Although they have little visual resemblance to the original onshore Christmas trees, they provide essentially the same functions. They furnish the flow paths and primary containment for the oil and gas production and the valves needed for both operation and safety (Leffler, Pattarozzi, & Sterling, 2011).

The valves can be operated by electrical or hydraulic signals; manually by a diver or by ROV (Remotely Operated Vehicle).

2.1.3. PIPELINE END TERMINATION

With the term **PLET (FLET)** it is intended the Pipeline (Flowline) End Termination. PLET is a system of piping, valve and connector, integral with the pipeline or flowline, used to connect the pipeline (or flowline) to a jumper.

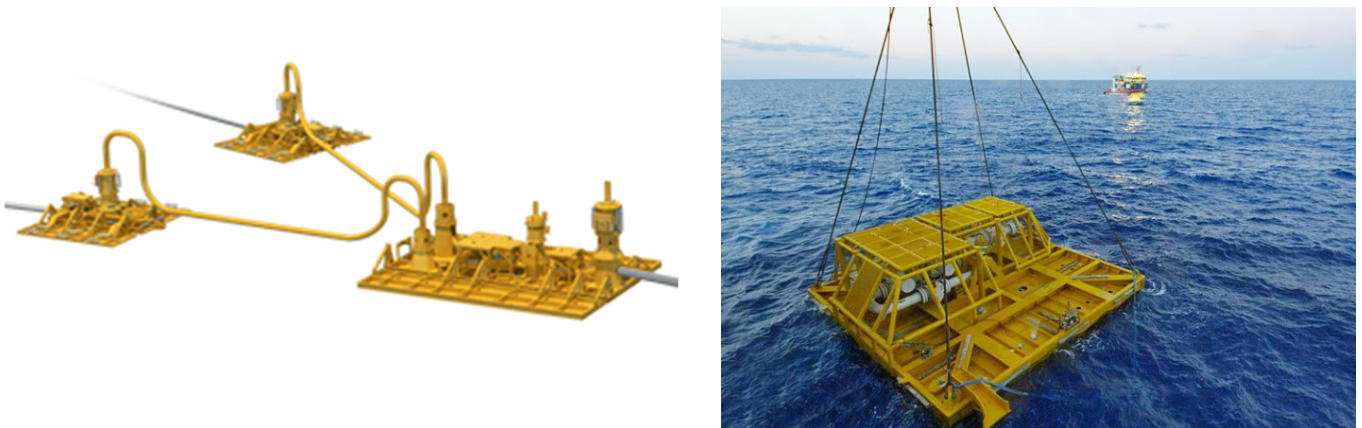


Figure 4 – Pipeline End Termination (PLET)

The PLET/PLEM (Pipeline End Manifold) is located at the end of a subsea pipeline, while the inline structure is located in the middle of the pipeline.

Commonly it is a frame structure, integral to the pipeline end, supporting the connection system and the isolation valve (if any). It is founded on mudmats and usually allows pipeline expansion.

Mudmat

Is a temporary seafloor support for subsea equipment (PLET, PLEM, Manifold) providing an adequate area for load distribution on the soil (Yarrarapu, 2015), made in steel, wood or fiberglass. The fundamental aspects considered in the design of mudmat are the bearing capacity of the soil, the resistance of the structure against sliding and overturning, together with occasional settlement of the mudmat.

2.1.4. SUBSEA MANIFOLDS

The **manifold** (Fig. 3) is an arrangement of piping or valves designed to combine, distribute, control, and often monitor fluid flow. Subsea manifolds have been used in the development of oil and gas fields to simplify the subsea system, minimize the use of subsea pipelines and risers, and optimize the flow of fluid in the system.

A manifold system can also provide functions for well testing, i.e. include a dedicated pipe header where the production of a single well can be isolated from the other.

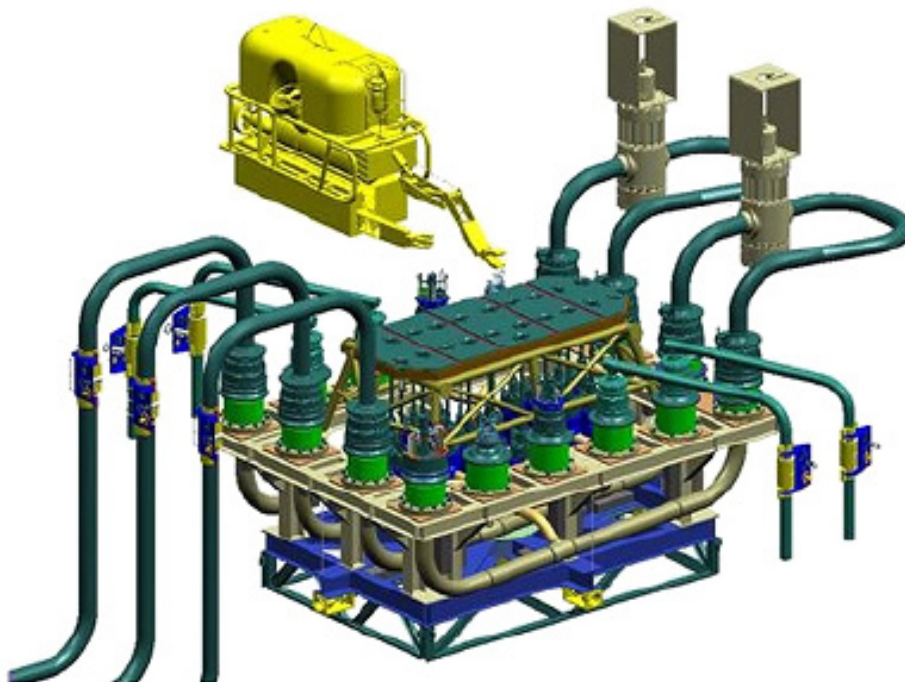


Figure 5 - Subsea Manifold and ROV

The manifold may be anchored to the seabed with piles or skirts that penetrate the mudline. Its size is dictated by the number of the wells and through put, as well as how the subsea wells are integrated into the system.

The numerous types of manifold range from a simple Pipeline End Manifold (PLEM) to large structures such as a subsea process system. (Bai & Bai, 2012).

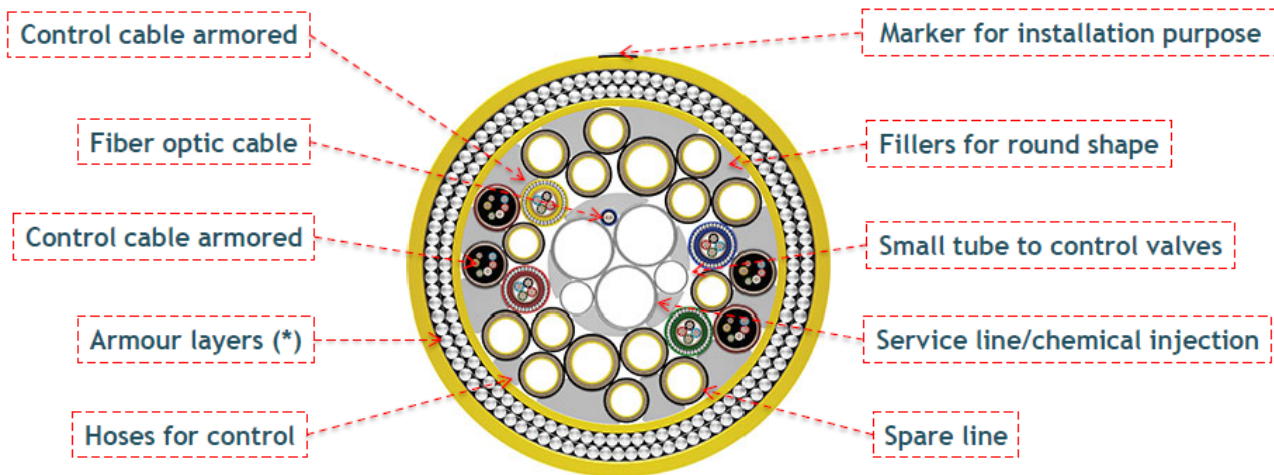
The manifold system can include control system equipment such as:

- Sensors for pressure and temperature monitoring;
- Flow meters for flow rate measurement;
- Distribution system for hydraulic and electric functions;
- Control module.

The manifold can be a “standalone” structure or can be a part of a drilling template. In this case the manifold can be installed separately later, after drilling and X-mas tree installation.

2.1.5. UMBILICAL SYSTEMS

An **umbilical** (Figure 6) is a bundled arrangement of tubing, piping and electrical conductors in an armored sheath that is installed from the host facility to the subsea production system equipment (Bai & Bai, 2012).



(*) for reinforcement and/or ballast



Figure 6 - Typical Subsea Umbilicals (Cross-Section)

Subsea umbilicals are used to control hydraulic valves, to transmit electricity to electrical subsea or topside systems and signals for surveillance and monitoring, to inject fluids into the production stream, to inject methanol and to operate electric pumps (power umbilical).

They conduct the flow necessary to keep the system alive, transmit the control fluid or electrical current necessary to control the functions of the subsea production and safety equipment (tree, valves, manifold, etc.).

Umbilical dimensions typically range up to 10 in (0.254 m) in diameter.

2.1.6. SUBSEA PRODUCTION RISERS

A production **riser** system consists of conductor pipes connected to floaters on the surface and the wellheads at the seabed. It is the primary device of the floating production system to convey fluids to and from the vessel (Bai & Bai, 2012) along a semi-vertical path.

There are various types of subsea riser systems used in deep-water (refers to water depths of more than 500 m) field developments, which can be classified essentially in *rigid* risers and *flexible* risers. A hybrid riser is achieved through a combination of these two types.

There are four main types of production risers: Steel Catenary Risers (SCRs), Top Tensioned Risers (TTRs), flexible risers, and hybrid risers.

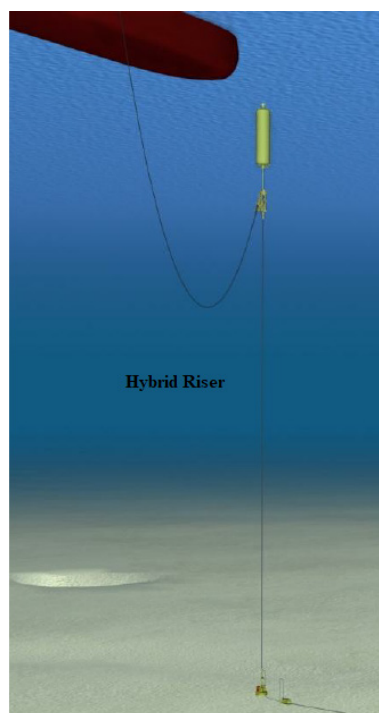
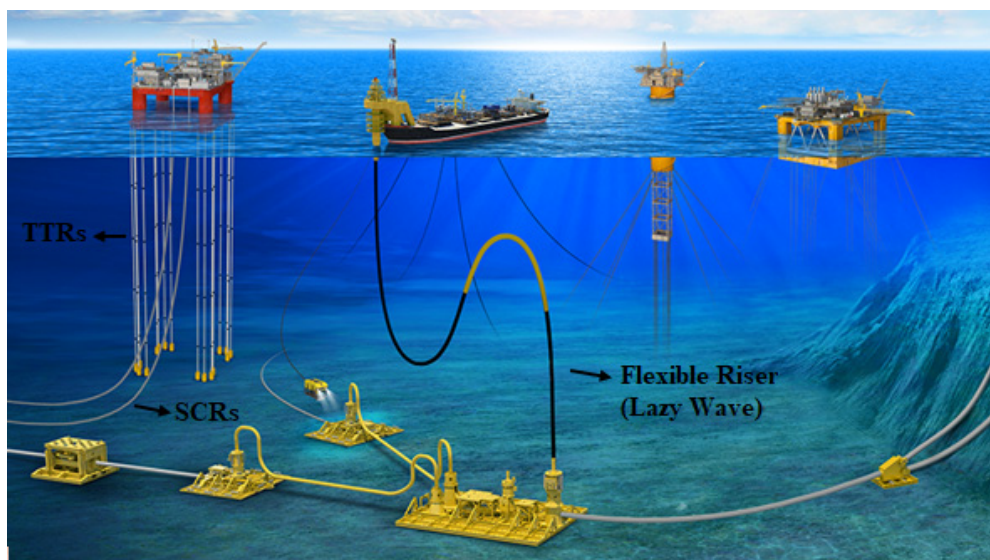


Figure 7 - Subsea Production Risers

SCRs were initially used as export lines on fixed platforms. The shape assumed by the SCR is controlled mainly by weight, buoyancy and hydrodynamic forces due to currents and waves. The rigid pipe of the SCR forms a catenary between its hang-off point (flex joint) on the floating or rigid platform and the seabed.

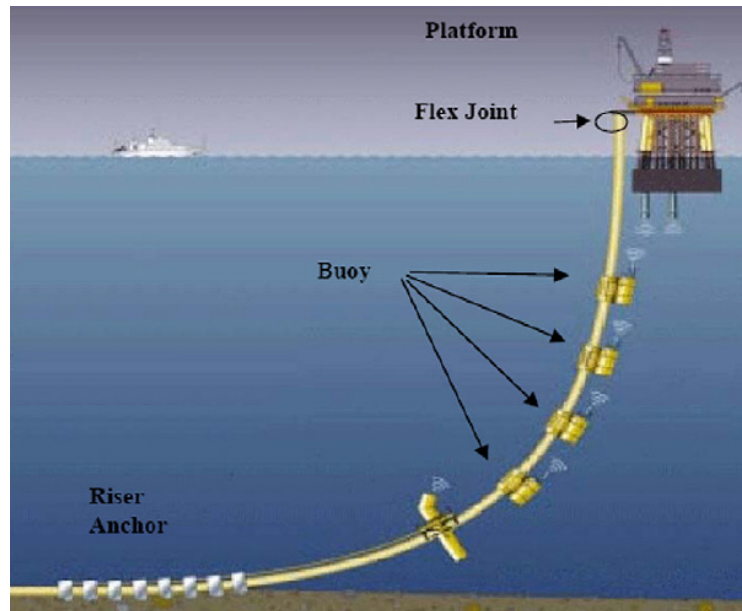


Figure 8 - Steel Catenary Riser configuration

The SCR is sensitive to waves and currents, due to the usually low level of effective tension on the riser. The fatigue damage induced by vortex-induced vibrations (VIVs) can be fatal to the riser.

TTRs are long circular cylinders used to link the seabed to a floating platform. These risers are subject to steady currents with varying intensities and oscillatory wave flows. The risers are provided with tensioners at the top to maintain the angles at the top and bottom under the environmental loading (Bai & Bai, 2012). TTRs are designed to give direct access to the well, with the wellhead on the platform. This type of riser has to be capable of resisting the tubing pressure in case of a tubing leak or failure.

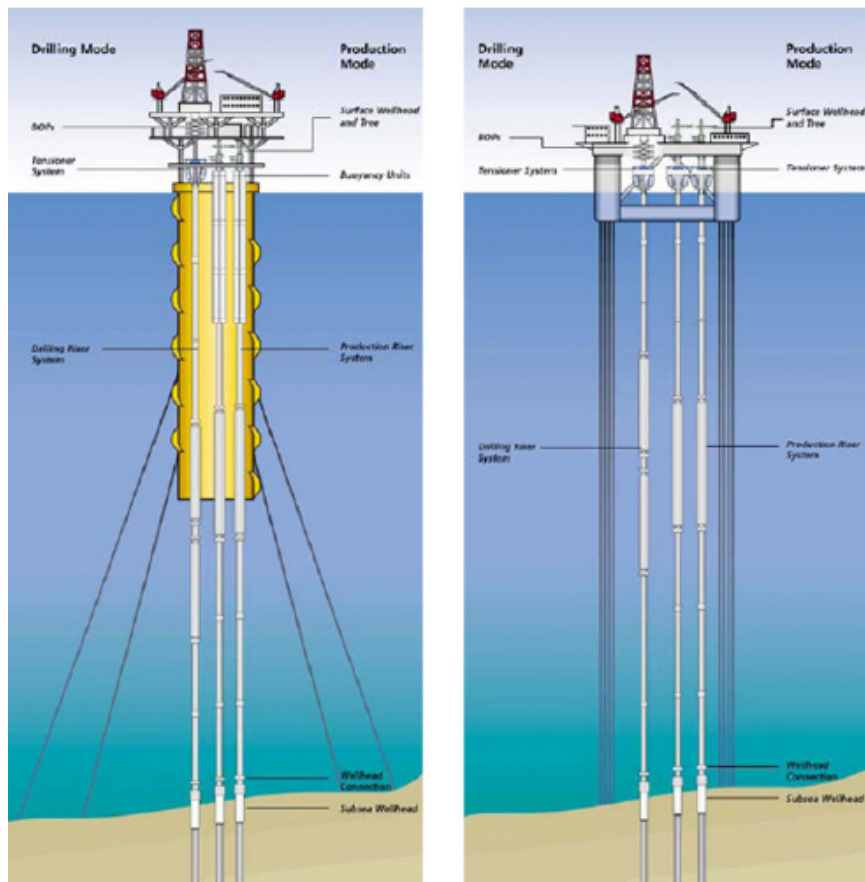


Figure 9 - Top Tensioned Riser Configurations

Flexible Risers have been a successful solution for deep-water or shallow-water riser and flowline systems worldwide. Flexible risers are the result of an extraordinary development program that was based on flexible pipes. The main characteristic of a flexible pipe is its relative low bending to axial stiffness ratio. This characteristic is achieved through the use of a number of layers of different materials in the pipe wall fabrication (Fig. 10). The flexible pipe composite structure combines steel armor layers with high stiffness, to provide strength, and polymer sealing layers, with low stiffness, to provide fluid integrity. The carcass forms the innermost layer of the flexible pipe cross section. The main function of the carcass is to prevent pipe collapse due to external hydrostatic pressure or buildup of gases in annulus. This modular construction, where the layers are independent but designed to interact with each other, means that each layer can be adapted and adjusted independently to meet specific field development requirements. Flexibility is the distinctive feature of a flexible pipe. A typical 8" (20.32 cm) inner diameter (ID) flexible pipe *can be folded securely at a radius of two meters or less*. This is why flexible dynamic risers are enabling technologies for floating production systems. This flexibility is also important for flow lines conditions of irregular seabed. The flexibility makes it possible to wrap the pipe on a coil for efficient transport and quick installation. The independent layers of a flexible structure allow it to be adapted to the precise needs of a specific development. Simple flexible pipe for medium-pressure water transport comprise only four layers. The most complex flexible pipe can have up to 19 layers. In addition to including new

thermoplastic or steel layers within the product, it is also possible to assemble thermoplastic tubes, electric cables or optical fibers around a flexible tube to produce an *Integrated Umbilical Service*. Since the steel wires are not in direct contact with the transported fluid, they do not require the same corrosion resistance as the steel tube. This means that our design experience and knowledge of the diffusion of gas through thermoplastic materials allow us to use carbon steel where the application of equivalent rigid tubes would require more corrosion-resistant alloys expensive. The combination of flexibility and modularity, together with corrosion and high pressure resistance, reusability and versatility show why the flexible pipe is a cost-effective solution.

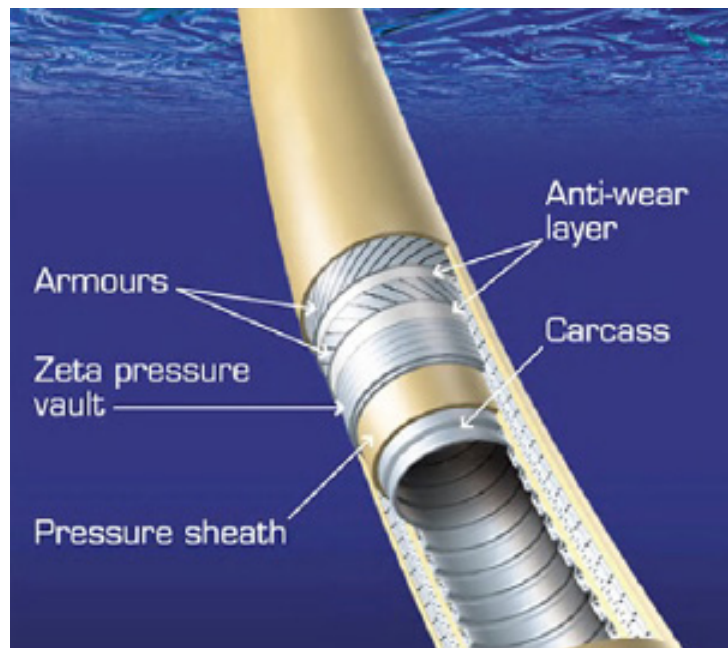


Figure 10 - Typical Cross Section of Flexible Pipe

The configurations are designed to absorb floater motions by change of geometry. Industry practice requires several types of riser configurations typically used in conjunction with floating production-loading systems (Fig. 11).

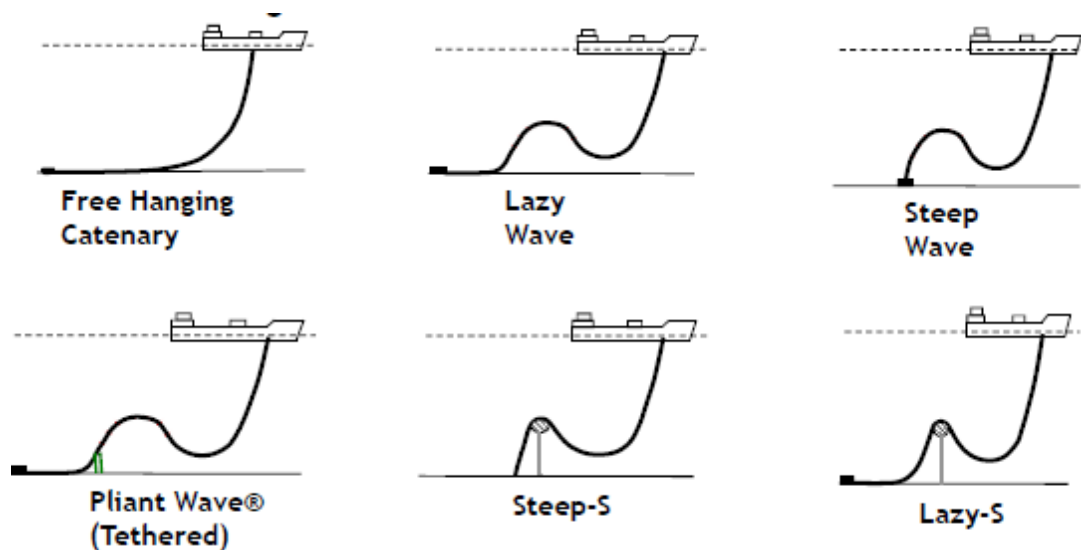


Figure 11 - Flexible Risers Configurations

Hybrid Risers consist of a vertical bundle of steel pipes supported by external buoyancy. The hybrid system is a combination of a rigid part for the larger part of the riser and flexible part for the connection with the floater.

2.1.7. SUBSEA PIPELINES

Subsea **flowlines** are the subsea pipelines used to connect a subsea wellhead with a manifold or the surface facility. The flowlines may be made of flexible or rigid pipe and they may transport petrochemicals, lift gas, injection water and chemicals (Bai & Bai, 2012).

Pipelines are operating at great depths, so that they are exposed to high level of external pressure. Furthermore, they are subject to high temperatures from the internal contents and to the action of due to pipeline walking and buckling. All these occurrences can damage the structures connected to the pipeline: the end connection, between flowlines or pipelines and the structures (subsea piping, manifolds, Christmas trees, platforms), is performed by *Jumpers and Spools*.

Pipelines Depth

With modern technologies submarine pipelines can be realized both in conventional-waters, that is sea areas with depths of 500 m, and in deep-waters ($h > 500$ m).

2.1.8. SUBSEA JUMPERS AND SPOOLS

In subsea oil or gas production system, a subsea **jumper** (or **spool** piece) is a short pipe connector used to transport production fluid between two subsea components like subsea piping, manifolds, Christmas trees, platforms.

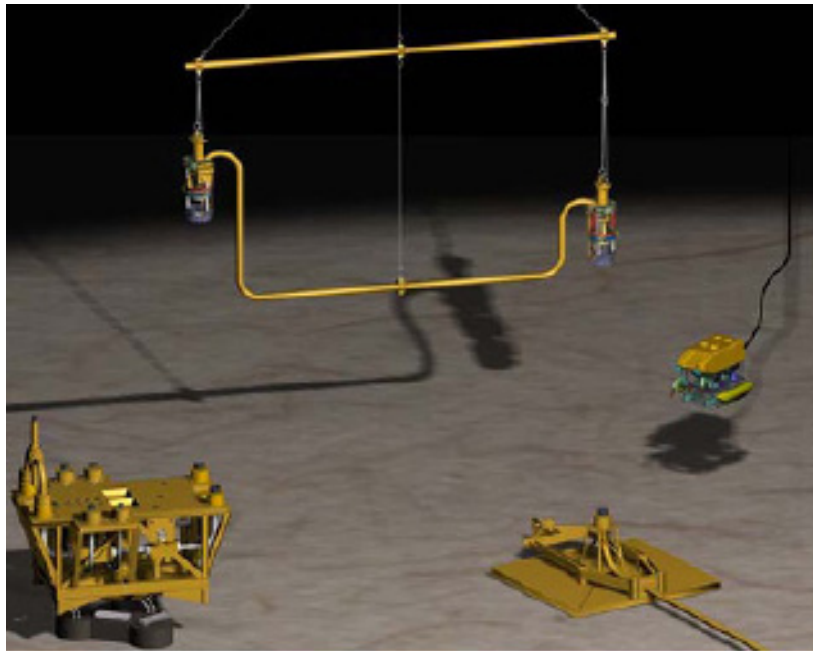


Figure 12 - Subsea Rigid Jumper

The jumper pipe spool should include an assembly of straight pipes and bends between the end connections configured to provide compliance during installation and operation.

The jumper **connection** system is configured with steel pipe and mechanical connections at each end for connection to the subsea facility's piping. The connector design is capable of resisting the design loads due to the combined effects of internal pressure, external bending, torsion, tensile, thermal and installation loads (Bai & Bai, 2012).

The main components of subsea jumpers are shown in Fig. 13:

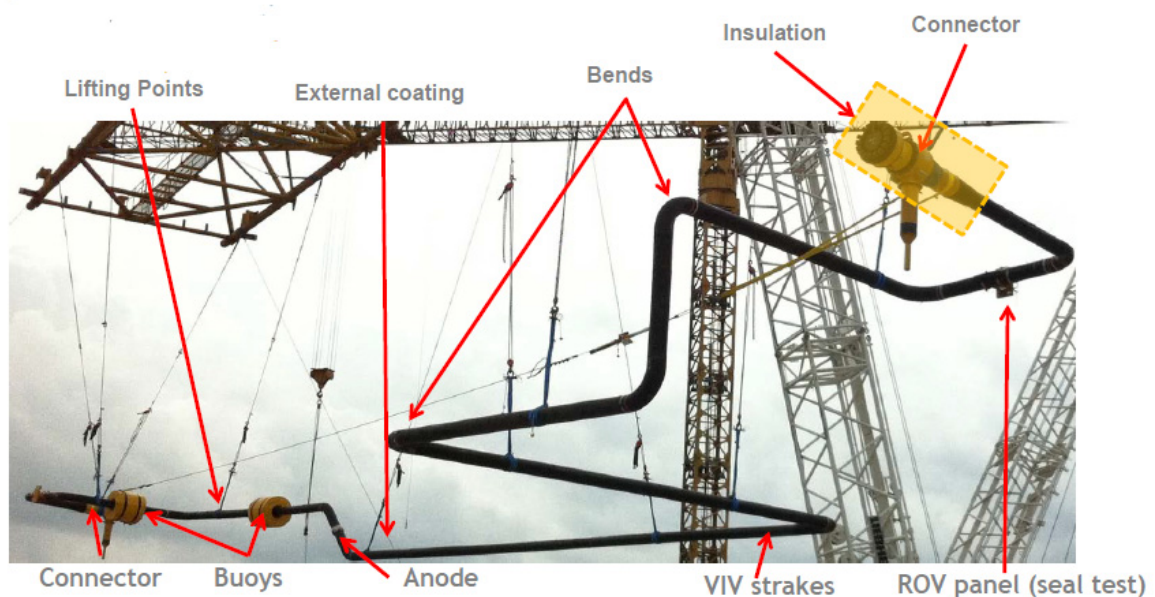


Figure 13 - Main Components

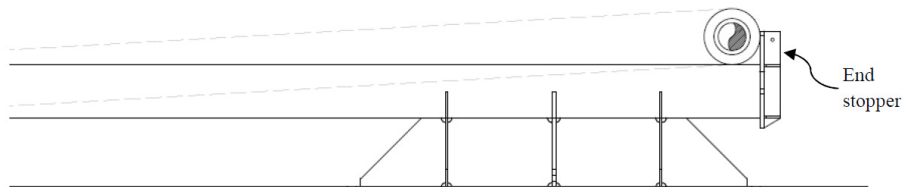
Buoyancy

The distributed buoyancy method distributes buoyancy modules at specific locations along the pipeline to buckle initiators and stress mitigation devices (Bai & Bai, 2014). Buoyancy is often added to jumpers to decrease the load on the terminations. Permanent or temporary buoyancy modules can be required to ensure adequate performance during operating or reducing interface loads during tie-in.



Buckle Initiators

Buckling is due to the temperature rise which, between fixed extremes, can unstable the pipe. For more severe design conditions, the designer shall ensure that the pipeline will buckle as often as required, which might involve artificial **buckle initiators** (Carneiro, Gouveia, Parrilha, & Cardoso, 2009). Buckle initiators are elements to artificially induce buckling in a controlled area.



If the pipe is a rigid type it is called **Subsea Rigid Jumper (SRJ)**; contrarily, if the pipe is a flexible type, is called **Subsea Flexible Jumper**.

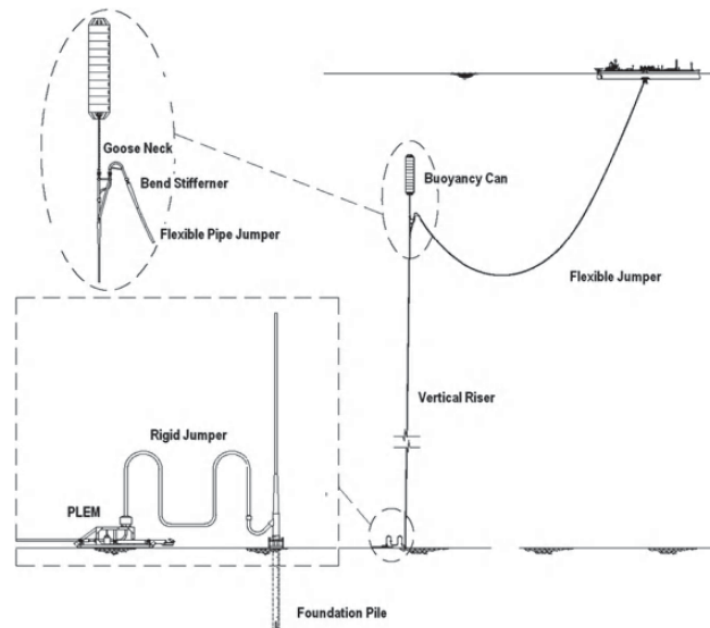


Figure 14 - Subsea Rigid and Flexible Jumpers

Two types of jumpers can be distinguished in function of their orientation: the **vertical** tie-in and the **horizontal** tie-in.

Vertical rigid jumpers are typical vertical tie-in systems and use mechanical *collet connectors* at each end. The connection at the extremities of the jumper pipe takes place through the connector hub. The jumper can have different configurations: M-shaped style and inverted U-shaped style.

The jumper configurations depends by the design parameters, interfaces with subsea equipment and the different modes in which the jumper will operate (Bai & Bai, 2012).

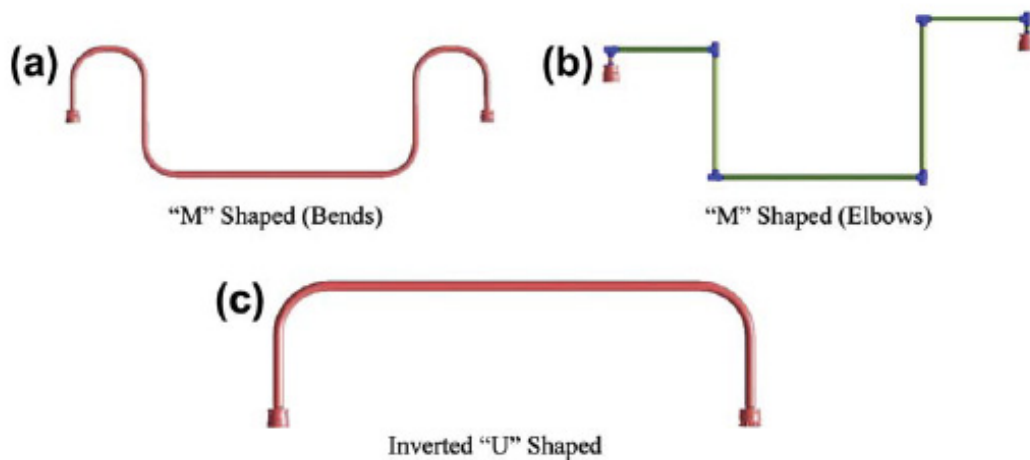


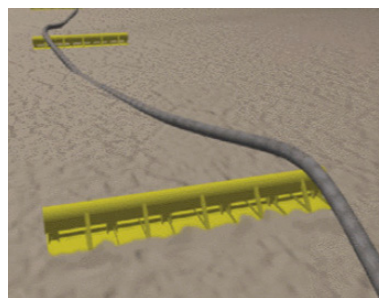
Figure 15 - Configurations of Vertical SRJs

They are characterized by a ‘floating’ configuration, spanning between the connections hubs. This mitigates the undesirable effects at the interface with the seabed by increasing its flexibility; it eases matters relating to design, metrology, fabrication and installation.

Horizontal spools are typical horizontal tie-in systems, usually laying on the seabed or, in particular conditions, on the *sleepers*, employing bolted joints connections. The typical configuration is Z-shaped type.

Sleeper

A sleeper is typically a large diameter pipe section, with or without a simple support base, pre-laid on the seabed perpendicular to the pipeline route to raise and support the pipeline above the seabed (Bai & Bai, 2014).



Types	Advantages	Disadvantages
M	Simple concept; Reliable strength and response	Fatigue sensitive; Dem and ing higher quality welds; VIV damage might be great; High load on connector
Z	Greater flexible; Reliable response intensity; Easy to adapt to the angle of the end	Fatigue sensitive; Dem and ing higher quality welds; VIV damage might be great
U	Long fatigue life; Simple design	Problems in manufacturing and installation; Higher load on connector; No proof of its reliability; VIV damage cannot be eliminated

Table 1 - Comparison of different Jumper configurations (Sun & Kang, 2015)

Links Saipem

<https://www.youtube.com/watch?v=3Bddl1aAlo4> (Hydrone)

<https://www.youtube.com/watch?v=tSNUC2WspgA> (Offset Installation Equipment)

Links Other Subsea Companies

<https://www.youtube.com/watch?v=z98oPpTilu0> (Spool Installation – Technip Norway)

https://www.youtube.com/watch?v=h-ke3Eux_rs (Vertical Jumper Installation – Oceaneering)

<https://www.youtube.com/watch?v=yTucNCAqBA>

Due to the remote-control operations, the exact positioning at the seabed is a challenge. Hence, jumper design will consider the complete range of possible configurations of the structures i.e. different lengths and angles.

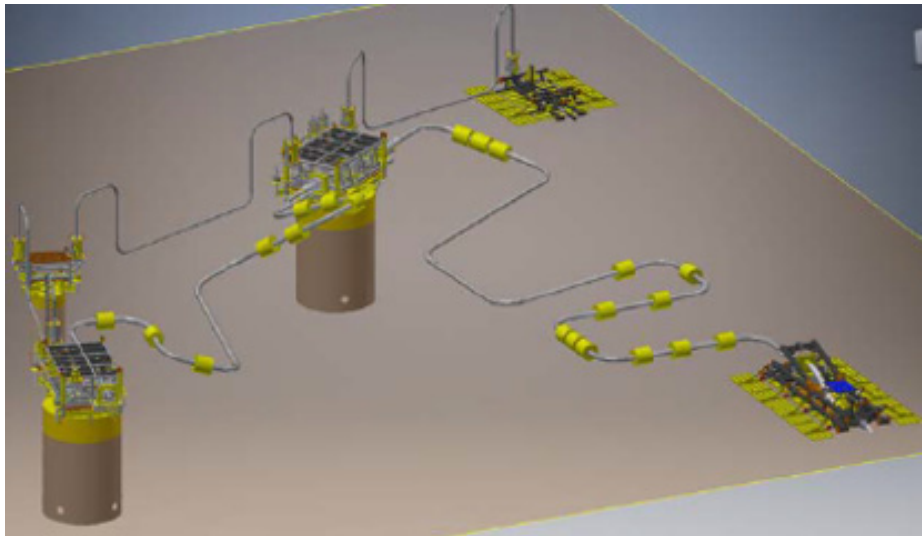


Figure 16 - Jumper configurations

A jumper or spool mainly serves two functions:

1. Complete the connection between pipelines and subsea structures and to be able to cope with installation tolerances;
2. Mitigate axial expansion of flowlines. In order to avoid expansion propagating to adjacent structures, spool-pieces with bends are installed to accommodate the expansions and prevent transmitting high loads into close structures.

They shall be designed to withstand:

- Large displacements due to expansion (pressure and temperature variations);
- PLET displacement due to lateral buckling or pipe walking;
- Riser displacement (wave and current induced motions at bottom of riser tower);
- Fabrication and installation loads (hydrotest, lifting, connection loads).

The design of a subsea jumper is dependent on the field layout. This will determine the length of the jumper and for a large part the geometry.

In the design phase of a subsea jumper, all of the operational and testing conditions will be modeled to see what the effects are on the jumper. Since the reservoir characteristics will change over the field life the internal pressure and temperature of the flow will also change. There can also be changes caused by the operation of the subsea system such as a shutdown and start-up.

Furthermore, the installation tolerances are applied in the design because a subsea jumper is installed in one piece on the bottom of the sea and this can be a very difficult operation. An installation tolerance can for example be a misalignment with a connector in position and rotation. The tolerances will also cause additional stresses in the jumper since it is not in the perfect position to transfer all the loads.

The construction of a subsea jumper is not straightforward: several sections of the jumper can be pre-fabricated.

Before these sections are welded together to form the jumper, highly accurate measurements are required between the hubs on the subsea structures and pipelines in order for the spool piece to be constructed within the tight tolerances required in order to join the two hubs together. The method of collecting these measurements is called 'Metrology'. There are several types of techniques currently available to support metrology surveys including: acoustics, inertial and dynamic laser scanning.

The aim of the design is to model the **entire life of the jumper**, which can be summarized in following phases:

1. INSTALLATION (Sun & Kang, 2015)

An example of a jumper installation method is:

Step 1: Use *installation vessel crane* to pick up the jumper from the vessel. First, the spreader beam is connected to the installation vessel crane with the locks and traction line equipment, then the jumper is connected with the spreader beam by riggings. Next, the crane lifts the spreader beam from the operation deck and then the spreader beam and riggings pick up the jumper.

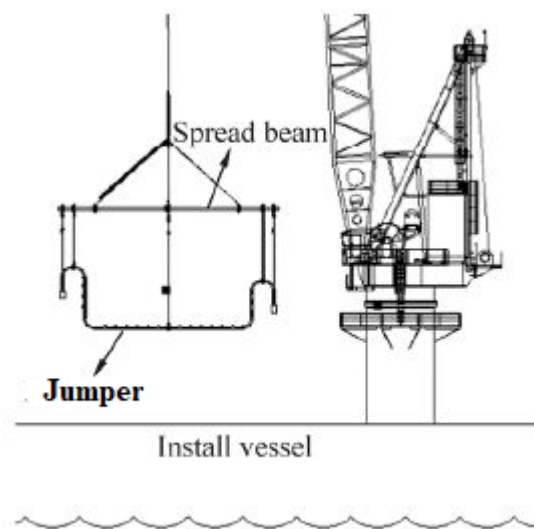


Figure 17 - Step 1: Pick up the Jumper

Step 2: Overboard the jumper and release the crane line until the jumper passes through the splash zone. After that, operate the crane to move the jumper to the outside of the vessel and then transfer it through the splash zone at a certain speed. Later on, connect the winch line with jumper locks, regulate the jumper and continue the installation. Finally, in the depths of about one hundred meters, the load will be transferred to the winch line and the crane line will be released with the help of ROV and then recover it (cf. e.g. Fig 5).

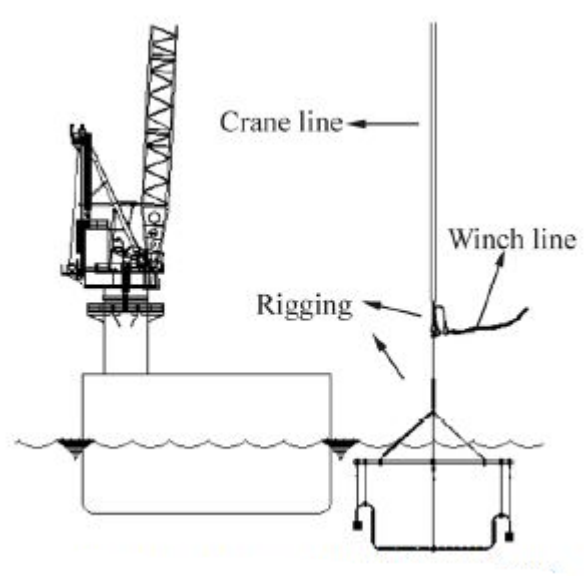


Figure 18 – Step 2: Deploy through splash zone

Step 3: Release the winch line until jumper is a few meters above seabed and make alignment of the connectors. When the jumper is approaching few meters away from the sea floor, use the ROV to monitor its location, direction and depth. Lastly, control installation vessel to move jumper just above the vertical position of underwater structures.

Connect the jumper with connection terminals. Then using the winch line and ROV to control the direction of the jumper and make sure the connector keep alignment with the connection terminal. Afterwards, the ROV locates the connector to the terminal and completes the installation and sealing work.

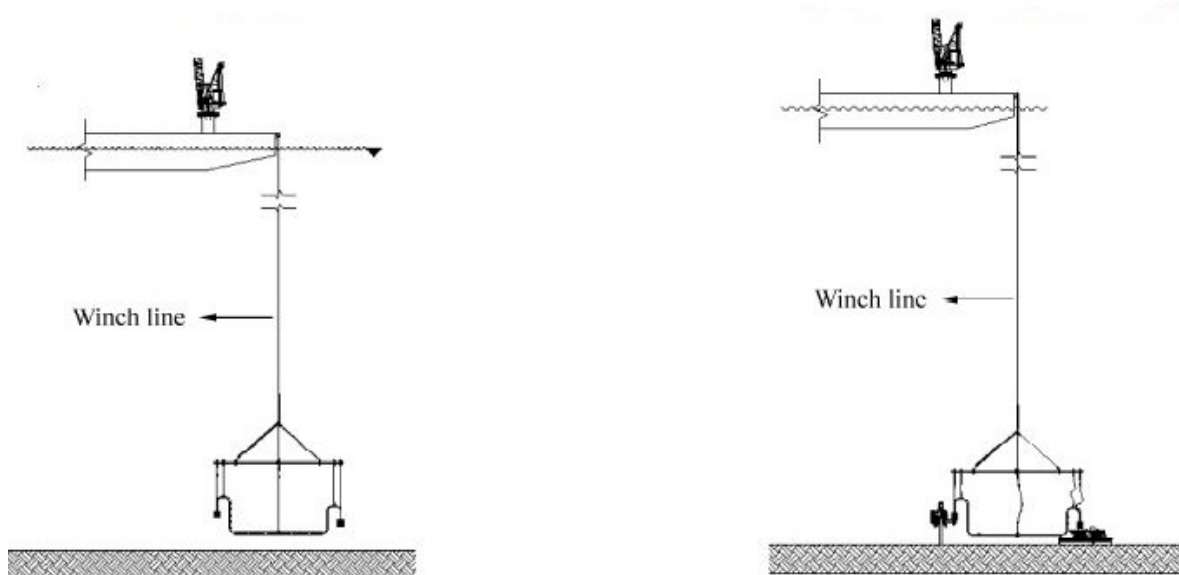


Figure 19 - Step 3: Jumper landing

2. **HYDROTEST:** Pre-commissioning activities are performed after the pipeline system is installed and all the tie-ins are completed, to assess the global integrity, qualify the system as ready for commissioning and start-up, confirm the safety to personnel and environment and confirm the operational control of the pipeline system (Guo, Song, Chacko, & Ghalambor, 2005). A hydrotest is one of the pipeline pre-commissioning activities. They are conducted to check the mechanical strength of the pipeline system and the integrity of the connections and it is carried out by pressurizing the system to a specified internal pressure, $P_{\text{hydrotest}} = 1.25P_{\text{design}}$, and holding it for a certain period of time to check whether there is a pressure drop.
3. **OPERATION:** Normal operating conditions.
4. **SHUT-DOWN.**

SRJs can be subject to significant static loads due to installation tolerances from fabrication and metrology, self-weight, internal and external pressures, thermal expansion, pipeline walking, seismic loads etc., as well as loads due to the interaction with the connected structures. The geometric configuration and loading conditions make the design of such systems particularly challenging (Bruschi, Parrella, Vignati, & Vitali, 2017).

For jumpers design there are also dynamic loads that have to be taken into account:

- **External loads:** the environmental loads caused by waves and currents. Jumpers are very sensitive to these loads due to their geometry and induced vibrations, VIV.
- **Internal loads:** loads induced by the internal flow such as *slug flow*. The many bends in a jumper configuration make the jumper particularly susceptible to these loads (FIV).

An excessive flexibility makes the jumper vulnerable to the external and internal flow induced vibrations (VIV and FIV), that is more susceptible to significant displacements due to dynamics loads like currents, high internal flow rate (coupled with slugging) or seismic events.

2.2. PIPE MATERIALS, COMPONENTS AND PARAMETERS

It is important to describe the characteristics of the material involved in offshore field and with primarily reference to the main pipe. The Standards (norm) and general prescriptions are generally given by the American Society of Testing and Materials (ASTM), together with its nomenclature and references, and American Petroleum Institute (API).

The main material used for submarine pipelines is steel. Despite the steel has the advantage of having a considerable specific weight and a good resistance it is highly sensitive to corrosion. Pipe steels must perform in difficult environmental conditions, such as the many corrosive and erosive actions of the sea, the dynamic cyclic and impact conditions, a wide range of temperature variations.

Thus, specialized criteria and requirements are imposed on the material qualities and their control. However, the following factors has to considering when selecting the correct material:

- *Cost.*
- *Resistance to corrosion effects.*
- *Weight requirement.*
- *Weldability.*
- *Fatigue endurance.*

The steel used for the pipeline must have high *strength*, i.e. the ability of the steel element to resist the longitudinal and transverse stress, consequences of the forces and distortions applied on the pipe. This resistance is obtained by using micro-alloyed low carbon steels to guarantee greater resistance to failure. However, steel has to maintain *ductility*, i.e. the ability of the pipe to absorb overstressing by deformation, impacts or shock loads and weldability. Finally, a very critical feature is the *fracture toughness*, namely the ability of the system, material-structural configuration, to prevent crack propagation.

The pipe sections are welded together to form a pipeline. High costs are associated with the manufacture of piping, so that the steels weldability is crucial. For this reason, the main factor determining a good weldability is the economy: the faster and easily the pipe can be welded, the faster it can be installed and the shorter the period of use of lay.

The pipe needs to conform to requirements of the **API Specification 5L**, with additional clauses to ensure that the material will be fit for the specific purpose. API Specification 5L details the mechanical properties of the steel, as well as methods for producing the pipe and testing finished pipe. One of the more important functions of API Specification 5L is the classification of dimensions and tolerances of the pipe joints, including standard diameters, wall thickness (termed schedule), lengths of joints, ovality, and out-of-straightness (Palmer & King, 2008).

Pipeline Grade /wall	Maximum Compositions %													
	C	Mn	Si	Al $\times 10^2$	Ca $\times 10^3$	Ni	N $\times 10^2$	Cu	V $\times 10^2$	Nb $\times 10^2$	Ti $\times 10^2$	B $\times 10^3$	P $\times 10^2$	S $\times 10^3$
Typical Formulations														
Basic API 5L	0.31	1.80											3	30
API 5L	0.16	1.56	0.35	4			1.2		7	5		1	3	15
Sweet Onshore	0.11	1.56	0.35	4		0.2	1	0.25	8	5			2.5	10
Sweet Offshore	0.08	1.56	0.30	4	3	0.2	0.8	0.25	8	4			1.5	5
Sour Offshore	0.05	1.00	0.30	4	5	0.2	0.7	0.25	6	5		4	1.5	1
Examples of Actual Pipeline Steels														
X65	16 mm	0.02	1.59	0.14						4	1.7	1	1.8	3
X65	25 mm	0.03	1.61	0.16		0.17				5	1.6	1	1.6	3
X65	25 mm	0.06	1.35			0.25		0.33	7	4	1.8		2.5	5
X70	20 mm	0.03	1.91	0.14						5		1	1.8	3
X70	20 mm	0.08	1.60					0.04		7				

Figure 20 - Typical compositions of pipeline steels (Palmer & King, 2008)

To ensure the durability of this material, namely the mechanical resistance due to chemical decay over time, it is necessary to provide the steel line with an efficient **cathode protection system**.

A coating is applied in order to protect the tube from corrosive environments and to provide protection against damage caused by abrasion and general wear. Pipe coating application is a standard practice and provides the following benefits:

- *Improved gas flow.*
- *Faster inspection and commissioning.*
- *Decreased cost of energy.*

Concrete or fiberglass coating provides further protection against abrasion. The addition of a concrete coating is also useful to compensate for the pipeline's negative buoyancy when it carries lower density product and to guarantee on-bottom stability. Furthermore, optional **insulation** may also be necessary in order to protect the pipe from rapid temperature fall, which may cause hydrate formation that obstructs the flow.

Cladding can be used sometimes in case of particularly severe corrosive conditions of the product content. It is a coating of high-cost corrosion resistant alloys applied on the pipe inner surface. Weld overlay cladding of carbon steel offers a wide choice of processes and flexibility to protect an almost infinite range of component shapes and sizes, with an equally wide range of base materials and cladding alloys (Lyssand, 2015).

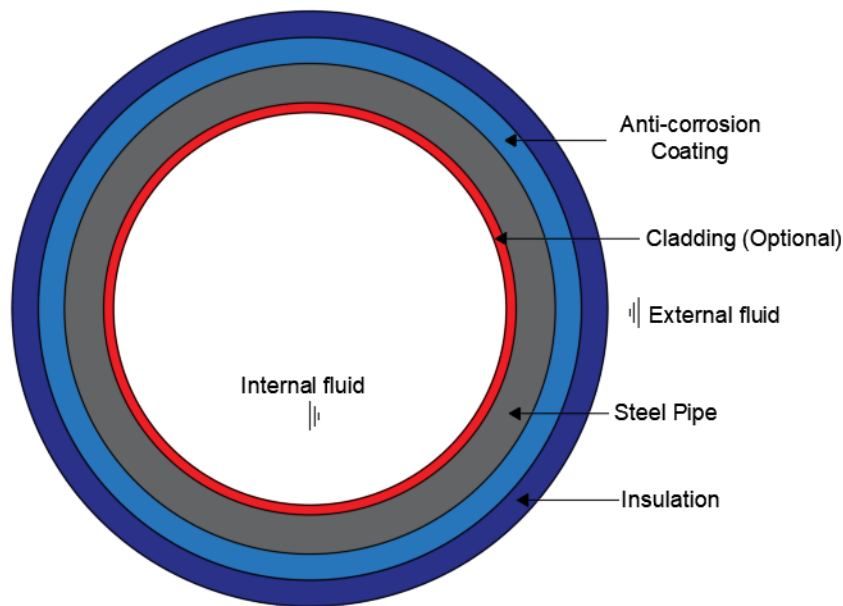


Figure 21 – Pipe Components

Geometric Characteristics

The pipe is generally identified by its *nominal diameter* and *nominal thickness*. The nominal pipe diameter is exactly the same as the **Outside Diameter (OD)** of the pipe (Peng & Peng, 2009). The OD is usually indicated in *inch* and it should be converted into *mm* if required.

The changes of direction of the pipe are made through several type of **Bends**. The **Radius** of curvature (**R**) of the bend is an important parameter and it should be well designed to comply with the applied stress, but also to assure correct flow of the product content. The most common bend is the so-called **long-radius elbow**, which has a bend radius equal to 1.5 times the nominal pipe diameter. Another type is the **short-radius elbow**, which has a bend radius equal to the nominal pipe diameter. An alternative is to make the curve directly by bending the pipe. To avoid excessive, the radius of this bends generally greater than three nominal diameter up to five diameters ($R = 3 \div 5 \text{ OD}$). All these different bends have different *wall thickness* requirements to be considered in the design and analysis (Peng & Peng, 2009). Another parameter, when considering the pipe to bent, is the **Tangent Length (TL)**: the manufacture of the “curved pipe” starts from the straight tube and the distance that I need to lever to bend it is just the *tangent length*. Generally **TL=OD**.

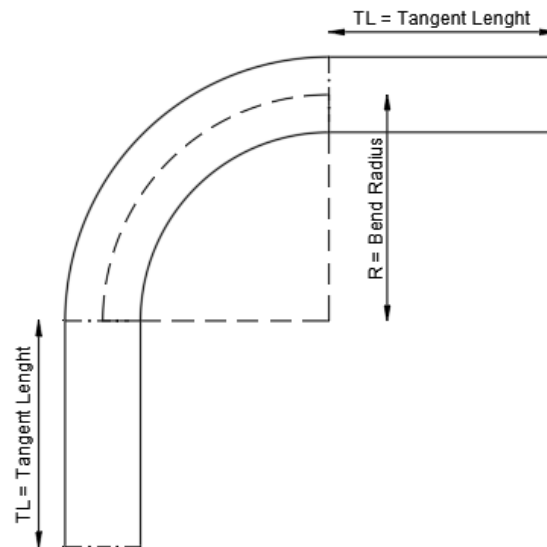


Figure 22 – Geometric characteristics of the pipe

The selection of the **Wall Thickness (WT)** is one of the most important and fundamental tasks in the design of subsea pipelines. While this task involves many technical aspects related to different design scenarios, primary design loads relevant to the containment of the wall thickness are as follows (Bai & Bai, 2014):

- Internal pressure loads.
- External hydrostatic pressure loads.
- Longitudinal functional loads.
- Bending loads.
- External impact loads.

The **Inner Diameter (ID)** is the nominal diameter (OD) less two times the wall thickness (and the eventual coating).

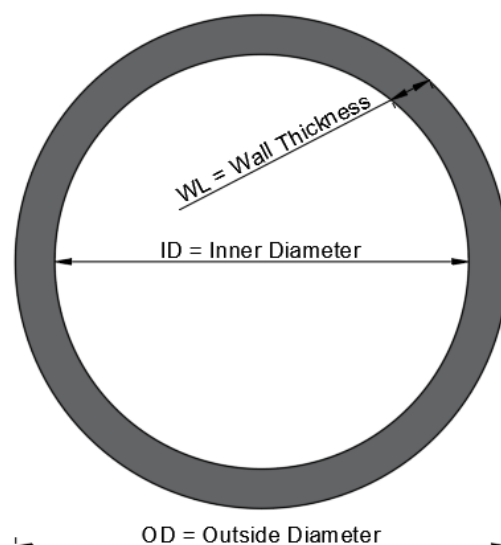


Figure 23 - Pipe Parameters

CHAPTER 3: *MULTIPHASE FLOW*

3.1. BACKGROUND

Transportation of hydrocarbon fluids through a pipeline and riser, in many cases will generate **multiphase flow**.

The adjective multiphase characterizes situations where several different phases such as liquids, gases, solids are flowing simultaneously. The boundaries between phases are called *interfaces*.

Due to the complexity of the multiphase flow, there are still many challenging theoretical problems that have not been solved so far, such as: *flow regime transition, flow instability, flow similarity, phase interaction* and so on.

One of the major difficulties in multiphase flow is that the phases are distributed in the pipe in particular ways; the various typical configurations are called **flow regimes**.

Since the beginning of multiphase flow research, a lot of research work has been performed and published. In particular, significant improvements and developments have been made for accurate descriptions and calculations of multiphase flow regimes in pipelines. There are various models for multiphase flow and are all based on the *conservation laws of mass, momentum and energy*. These models can be classified into three categories: *theoretical analysis* (based on different mathematical and physical principles); *experimental study*, to discover the physical phenomena and to calibrate the theoretical results (based on field observations and laboratory simulations); *numerical simulation* (solution of the three dimensional Navier-Stokes equations).

In the recent years the use of numerical methods such as **Computational Fluid Dynamics (CFD)**, has increased in the area of oil and gas field multiphase flow modeling, owing to the advent of powerful computers in combination with more efficient software tools. CFD has been used as a powerful tool for hydrodynamic prediction, design and optimization of several chemical engineering equipment: pipes and pipe bends, particulate flows, bubbly flows, etc. Very important phase of the analysis is an efficient and robust post-processing of the results, via graph, image, video, table and algebraic manipulations.

The basic parameters to describe a single-phase flow are *velocity, mass flow rate and volumetric flow rate*. Moreover, in multiphase flow are the *mass flow rate, volumetric fraction and velocity of each phase* are also the important parameters (Sun B. , 2016).

Understanding of fluid behavior and *flow regimes*, throughout an entire structure, is key to oil field production. To properly design offshore pipelines, it is critical to recognize the impacts of multiphase flow (Guo, Song, Chacko, & Ghalambor, 2005). All of the *flow assurance* issues, associated with offshore pipeline operations, are correlated to the multiphase flow.



Flow Assurance

Is the analysis of thermal, hydraulic and fluid-related threats to flow and product quality and their mitigation using appropriate equipment, chemicals and procedures.

Target of the **flow assurance** is to allow the transport in a safely and reliable way of the well fluids from the reservoir up to the treatment plants along the complete operating life of the production system and considering all the potential operating conditions (*steady state, transients and possibly emergency*).

The focus of this thesis is on *two-phase flow*, in particular on the *gas-liquid flow* in pipelines, with particular regards to the jumpers.

3.2. TWO-PHASE FLOW

The **two-phase flow** is much more complicated than a single-phase flow. Two-phase flow is a process involving the interaction of many variables. The gas and liquid phases normally do not travel at the same velocity in the pipeline, because of the differences in density and viscosities. For an upward flow, the gas phase, which is less dense and less viscous, tends to flow at a higher velocity than the liquid phase. For a downward flow, the liquid often flows faster than the gas because of density differences (Bai & Bai, 2012).

For a two-phase flow, most analyses and simulations solve mass, momentum, and energy balance equations based on one-dimensional behavior for each phase. Such equations are used as a framework in which to interpret experimental data. Reliable prediction of multiphase flow behavior generally requires use of data or experimental correlations. Two-fluid modeling is a developing technique made possible by improved computational methods (Bai & Bai, 2012).

The focus will be put on the **gas–liquid flow**, which is the most complex because the interfaces are deformable. This characteristic, coupled with the naturally occurring turbulence in gas–liquid flows, makes the study highly hard.

Some simplification is possible, by classifying the types of interfacial distributions under various headings, known as **flow regimes** or **flow patterns**.

Due to the differences in the physical properties between liquid and gas (mainly the density), several flow patterns can occur when gas and liquid flow simultaneously inside the pipeline. The flow regimes differ from each other by having different *gas-liquid interfaces*. The mechanisms of mass, momentum, and energy transfer between the phases are different in the different flow regimes. Despite many classifications are available in the literature, gas-liquid flow regimes can be divided into three main categories (SAIPEM Group, 2020):

1. **Dispersed**: one phase is distributed throughout another continuous phase. Within the dispersed flow pattern, many subcategories can be defined, e.g. **bubbly flow** where bubbles of gas of different size (generally small compared to the diameter of the tube) and shape are dispersed in a continuous liquid phase.
2. **Separated**: the phases are not mixed. Furthermore, the separated flow regime can be divided in many subcategories: **stratified flow**, where the light phase is flowing on top of the heavy fluid; **annular flow**, when the thin liquid layer flows along the inner wall of the tube (to create an annulus) and the central core of the flow consists of the gas phase.
3. **Intermittent**: it can be considered as the most complicated flow regime, in which the phases are not uniformly distributed throughout the pipe and the flow regime evolves with time and position. In a similar way to previous pattern the intermittent flow regime can be split in different types: **slug flow**, when a large volume of liquid

is followed by a bubble of gas; **churn flow**, characterized by the presence of a very thick and unstable liquid film, often oscillating up and down.

Thus, it is important to know the different flow regimes in both horizontal and vertical flows.

3.2.1. GAS-LIQUID FLOW REGIMES IN HORIZONTAL PIPE

In the horizontal, or near horizontal, pipe if the gas and liquid are flowing at a slow velocity the gas and liquid will completely separated from each other. Due to the gravity force, the gas will flow on top of the liquid and the gas-liquid interface is smooth. This flow regime is called **stratified smooth flow**.

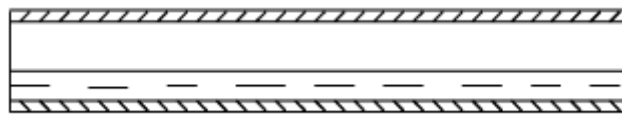


Figure 24 - Stratified Smooth Flow

When gas or liquid velocity increases, some waves will be generated at the gas liquid interface. The gas liquid interface becomes wavy and rougher. This flow is called **stratified wavy flow**.

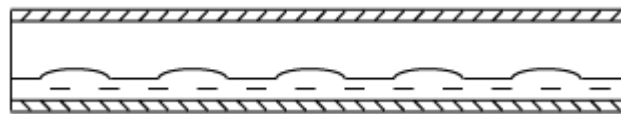


Figure 25 - Stratified Wavy Flow

As the flow velocity continues to increase, the waves at the interface continue to grow and probably some will be large enough to touch the top of the pipe to create a *liquid slugs*. This flow is called **slug flow**. In slug flow, liquid slug is followed by a gas zone, named *gas pocket*, containing a stratified liquid layer flowing at the bottom of the pipe, while the liquid slugs may be aerated by small gas bubbles.

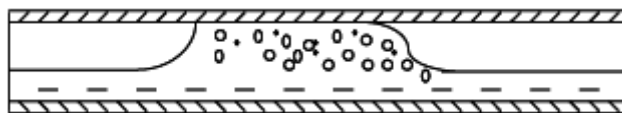


Figure 26 - Slug Flow

If the gas velocity further increases, the gas will flow as a core in the centre of the pipe and the liquid will flow as a ring around the pipe wall: **annular flow**. The liquid ring may not be uniform along the entire circumference, but is thicker at the bottom of the pipe than at the top. Some small liquid droplets may be contained in the gas core. In the annular flow regimes, the liquid in the pipe flows as a film around the wall of the pipe and it is often observed under high gas flow velocity.

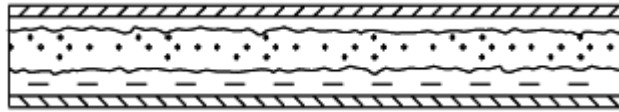


Figure 27 - Annular Flow

Finally if the liquid content is very high, compared to the gas content, the gas can become dispersed in the liquid as bubbles which are not uniform in size and most of the bubbles are in the upper portion of the pipe due to the buoyancy effects: **dispersed bubble flow**. With very low gas flow and high liquid flow, the gas will flow as discrete bubbles within a continuous liquid phase.

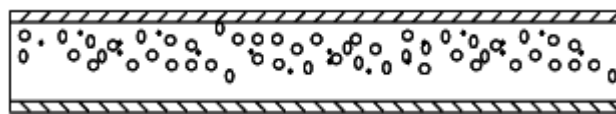


Figure 28 - Dispersed Bubble Flow

Flow regimes for two-phase flow through a horizontal pipe are summarized as follows:

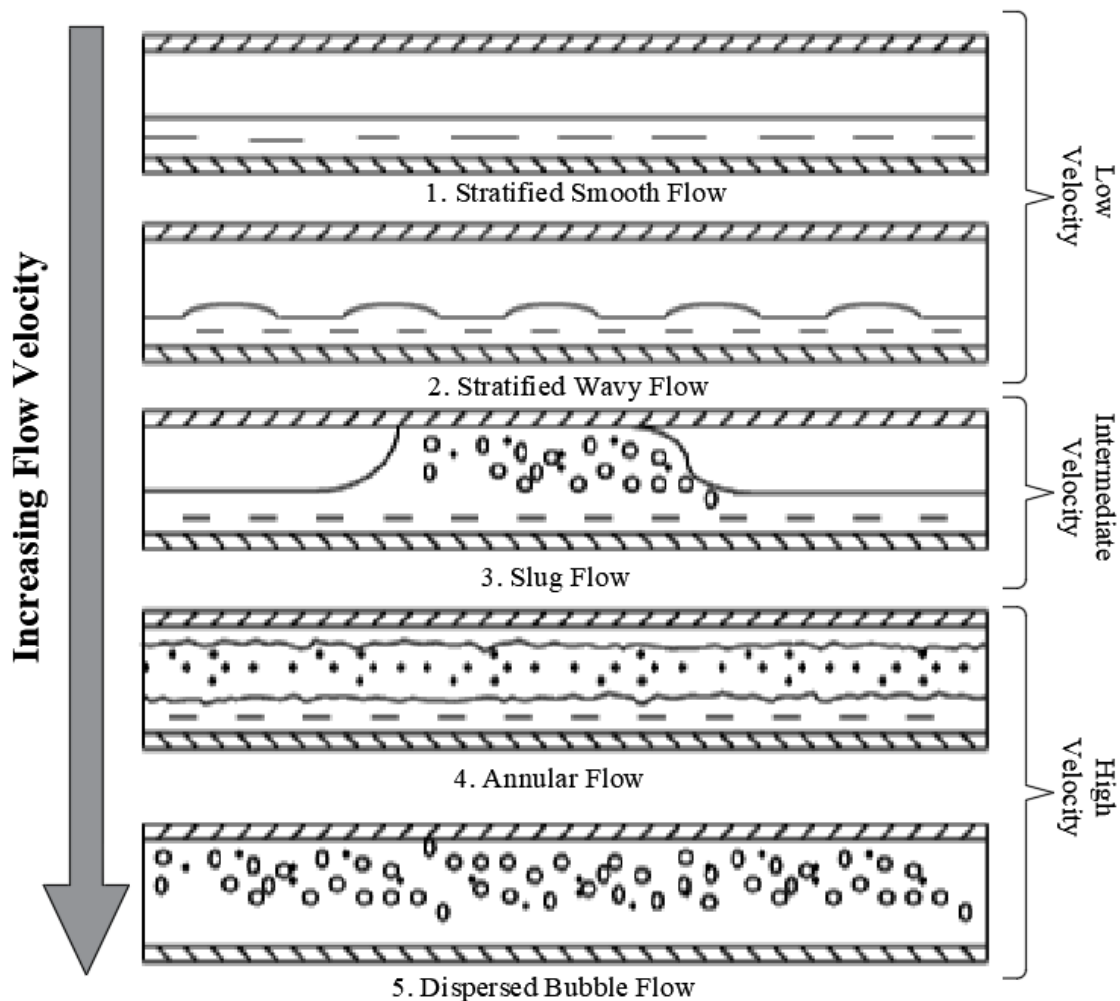


Figure 29 - Gas-liquid flow regimes in horizontal pipe

3.2.2. GAS-LIQUID FLOW REGIMES IN VERTICAL PIPE

The flow regimes identified in vertical pipelines are often rather different from that in the horizontal pipelines. Two-phase flow in a vertical pipe tends to be more symmetric, since gravity acts equally through the cross section although the gravitational force plays a more dominant role in vertical pipes.

When the gas flowrate is very low, the gas tends to flow as discrete bubbles in a continuous liquid phase: **bubble flow**. The bubbles are randomly dispersed as small bubbles of various sizes in the fluid flowing upwards.

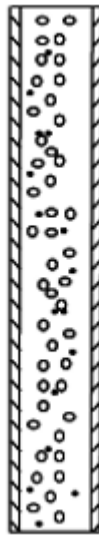


Figure 30 - Bubble Flow

As the gas velocity increases, the bubbles will keep growing in size. When bubble concentration increases, the larger and faster bubbles capture the smaller bubbles becoming even larger. The bubbles, with a “bullet” shape, have the same inner diameter of the pipe: **Taylor bubbles**; the flow regime will transit to the **slug flow**. The Taylor bubble, also named as *gas pocket*, is usually separated by *liquid slug*, which often contain some small gas bubbles. Because the density of the gas is small, the pressure drop across the gas bubble is not enough to support the liquid film surrounding the gas bubble and the liquid film falls down. The falling liquid film is caught up by the liquid slugs, which separate successive Taylor bubbles (Guo, Song, Chacko, & Ghalambor, 2005).

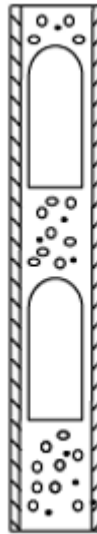


Figure 31 - Slug Flow

In slug flow, the fraction of an element of pipe, which is occupied by liquid at same instant, *the liquid holdup*, along the pipe axis is not uniform, but intermittent. If the flowrate increases, the slug flow will become unstable and leads to **churn flow** it is formed by the breakdown of the Taylor bubbles in slug flow and is very similar to slug flow, but more chaotic. At the same time, the liquid slugs between Taylor bubbles are penetrated by gas bubbles and start to fall downward.

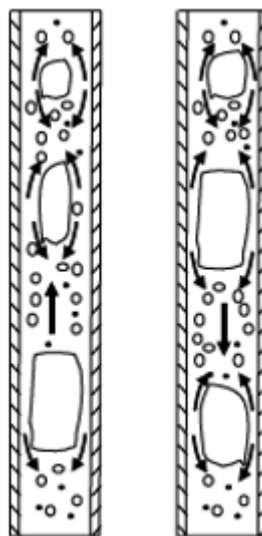


Figure 32 - Churn Flow

As the liquid falls down, the liquid forms a bridge at a lower position and then is lifted again by the gas. This sequence repeats itself as fluids flow upward. Thus, in churn flow, the liquid slugs have oscillatory motions (Guo, Song, Chacko, & Ghalambor, 2005). When the gas flowrate become very high, the gas will flow as a core in the centre of the pipe

(some liquid droplets) and liquid will flow as a film along the pipe's inner wall: it is the **annular flow**.



Figure 33 - Annular Flow

Engineering applications uses simplified methods to predict flow regimes inside the pipeline. Thus, flow regime maps were developed to define the various flow regimes and their transitions. These flow maps are based upon either experimental data or mechanical models. A lot of work is available in literature to generalize flow map, in order to make them applicable to a wide range of pipeline diameters and fluid characteristics.

A much more widely used flow regime map, for horizontal and vertical gas liquid two-phase flow, was developed by Taitel and Dukler (1976). The flow map plots the superficial gas velocity against the superficial liquid velocity and shows the prevailing regime. The superficial velocities are the gas (U_{sg}) or liquid (U_{sl}) flow rates divided by the pipe cross-sectional area.

3.2.3. BASIC FLOW PARAMETERS

Superficial velocity: the superficial velocity of liquid or gas is defined as the ratio of the liquid or gas volumetric flowrate to the total pipeline cross-sectional area.

$$U_{sl} = \frac{Q_l}{A}$$
$$U_{sg} = \frac{Q_g}{A}$$

Where:

- U_{sl} = liquid superficial velocity;
- U_{sg} = gas superficial velocity;
- Q_l = liquid volumetric flowrate;
- Q_g = gas volumetric flowrate;
- A = pipeline flow cross-sectional area.

Mixture velocity: the fluid mixture velocity is defined as the sum of the superficial gas and liquid velocities (U_m).

$$U_m = Q_{sl} + Q_{sg} = \frac{Q_l + Q_g}{A}$$

Liquid holdup: liquid holdup is defined as the ratio of the liquid volume in a pipeline segment to the whole volume of the pipeline segment. It's a function of both space and time.

$$H_l = \frac{V_l}{V}$$

Where:

- H_l = liquid holdup;
- V_l = pipeline segment volume occupied by liquid;
- V = whole pipeline segment volume.

Mixture density: The density of gas and liquid homogeneous mixture is expressed as:

$$\rho_m = \rho_l H_l + \rho_g (1 - H_l)$$

Where:

- ρ_m = gas-liquid mixture density;
- ρ_g = gas density;
- ρ_l = liquid density.

(Guo, Song, Chacko, & Ghalambor, 2005)

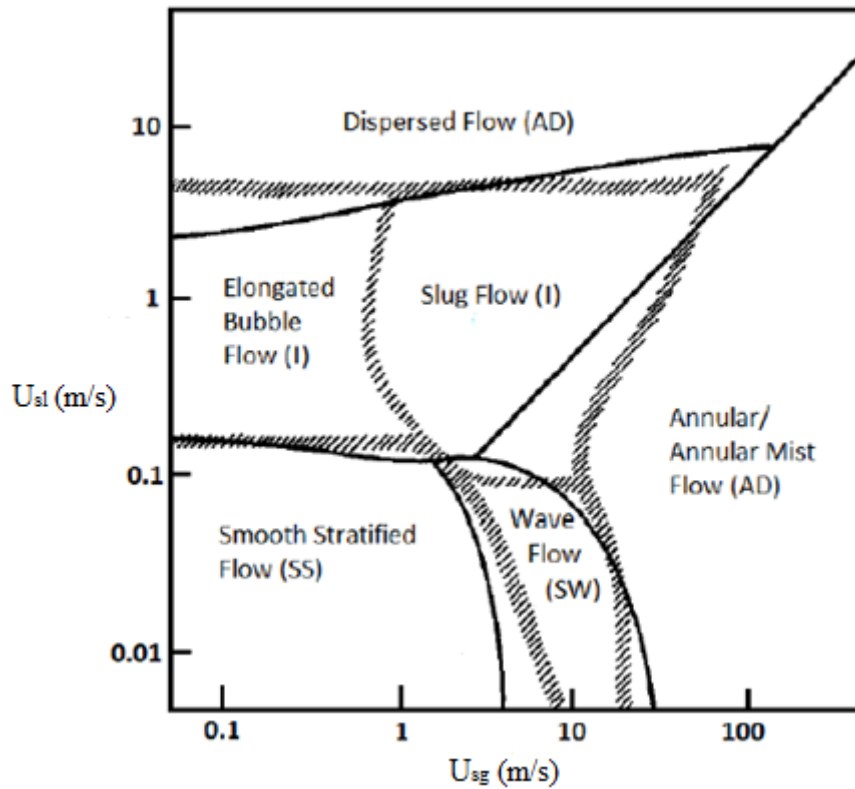


Figure 34 - Generalized flow map for multiphase flow in a horizontal pipe (Taitel, Barnea, & Duckler, 1980)

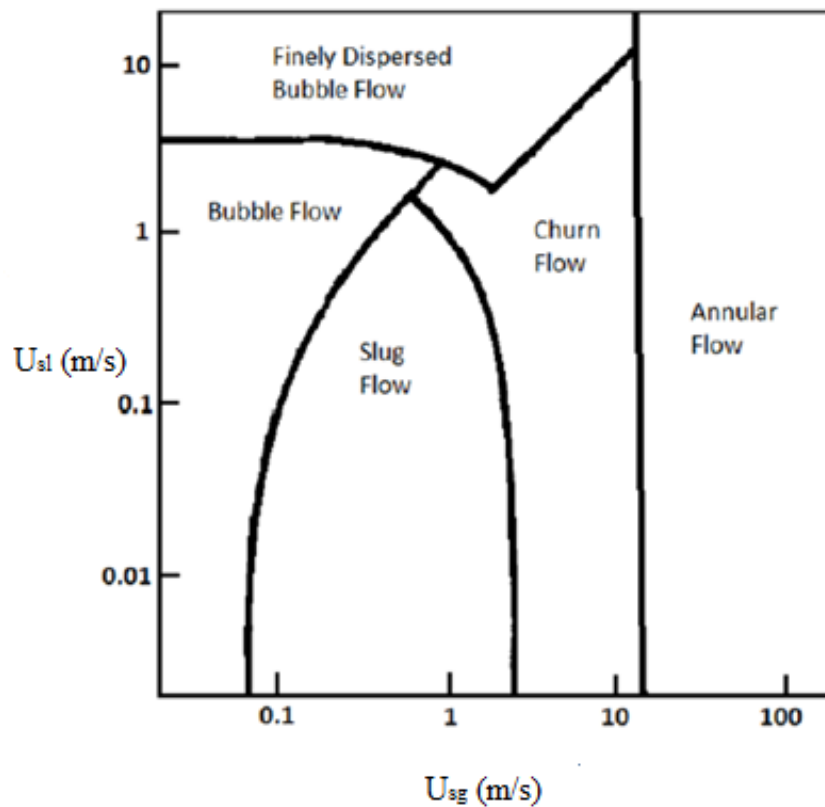


Figure 35 - Generalized flow map for multiphase flow in a vertical pipe (Taitel, Barnea, & Duckler, 1980)

3.3. SLUG FLOW

Slug flow is an intermittent flow, characterised by an alternating flow of liquid slugs and gas pockets (cf. 3.2.1-2). This is one of the most undesired multiphase flow regimes, due to the associated instability, which imposes a major challenge to *flow assurance* in the oil and gas industry. The oil and gas industry encounters slug flow in the course of their production activities both in horizontal and vertical pipe. The likelihood of slug flow is both a function of the incoming fluid as well as the pipeline layout. The potential for slug flow should be assessed at an early stage of flowline design. Where slug flow is expected, *flow assurance* studies should include careful evaluation of slug parameters for use in flowline mechanical design. *Slug frequency*, *slug length* (L_L), *bubble or pocket length* (L_P), *slug density* (ρ_L) and *bubble or pocket density* (ρ_P) should be carefully estimated for the range of hydraulic conditions expected during the life of the field.

Slug flow can cause large pressure and liquid flowrate fluctuations inducing significant *mechanical loads* for subsea structures (jumper, riser). Thus, this intermittent flow can have an impact on production, on receiving equipment, on control systems and can be induced *dynamic mechanical loads*. Slug flow is causing time varying stresses in pipes, connectors and supports and consequently causes structural fatigue damage and failure: at each change in direction of flow, a resultant force must be resisted by the piping or pipe support systems. Unrestrained piping bends, elbows and tees are subject to *deformations*, *cyclic stress* and *fatigue* resulting from the dynamic fluid forces associated with slug flow.

This flow regime can generate rapid *variations* of the *mass distribution* and *pressure perturbations* along the pipe, which may induce large vibrations (FIV). Transient stresses due to these vibrations consequently cause fatigue failure, local buckling or even excessive bending and breaking. These fluctuated stresses in the pipelines can strongly disturb the normal operation, accelerating pipeline corrosion and causing severe damage in the pipe wall (Mohammed A. O., Al-Kayyem, Nasif, & Timec, 2019). Pressure variation, resulting from slug passing, can be either a source of high stress, a source of resonance by lock-in of a mechanical mode with a fluid excitation frequency. Such FIV phenomenon should be consequently accounted for in the engineering design process (Bakkouch & Minguez, 2013).

Over the past decades, a great deal of work has been done to develop numerical tools capable of identifying this complex multiphase flow: **OLGA**, **LEDAFLOW**, **PIPESIM**, etc. Despite these solvers are *one dimensional* (1-D), they are capable to reproduce with a good level of accuracy the involved physics.

A more general approach is to perform a **Fluid Structure Interaction (FSI)** analysis. In this case, it appears fundamental to recover at the best the main flow features in characteristic piping systems. Furthermore, the numerical solver must be able to recover the *occurrence of the slug*, the *passing frequency* and the *resulting pressure variation*. To complement a *dimensional analysis* of the multiphase flow, the **Computational Fluid Dynamics (CFD)** can be

used in engineering studies. Among the most used CFD software there are: FLUENT (ANSYS) and CFX (ANSYS).

3.3.1. SLUG FLOW MECHANISMS

In oil field industry, several operating conditions generate liquid slugs flow in pipelines. Some of these mechanisms can be identified as follows (Ragab, 2008):

- **Flowrate changes:** if a pipeline, operating in stratified flow, is subject to an increase in gas flow rate or to total production rate, one or more slugs may be produced when the equilibrium level drops towards a new state condition. Therefore, slugs may be produced as a result of *transient* effects along the pipeline.
- **Start up and blow-down operations:** when a pipeline is *shut down*, the liquid will drain to the low points in the line, and when the line is restarted, this liquid may exit the pipeline in the form of slugs. Slugs may also form during *depressurization* due to high gas velocities, and so transient simulations can be used to estimate both of these types of slugs.
- **Pigging operations:** when “pigs” are run through pipelines. Pigging produces the largest amount of slugs.
- **Terrain induced:** slugs caused by significant elevation changes along the pipeline, such as topographic features or vertical risers. They are system specific and more difficult to model than the other types of slugging.

Pig

Device designed to inspect pipelines from inside: structural integrity, inventory control, maintenance, data logging, cleaning, de-waxing.

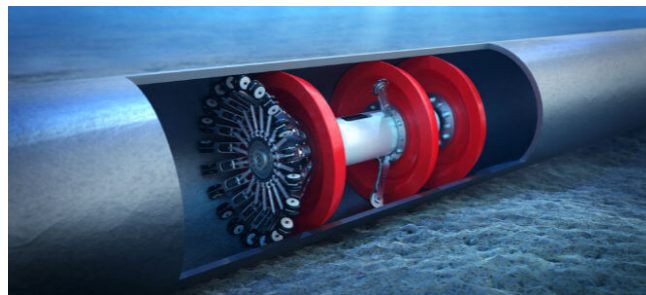


Figure 36 - Pigging Operation

3.3.2. CLASSIFICATION OF SLUG FLOW

There are different types of slugs, according to the formation mechanism:

1. **Terrain slugging:** is caused by the elevations in the pipeline, which follows the ground elevation or the seabed. Liquid can accumulate at a low point of the pipeline until sufficient pressure builds up behind it. Once the liquid is pushed out of the low point, it can form a slug.
2. **Hydrodynamic slugging:** is caused by gas flowing at a fast rate over a slower flowing liquid phase. This is associated with undesirable flowline geometry and bathymetry. Hydrodynamic slugging occurs at moderate gas and liquid flow rates, over a wide range of flow conditions. The gas will form waves on the liquid surface, which may grow to bridge the whole cross-section of the line (fig. 33). This creates a blockage on the gas flow, which travels as a slug through the line. An accepted mechanism for this wave growth is the **Kelvin-Helmholtz instability**. The gas at a higher velocity than the liquid mainly pushes the slug.

Hydrodynamic slugging can produce high frequency loading cycles that cause challenges for the fatigue design of *risers*, *pipelines* and *spools*. Hydrodynamic slugs are initiated by the slow growth of small perturbations at the liquid-gas interface due to hydrodynamic instability of the flow under conditions at a given location in a structure at a given instant in time. The slugs produced by such a process are initially relatively short but, depending on topography and pipe configuration, can grow.

3. **Operation induced slugging:** is due to certain operations performed during production. The following operations can generate a huge number of liquid slugs: ramp-up (increasing production) and turn-down; pigging, where the pig is designed to push all or most of the liquid content of the pipeline to the outlet (this operation intentionally creates a liquid slug); depressurisation.
4. **Severe slugging:** also known as 'riser-based', it is caused by liquid accumulation at the bottom of the riser until sufficient pressure is generated behind it to push the liquids over the top of the riser. Behind this slug of liquid, follows a slug of gas, until sufficient liquids have accumulated at the bottom to form a new liquid slug. This type of slug flow is caused by the undulations and dips in the pipeline geometry, topography and network.

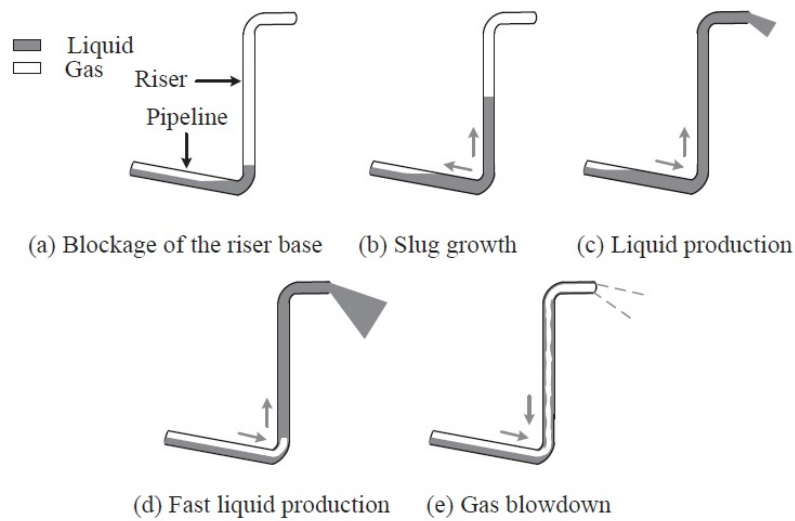


Figure 37 - Example of Severe Slugging

To conclude, “steady state” slug flow can be classified as either hydrodynamic slugging or terrain induced slugging governed by the site-specific elevation profile of the flowline. Severe slug flow is typically related to the latter condition.

“Transient slug conditions can in addition occur during start-up, operational changes of flowrate and pigging operations. Slug volumes seen during pigging are usually the largest slug volumes seen during normal operation” (DNV-OS-F201, 2010).

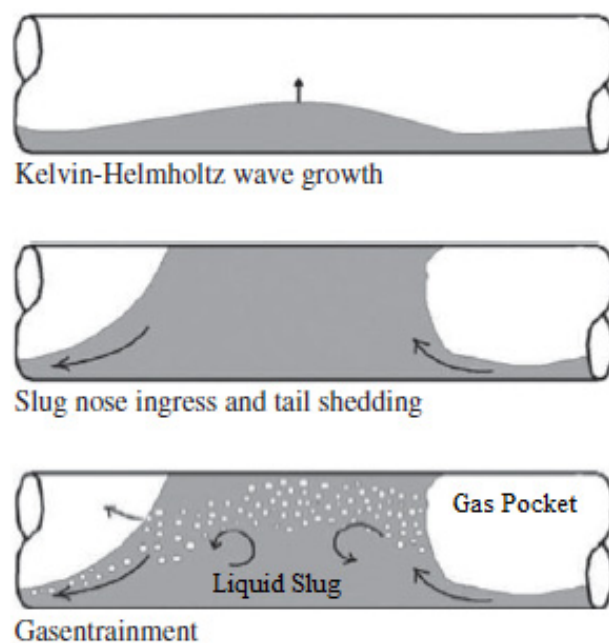


Figure 38 - Example of Hydrodynamic Slug Initiation

Initiation of hydrodynamic slug: hydrodynamic slug flow depends mainly on fluid properties and flowrates, pipe diameter and inclination. Once slug flow exists at a given location of the pipe, a hydrodynamic slug may also initiate at an adjacent section.

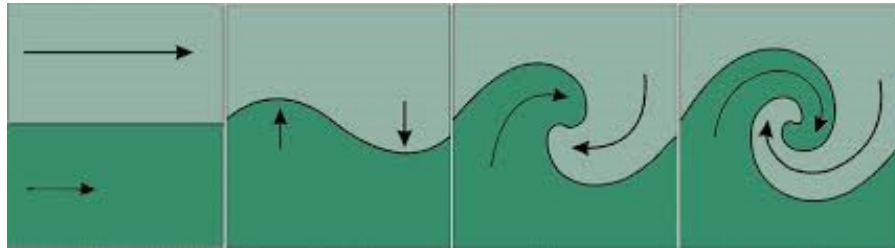


Figure 39 - Kelvin Helmholtz Instability

Initially, the gas-liquid interface is lifted to the top of the pipe when the velocity difference between gas phase and liquid phase is high enough. This wave growth is triggered by the *Kelvin-Helmholtz instability*. Once the wave reaches the top of pipe, it forms a slug. The slug is pushed by the gas and so travels at a greater velocity than the liquid film, and more liquid is then swept into the slug. A main part of the frictional pressure drop in multiphase flow is thought to be due to the turbulent region within the slug. Thus, the size of the turbulent region can have a significant effect on the frictional pressure losses in a pipeline.

3.3.3. SLUG MITIGATION AND CATCH

To ensure a stable production and transportation operations, methods for slug mitigation is required:

- **Change operating process conditions.**
- **Slug catcher:** is a “container” located at the outlet of the pipeline just before the processing equipment. It should have a sufficient buffer volume to store the largest slugs expected from the upstream system. The buffered liquids can be drained to the processing equipment at a much slower rate to prevent overloading the system. *Slug catchers* are designed in different forms: *vessel type*, *finger type* and *parking loop*. *Vessel type* is the most conventional vessel, simple in design and maintenance.

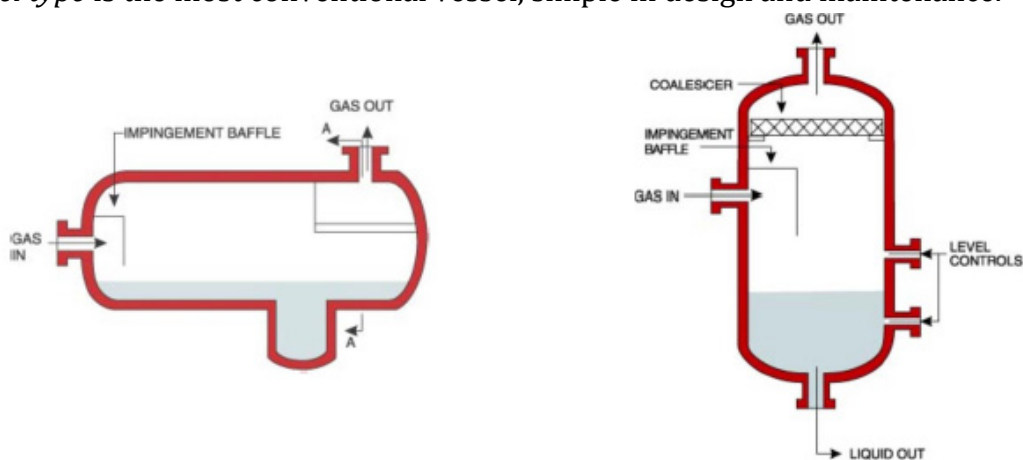


Figure 40 - Vessel Type

Finger type consists of several long pieces of pipe ('fingers'), which together form the buffer volume. The advantage of this type of slug catcher is that pipe segments are simpler to design than a large vessel, for high pressures often encountered in pipeline systems. A disadvantage is that its footprint can become excessively large.



Figure 41 - Finger Type

Parking loop combines features of the vessel and finger types. The gas-liquid separation occurs in the vessel, while the liquid is stored in the parking loop-shaped fingers.

- **Choking:** this method has shown to be effective for severe slug mitigation. Choking helps eliminate riser slugging by increasing the pressure drop across slugs. It changes the slug flow to bubble flow regimes. The choke has been found to eliminate severe slugging by increasing the back pressure proportionally to the velocity increase at the choke. If the acceleration of the gas front up the riser is stabilized before reaching the choke, steady flow will eventually occur.
- **Gas injection:** is based on injection of some gas at the bottom of the riser. The primary benefit of gas injection is to reduce the hydrostatic head in the riser and thus, reduce the pipeline pressure. The injected gas also tends to carry the liquid and, thus, keep the liquid moving up the riser. When sufficient gas is injected the liquid will be continuously lifted and a steady flow will occur. Gas injection plays on decreasing the slug length. One of its drawbacks is increasing compression cost. The drawback of gas lift is the large gas volumes needed to obtain a satisfactory stability of the flow in the riser.

3.3.4. PREDICTION OF SLUG FLOW

Due to the number of parameters that can affect the flow regime in a pipe, prediction for multiphase flows represents a very complex problem and poses a significant challenge for current mathematical methods. **Theoretical analysis, experimental measurements, and numerical simulations** have been undertaken over the years to characterize slug parameters such as *slug frequency, slug translational velocity, slug body holdup* and *slug length*.

The main macroscopic models for multiphase flow are: the *homogeneous flow model* and the *separated flow model*. These models are all based on the conservation laws of mass, momentum and energy.

Homogeneous flow model: assumes that the multiphase mixture behaves much like a *homogeneous single-phase fluid*, with property values that are some kind of average of the constituent phases. Once one decides which kind of averaging procedure to use, the computation procedure is that of a single-phase system. Note that, the assumption of homogeneity pre-supposes a condition of no slip, that is, that all phases move with the same velocity. Consequently, in-situ liquid fraction or liquid holdup is the same as the input fraction.

Separated flow model: recognizes that the phases are segregated or separated and that they *move with different velocities*. Hence, the slip between the phases requires to be known in addition to the frictional interaction of the phases with the wall and among themselves. In the simple versions of the separated flow model, the *frictional interactions* among the phases *are ignored*. Consequently, even for the simplest model in this category, empirical correlations for computing liquid holdup and wall shear are needed, unlike the homogeneous model, where only wall shear is required.

However, as regards the numerical analysis, there are several modelling tools that can be used to simulate oil-water-gas multiphase flow and to predict the likelihood of slug flow in

a pipeline and riser under operating conditions.

The slugging prediction can be carried out using 1-D tools like a *PIPESIM* (Schlumberger), *OLGA* (Scandpower Petroleum Technology), *LedaFlow* (Kongsberg) etc. or using 3-D general purpose tools, like *CFD*.

PIPESIM: steady-state multiphase simulation software can predict hydrodynamic slug distributions along the flowline and riser.

OLGA: is a thermo-hydraulic 1-D flow simulator that is considered a market leader in modelling multiphase flow and predicting and characterizing slug flow. *OLGA* is verified against large scale experimental as well as field data as part of a research and development program known as the “*OLGA Validation and Improvement Program*” (OVIP). Due to its facility for tracking individual slugs, *OLGA* is widely used as a multiphase simulator tool for predicting and characterizing slug flow.

LedaFlow: is a fully transient multiphase flow simulator for single, two-phase and three-phase flow. It is based on a representation of multiphase physics from large-scale experiments and field data and uses the equations for mass flow (describing the continuous and dispersed phases), while enthalpy and energy equations are solved for the continuous phases only. The basic *LedaFlow* concept is based upon capturing small scale dynamics by refinement of grid size. By using a scale which is comparable to the pipe diameter, individual slug and wave dynamics may be captured numerically on a small grid.

CFD: uses full 3D methodology to simulate slug flow. The fluid domain is discretized into a large number of cells. For each cell, the Navier-Stokes and the conservation equations are used to characterize the flow. The interactions between the different fluid phases are simulated explicitly. The results from CFD simulations are generally considered to give a more refined prediction of localized slug flow, but are limited by the significantly longer computing times compared to 1-D simulators. It is not considered realistic with the current technology to use CFD to simulate slug flow for multiple load cases through long lengths of pipe over large time intervals! CFD is used for the simulation of short sections of pipe where detailed analysis of localized slug flow conditions is required.

3.3.5. SLUG FLOW PARAMETERS

Due to the several mechanisms involved in the slug flow, it is a complex matter to characterize the phenomenon. The slug flow is idealized by means of the so-called **Slug Unit** (Figure 42).

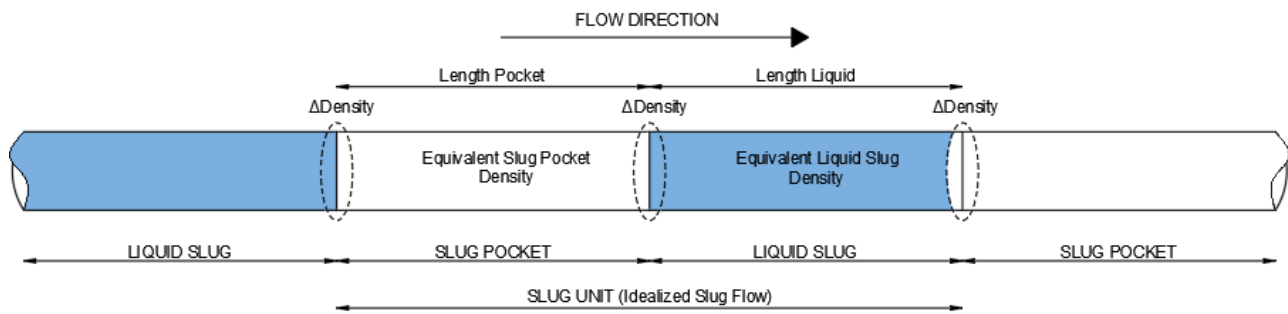


Figure 42 - Representation of SLUG UNIT

The parameters required to define slug flow are as follows:

- **Slug Unit: Slug Pocket + Liquid Slug**
- **Slug Pocket:** part of the slug unit occupied by gas.
- **Liquid Slug:** part of the slug unit occupied by liquid.
- **Liquid Slug Length:** is the length of the liquid slug body for a slug unit (L_L).
- **Slug Pocket Length:** is the length of the slug pocket body for a slug unit (L_P).
- **Equivalent Density of Liquid Slug (ρ_L).**
- **Equivalent Density of Slug Pocket (ρ_P).**
- **Representative slug unit velocity (v_{slug}):** is the velocity at which the slug unit will be assumed to travel along the model and typically it is the velocity used to calculate all global slug induced loading, unless specified otherwise. It needs to be defined by flow assurance engineers.
- **Frequency:** is the number of slug units travelling a section of the pipe over a unit of time. The slug frequency changes depending on the nature of the flow and the pipe inclination, whether turbulent flow is developed or not.
- **Occurrence data and time history data.**

3.3.6. SLUG FLOW INPUT DATA

It is important to define the loads arising from the slug flow along the jumper. To calculate these loads it is necessary to have specific input data, which depend mainly on the layout of the field, the length of the jumpers and flowlines. With *flow assurance* software [see § 3.3.4], it is possible to estimate the slug parameters for each particular jumper and for the entire field lifetime. For the structural response assessments of a relatively short configurations (spools, jumpers) the most frequent strategy adopted is the “**Specific Point Strategy**” (see *Box* below).

Slug Flow Data Extraction (SAIPEM Group, 2020)

Slug flow prediction tools using one of two strategies:

Complete System Strategy: consider the total number of slugs in a system at any one time or a series of time increments.

Specific Point Strategy: generating a time-history of slug units at entry to a jumper. The focus is on predicting slug flow over time at a specific point in the system.

A typical approach is the “**Time History Approach**” and the data format can be given as follows:

Slug Unit No.	Entry time (s)	Liquid Slug		Slug Pocket		Slug Unit Velocity (m/s)
		Lenght (m)	Equivalent Density (kg/mc)	Lenght (m)	Equivalent Density (kg/mc)	
1	0	120	950	200	210	10
2	100	80	825	150	225	8
--	--	--	--	--	--	--
--	--	--	--	--	--	--
--	--	--	--	--	--	--
--	--	--	--	--	--	--

Table 2 - Data Format (Time History Approach)

With this approach, a tabulated series of slug units is prepared, defined by their length, equivalent density, *representative slug unit velocity* and a time stamp. Time stamp is usually associated with the time at which each liquid slug front appears at a specific point in the jumper system. Data can also be provided between entry time stamps, to describe the evolution of slug units in this period (SAIPEM Group, 2020).

Once the input data are known, they must be converted into a format appropriate for the **structural response analysis** program so that the loads and stress cycles on the jumper, due to slugging, can be calculated.

CHAPTER 4: STRUCTURAL RESPONSE ANALYSIS

4.1. LOADS DUE TO SLUG FLOW

The passage of slug flow through risers, pipelines, **jumpers** and **spools** causes a *time dependent variation in structural loads* that significantly affect the components design.

The main structural loads can be identified as follows:

4.1.1. GRAVITATIONAL LOADS

Gravitational loads are due to the mass of the internal pipeline content. In particular, the presence of gas pockets and liquid slugs generates weight variations inside the pipe and therefore different gravitational loads. The *weight variations* due to the passing of the slug though the jumper is easily modelled as a *time-dependent distributed gravity load* on the horizontal sections of the jumper.

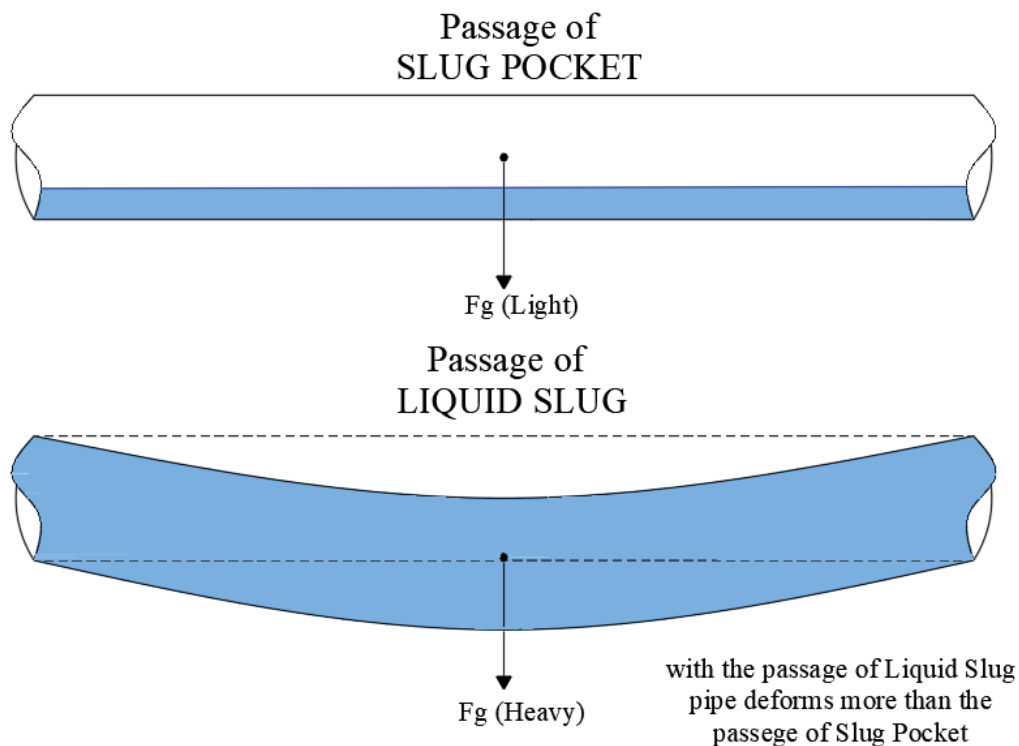


Figure 43 - Gravitational Effects

4.1.2. CENTRIFUGAL FORCE

Internal fluid flowing through a curved pipe induces a centrifugal force on the bend. When the flow passes a turning bend, it imposes an *impact-type force* to the bend due to a change in the flow direction, and thus a change in momentum. It also exerts a force on the bend upon leaving it (Peng & Peng, 2009).

This type of load will deform the jumper and keep it in that position until all the slug has passed the curve. However, the first passage certainly induces a transitory vibration. In similar manner, once the slug exits the bend the load decreases, so that the jumper will vibrate until it returns in the un-deformed configuration.

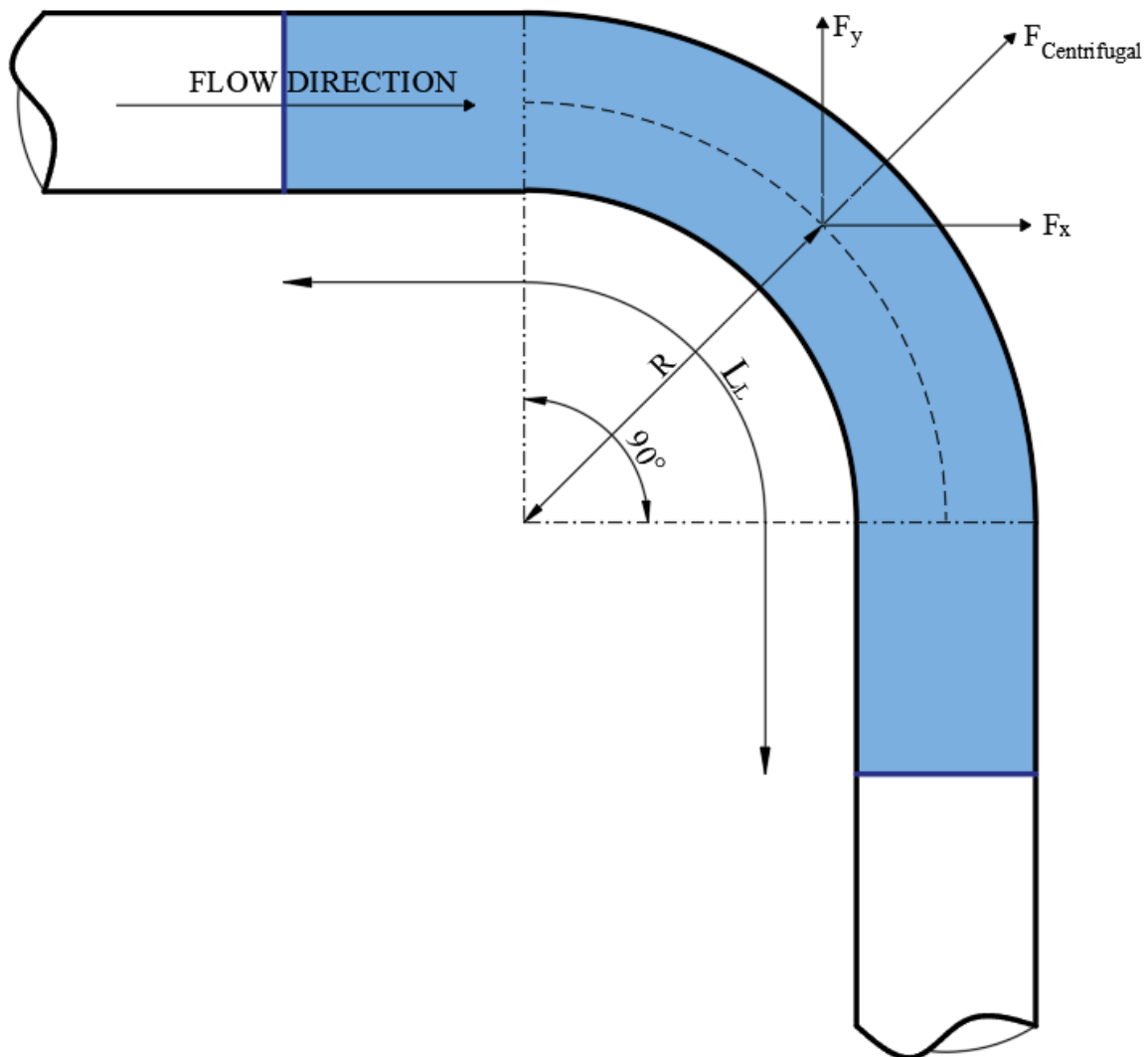


Figure 44 - Centrifugal Force

The orthogonal components of the total force change can also be expressed as [see Appendix B]:

$$F_{slug} = F_{centrifugal} = \rho_{slug} A v_{slug}^2$$

$$F_x = \rho_{slug} A v_{slug}^2 (1 - \cos\theta)$$

$$F_y = \rho_{slug} A v_{slug}^2 (\sin\theta)$$

For the **static** load case condition, the centrifugal force can be gathered in a global force, applied at the centre of the bend (Figure 44).

The **time-dependent force**, exerted for flowing fluid on the jumper bends, is shown in Figure 45. , with a typical trapezoidal path in time.

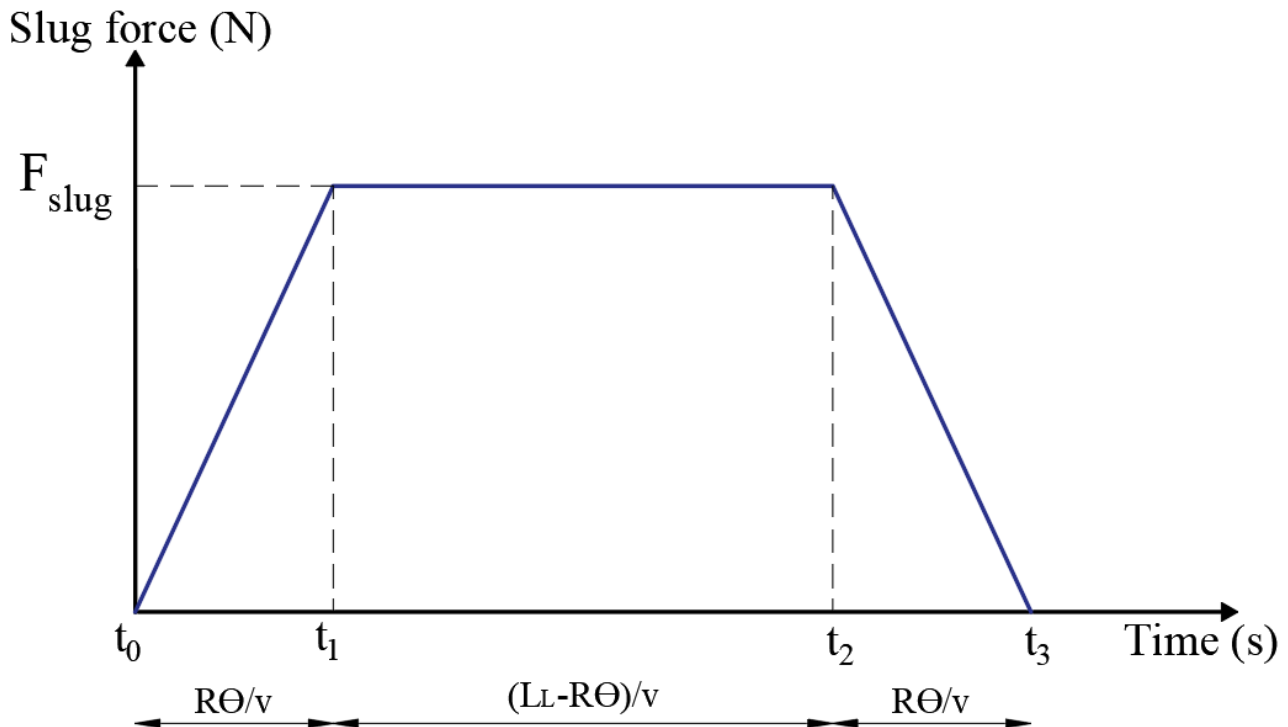


Figure 45 - Bend Impact Force history due to Slug Flow

Where:

- t_0 = time when the front of liquid slug enters the bend;
- t_1 = time when all the liquid slug occupies the bend length ($R\theta$);
- t_2 = time when the tail of liquid slug reaches the start of the bend;
- t_3 = time when the liquid slug exits the bend;
- R = bend radius;
- v or v_{slug} = representative slug unit velocity;
- L_L = liquid slug length;
- θ = bend angle;
- $F_{slug} = \rho_{slug} A v_{slug}^2$. Maximum slug force.

$R\theta/v$ is the time for the liquid slug to occupy the whole bend. At time t_1 , $F(t)$ exactly holds F_{slug} , i.e. the maximum force. $(L_L - R\theta)/v$ is the time for the *tail* of the liquid slug to reach the start of the bend. When the tail reaches the start of the bend, the force starts to ramp down. The tail then takes a time of $R\theta/v$ to pass around the bend (Figure 46).

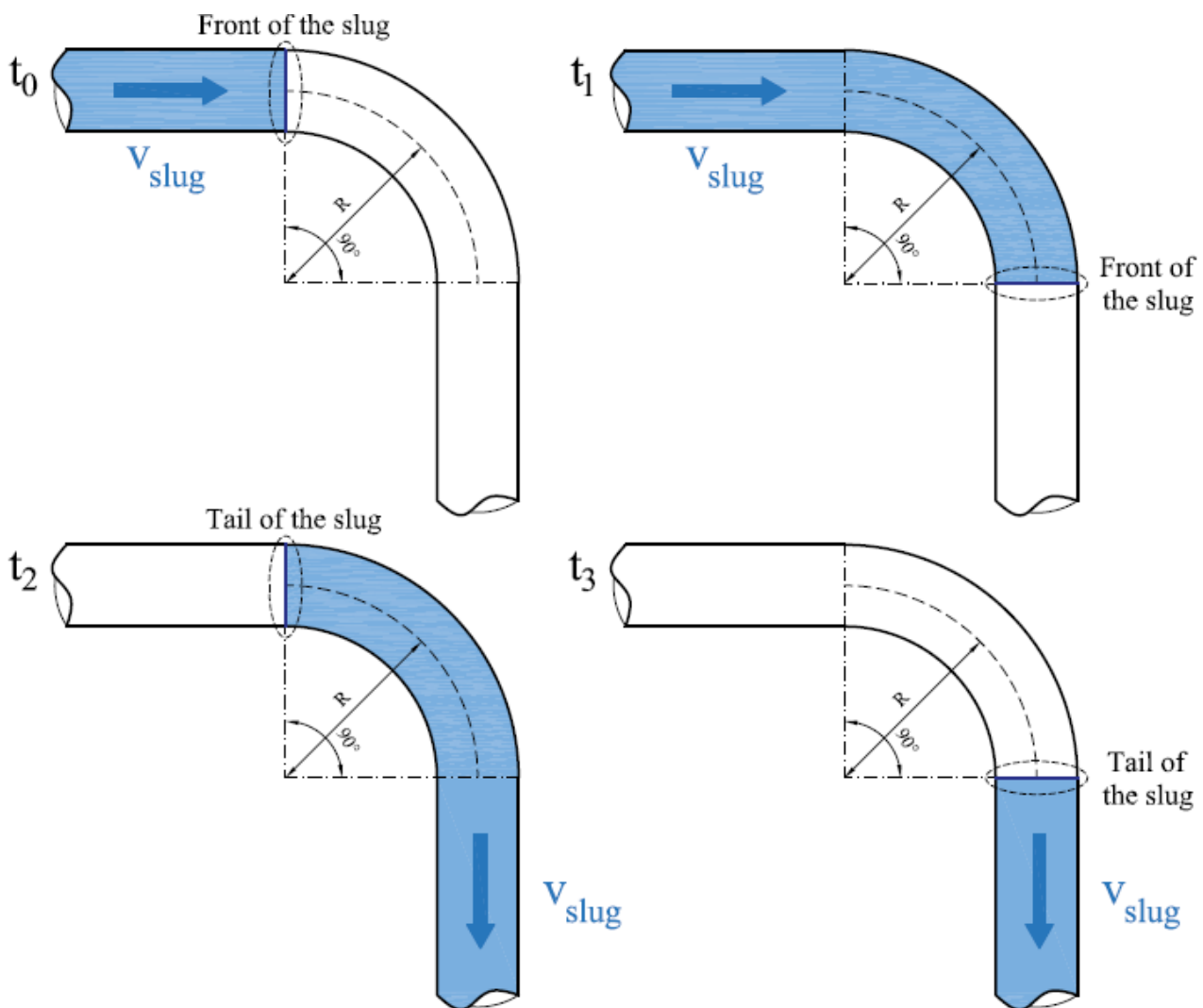


Figure 46 - Position of liquid slug with time

While these forces can be considered as constant, when the liquid slug flowing in the pipe has a constant density and velocity, in reality there is a *time-dependent variation* in most field layout.

In this thesis, the passage of the slug is simulated by assigning (on each node) simply a **time-dependent force**. However, this action is actually caused by a traveling **variable mass**. We neglect the influence of the moving mass (**forces without mass hypothesis**), even if it would expect that the *response* of the structure could be *significantly influenced by the variable mass, in time and space*.

In addition, in flowing **pocket** and **vertically orientated bends**, these impact forces can fluctuate and the time-history is very difficult to predict due to changing equivalent density and phase velocities.

In case of vertically orientated bends, it is necessary to take into account the periodic "fall-out" of part of the liquid phase:

- It generates a variation of the average velocity;
- Force is variable.

Hypothesis:
 $L_L < L_{bend}$

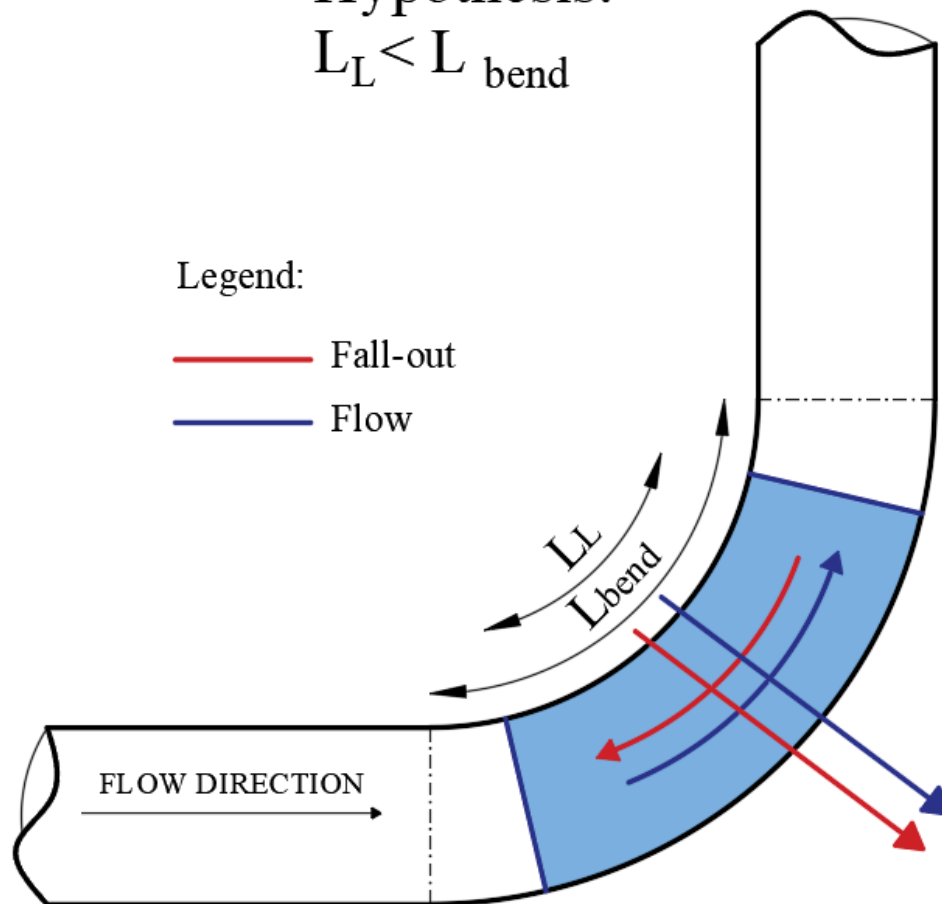
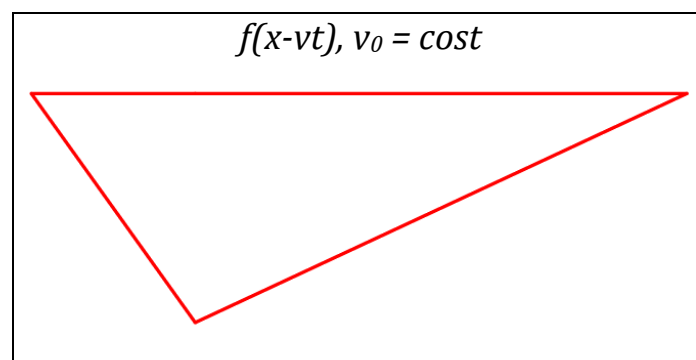


Figure 47 - Bend impact forces

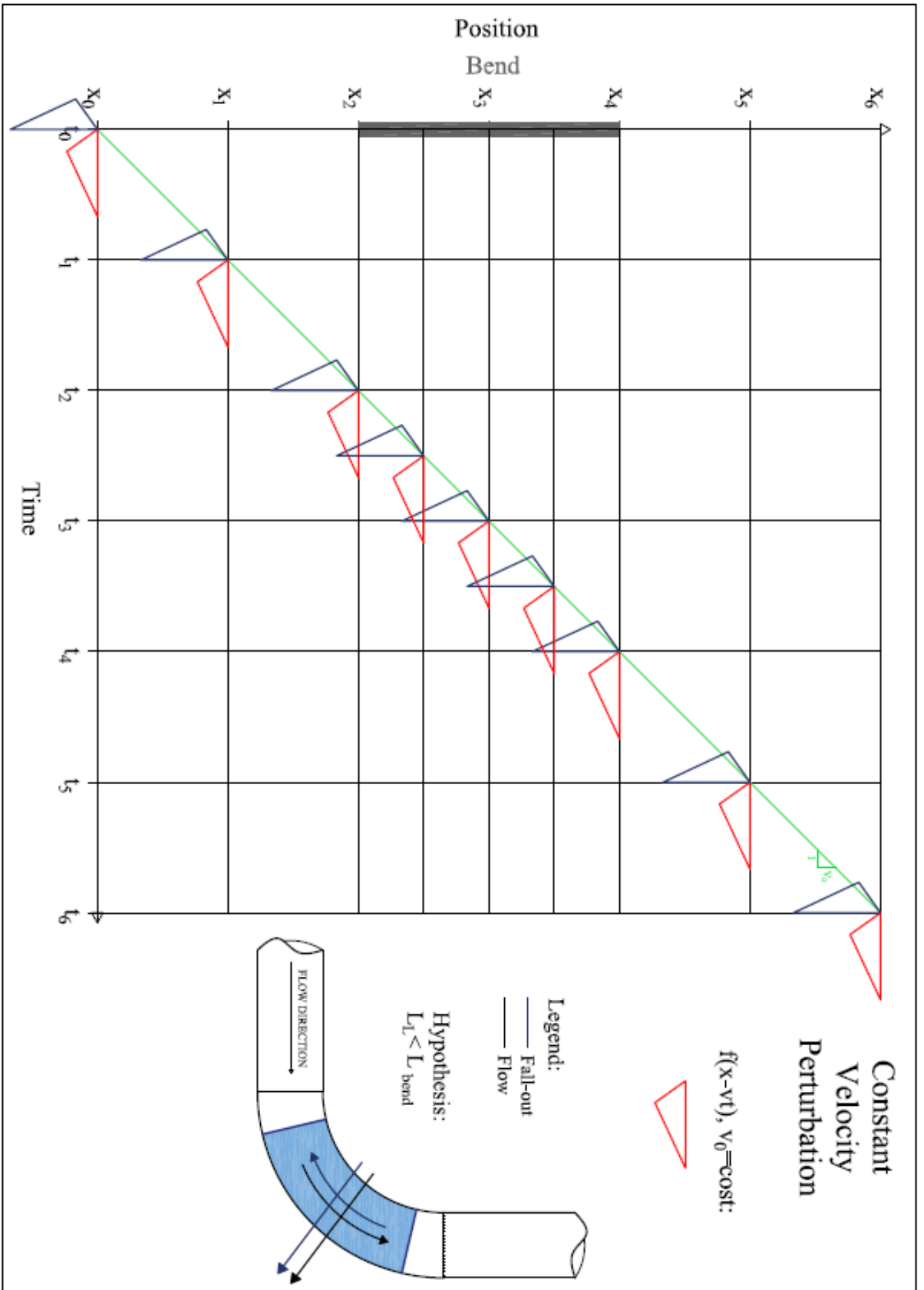
Even if the flow moves in the opposite direction, the resultant forces are in the same direction.

The simulation of the slug flow, in a vertical bends of the jumper, can be qualitatively sketched as a **moving perturbation**, whose force distribution is **variable** in both **velocity and intensity**. It drastically simplify the very complex phenomenon, by gathering together both the contribution of the main *progressive* flow and the partial secondary fall-out.





First, as an introduction to the model, let consider the perturbation shape-function $f(x-vt)$ moving at constant velocity, say v_0 : in the first quarter it *grows rapidly*, then *drops more slowly*. The scheme, showing both the time and spatial evolution, for constant velocity motion is the following:

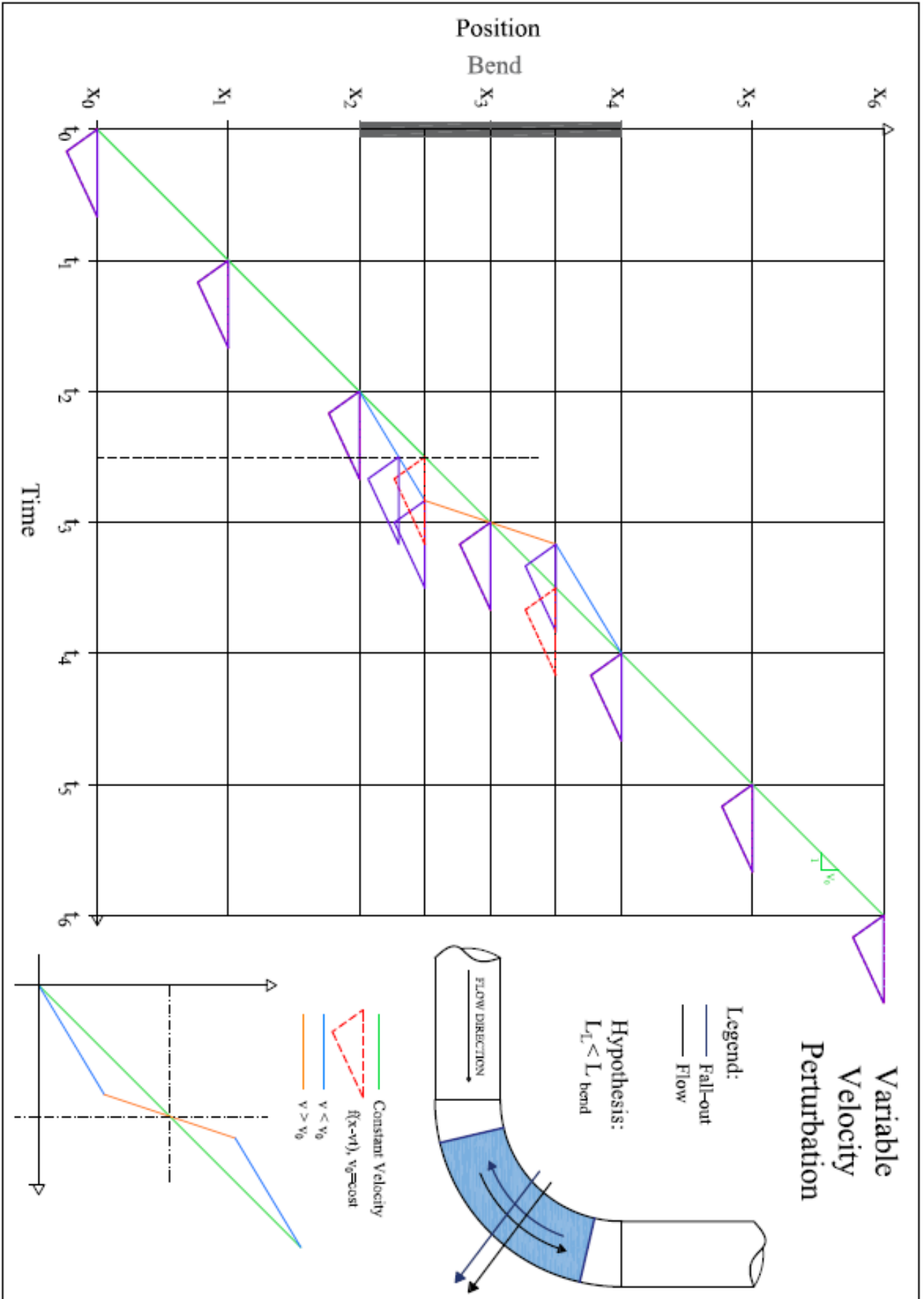


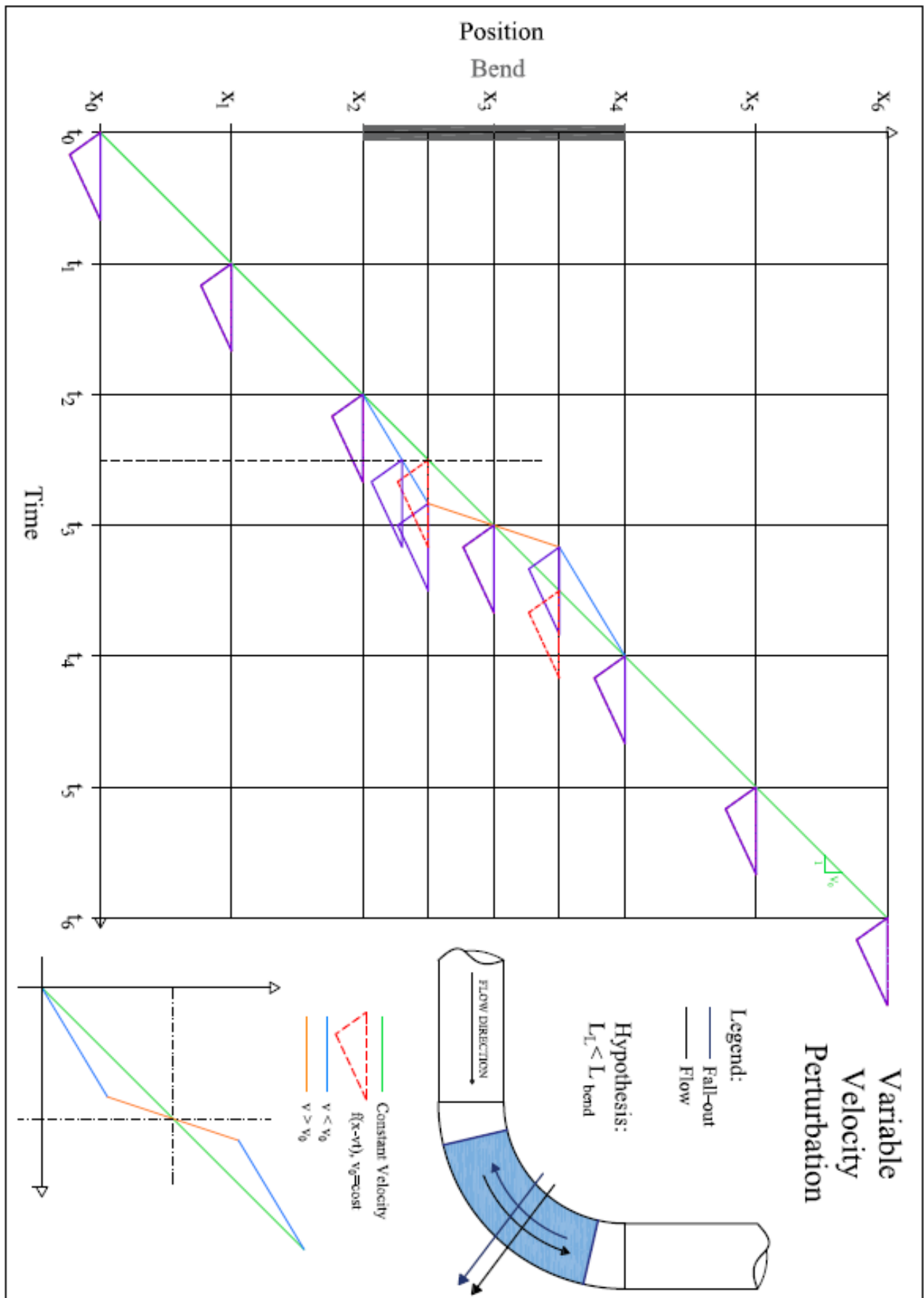
Now let us consider the case in which the same perturbation moves with a **variable velocity**: lower than v_0 at the start and exit of the bend and higher than v_0 in the central part, *maintaining a constant average velocity*. Note that, for the sake of simplicity, we consider the forces depending on the *average velocity* of the flow, by ignoring that part of the fluid *locally* goes back and forth (in a portion of the cross section of the pipe).

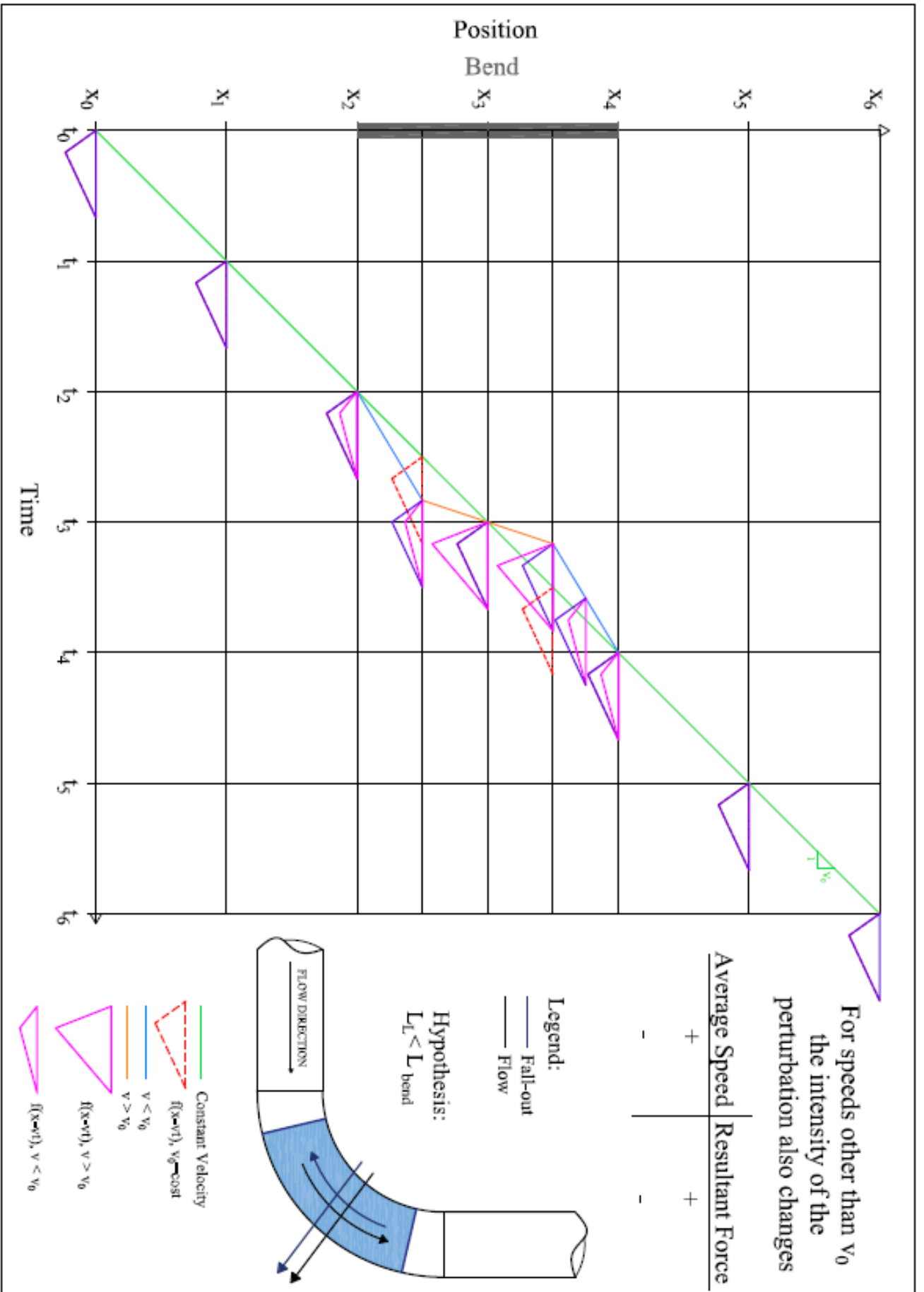
The effect is a *different evolution of the perturbation position* at time t : compared to the case of constant velocity, it will be more backward in the case of lower velocity and more advanced in the case of higher velocity.

In fact, in correspondence with the *dotted line* (between t_2 and t_3), it can be seen that the position of the perturbation following v_0 is more advanced than that following $v (< v_0)$. When the propagation velocity is lower (because in our scheme a little quantity of the fluid is going backwards), then there will also be a lower force.

However, when the velocity is higher, then the force will also be higher.

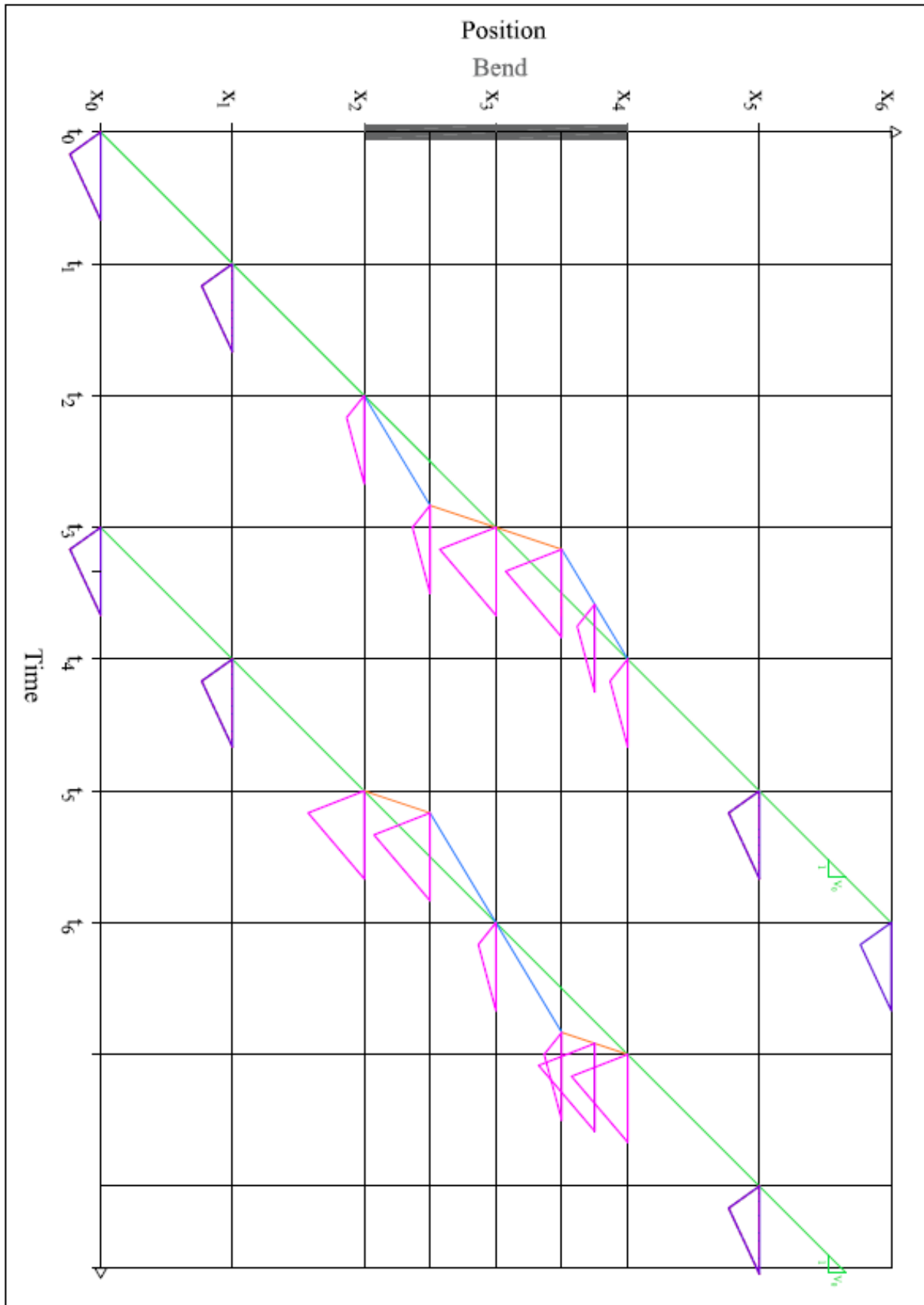








Finally, the situation in which the slug has just passed is represented and then when the next slug arrives it will have an opposite situation.



4.1.3. OTHER CONTRIBUTORS

Dynamic Pressure (end cap compressive effect), *Inertia Forces* (pipe acceleration and mass of slug unit composition), **Resonance** (amplification of response due to periodic driving forces) and *Fluid friction* (force exerted on pipeline due to frictional effects between the flowing fluid and pipe wall).

The forces also change rapidly in the case of intermittent flow at transitions between liquid slugs and pockets. These rapid changes in force and mass can lead to dynamic effects depending on configuration type and boundary conditions (SAIPEM Group, 2020).

The use of these forces with a *time-dependent amplitude*, allows representing the passage of the slug characterized by a particular length. Dividing the length of the slug by its velocity, the time necessary for the slug to cross jumper components (bends, straight pipe) are achieved. In this way, each slug is tracked through time as it travels through the jumper. This also allows representing any particular *slugging regime* and *frequency*. With this analysis, a stress-time history for a point or node in the Finite Element model is obtained.

To understand the loading described for jumper, it is important to remember that numerical analysis requires an **idealised representation of slug flow** [Slug Unit, see Figure 42]. In addition, structure is usually modelled using a **beam based Finite Element (FE)** under large displacement and small strain. Slugs are typically modelled as a 'train' of alternating liquid slugs and pockets with each liquid and pocket giving rise to changes with time in the mass and forces applied to each beam.

A final remark: in the above models, the flow regime is implicitly considered **independent** of the **structural behaviour**. In particular, the influence of the dynamic of the structure is bypassed by inheriting the results obtained from the *flow assurance* for a very great number of regimes, in fixed pipelines. This is a row approximation, of course, physically rather questionable. However, a comprehensive Interaction analysis for a realistic structural section (jumper + pipeline + riser) is still prohibitive.

4.2. STRUCTURAL ANALYSIS

Structural analysis is performed using global analysis methods with FEA software tools. There are several FEA tools such as Flexcom, ORCAFLEX, AUTOPIPE, ANSYS and ABAQUS. The most used for modelling the structural behaviour of subsea pipelines, risers and jumpers and spools is **ABAQUS** [see Appendix A].

4.2.1. ANALYSIS CLASSIFICATION

The global analysis to evaluate the effects of the slug on the jumpers generally involves one of the following methodologies:

- **Regular Slug Trains:** the same slug type is repeatedly passed through the jumper.

- **Irregular Slug Trains:** different slug types are passed through the jumper.

Slug Trains (SAIPEM Group, 2020)

The 'train' analogy is used to denote a string or series of slug units being passed through a piping system.

Moreover, in each methods, the slug units can be:

- **Variable:** slug units have global properties that vary with time as they pass through the jumper configurations. These slug units can accelerate, decelerate, elongate, contract.
- **Fixed:** slug units do not change properties as they pass through a jumper configuration.

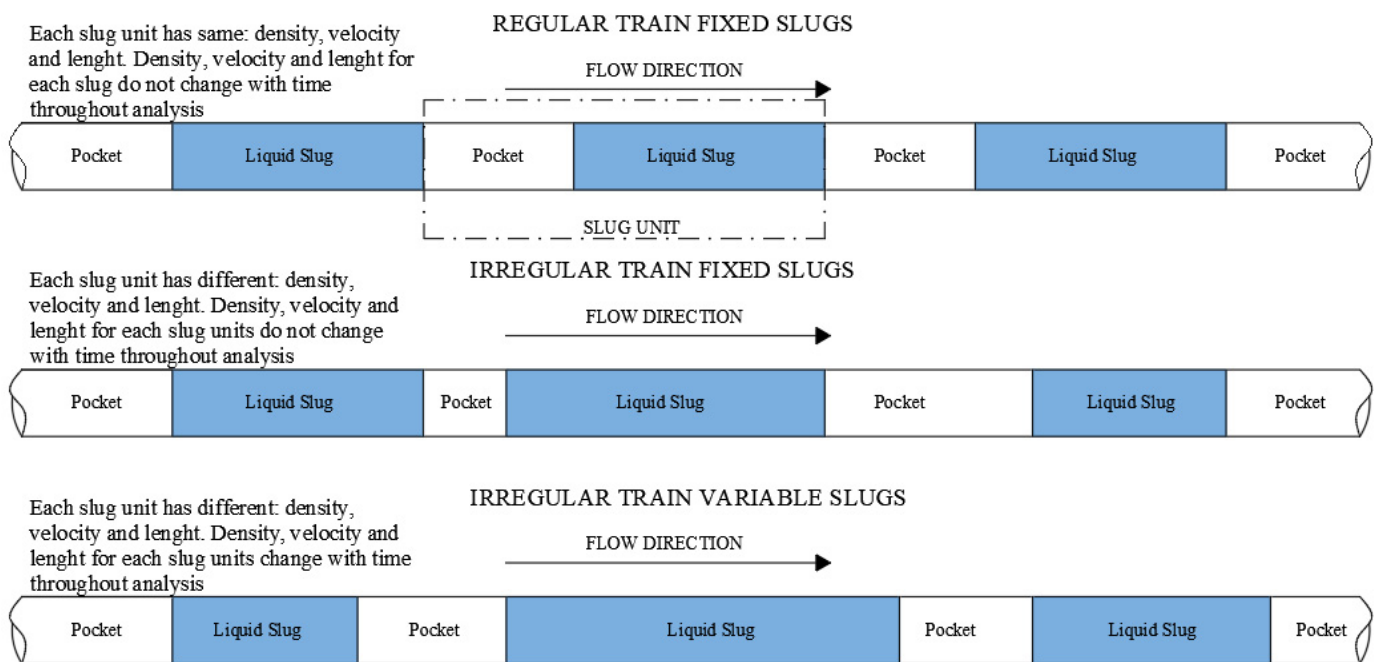


Figure 48 - Slug "Trains"

It is important to *verify* that the slug loads do not excite the natural frequencies of the jumper, therefore that there is no resonance. **Resonance** generates an **amplification of the response** in piping systems, which causes an **increase in fatigue damage**.

Resonance

is the tendency of a system to oscillate with greater amplitude near a modal frequency, in the presence of periodic driving forces. Resonance can occur in pipeline systems when slug loading conditions excite natural frequencies.

The number of consecutive slug units to be included in each analysis should be decided on the basis on an evaluation of the processed slug data. Usually, the number of slug units required to achieve steady state response is included in each simulation. However, a large number of consecutive identical slug units may be overly conservative and may not be reflective of actual anticipated flow conditions (i.e. creating inapplicable resonance amplification) (SAIPEM Group, 2020).

CHAPTER 5: PIPES DYNAMICS WITH VARIABLE AND MOVING MASS

Systems with time variable masses are present in physics and engineering (robotics, transport systems, excavators, chemistry) and in *fluid-structure interaction problems* (Irschik & Belyaev, 2014) (Belluzzi, 1994).

Travelling loads or **moving loads** problem is fundamental in the study of structural dynamics. Its importance is evident in numerous applications in the field of transport. Some examples of structural elements designed to withstand moving masses are bridges, walkways and **pipeline**.

A beam, or a pipeline, under moving loading condition can be analyzed following to two limit schemes: first, the mass of the moving load is negligible with respect to the mass of the beam (and the velocity is reasonably moderate); on the other hand, the mass of the beam is small, in comparison with the moving mass. In the later case, the beam is devised as a (variable) elastic constraint, and the question becomes a rigid body dynamic problem. Both situation are full covered by the usual methods of the structural dynamics: modal or spectral analysis or direct integration.

The problem of the moving slug in pipeline belongs, properly, to neither of the above schemes. The theoretical and numerical apparatus to face this formidable problem is very complex, even more for a train of slugs whose frequency, length and distancing is greatly variable.

The dynamics of fluid-carrying pipes have been extensively studied in recent decades. The equation of motion describing a Euler-Bernoulli beam is shown below in its simplest form:

$$EJ \frac{\partial^4 w(x, t)}{\partial x^4} + m \frac{\partial^2 w(x, t)}{\partial t^2} + M_f (U^2 \frac{\partial^2 w(x + ut, t)}{\partial x^2} + 2U \frac{\partial^2 w(x + ut, t)}{\partial t \partial x} + \frac{\partial^2 w(x + ut, t)}{\partial t^2}) \delta(x + ut) = 0$$

where $w(x, t)$ is the transversal displacement, x the axial coordinate, t the time, EJ the bending stiffness of the pipe, m the mass per unit length of the pipe, M_f the moving mass and U is its velocity, assumed constant; δ is the Dirac delta *distribution* locating the moving mass along the beam. In this equation are neglected gravity, internal and external pressure, damping, shear deformation and global axial forces (second order instability effects) as well as large displacement. The pipe is a Euler-Bernoulli beam. The three term can be easily interpreted:

- $M_f U^2 \frac{\partial^2 w}{\partial x^2} = M_f U^2 \frac{1}{r}$ is the *centrifugal force* ($1/r$ being the curvature)
- $M_f 2U^2 \frac{\partial^2 w}{\partial x \partial t}$ is the mutual contribution of the velocities of the beam and of the mass

- $M_f \frac{\partial^2 w}{\partial t^2}$ is the *force of inertia* of the mass (on the beam)

The fluid internal forces are modelled according to a slug flow model. This means that the fluid is shaped like an infinitely flexible cylinder that travels through the pipe. All the points of the fluid have a constant velocity with respect to the pipe.

Let consider a very slender body, like a pipe, where the diameter does not vary over the length of the pipe. The transversal acceleration of the fluid can be found by considering the lateral velocity of a fluid particle relative to the pipe.

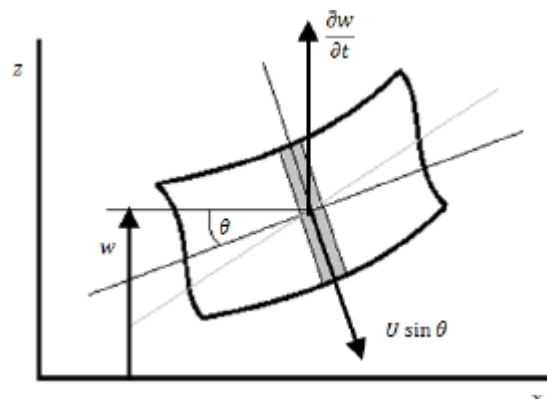


Figure 49 - Cross section of an infinitely long slender cylinder (H.E.J. van der Heijden, 2013)

The contribution of the slug in the equation of motion can be better understood considering the simpler scheme of a beam with a moving mass. This system has been extensively studied and has been employed in many applications, including slugs. (Reda, Forbes, & Sultan, 2011) compares a simply supported beam with a moving force and a moving mass in order to simulate the motion of a free pipe span under slug load. The difference between force and mass is the terms due to the inertia of the mass, sketched above. It is concluded that the mass model, that is with inertia, provides better results when the mass of the slug cannot be neglected compared to the weight of the beam.

The equation of motion of a beam with a moving lumped mass is the following:

$$EJ \frac{\partial^4 w}{\partial x^4} + m \frac{\partial^2 w}{\partial t^2} + m_{slug} \delta(x - u_s t) \left(g + \frac{\partial^2 w}{\partial t^2} \right) = 0$$

where g is the gravity acceleration and the δ *distribution* is again used to synthetically describe the slug as a lumped mass.

Slug flow has two parameters: mass and velocity. However, the slug flow velocity will be close to the gas velocity in this two-phase system and it will be cautiously assumed be equal to the gas velocity: the slug and gas velocities are equal to the *same* constant. The only time-dependent parameter should be the density or mass of the slug.

The pipe is immersed in water, so the effects of *damping* and *added mass* have to be included (due to the Fluid Structure interaction, during the vibration); in addition, it should be take into account both the external and internal pressures (in several load cases combination).

Added mass

As the pipe moves, the surrounding water will be moved. The acceleration due to the displacement of the surrounding water will add inertia to the system. The velocity of the pipe causes the added damping as it moves sideways. This velocity will cause resistance, which will bring energy out of the system and therefore dampens it.

The equation of motion for this problem is as follows (H.E.J. van der Heijden, 2013):

$$\begin{aligned} \left(1 + \alpha \frac{dw}{dt}\right) EJ \frac{\partial^4 w}{\partial x^4} + (\rho A + M_a) \frac{\partial^2 w}{\partial t^2} + \Delta m \delta(x - u_s t) \left(g + \frac{\partial^2 w}{\partial t^2}\right) \\ + m_0 \left(\frac{\partial^2 w}{\partial t^2} 2u_g \frac{\partial^2 w}{\partial t \partial x} + u_g^2 \frac{\partial^2 w}{\partial x^2}\right) + (A_e p_e - A_i p_i) \frac{\partial^2 w}{\partial x^2} + c \frac{\partial w}{\partial t} \\ = (\rho A + m_0)g \end{aligned}$$

where EJ and ρA are the bending stiffness and the mass of the beam respectively. For the slug, Δm is the mass and u_s the slug velocity. For the gas: m_0 is the mass and u_g is the velocity. The internal pressure, p_i , and the external pressure, p_e , together with the internal and external transverse area, A_i and A_e , constitute the pressure contributions. The damping coefficient c represents the added damping. The damping of the material is also included, in the more realistic the Kelvin-Voigt form, by introducing the α coefficient.

A way to solve the above differential system is the Galerkin method, which discretizes the unknown function with a finite number of parameter, $q_i(t)$, leading to a possible numerical solution. The unknown displacement is therefore written as:

$$w(x, t) \cong w_N(x, t) = \sum_{i=1}^N \varphi_i(x) q_i(t)$$

where φ_i are the *shape form*. These functions, defined in the domain $D=[0;L]$ (with L =pipe length) satisfy both dynamic and kinematic boundary conditions.. In general the $q_i(t)$ have to satisfy a ordinary differential equation. For shape form, both auto-functions and modal shapes can be used as they meet the boundary conditions in the same domain $D=[0;L]$.

In order to find a suitable φ , the general solution of a Euler-Bernoulli beam is used: a simply supported beam, in the simplest form:

$$EJ \frac{\partial^4 w}{\partial x^4} + \rho A \frac{\partial^2 w}{\partial t^2} = 0$$

This partial differential equation can be solved using the method of separation of variables in which the solution $w(x,t)$ can be expressed as two unknown functions of x and t . It is easy to verify that the temporal function is a sinusoidal function. This means that it can be written as:

$$w(x, t) = W(x) \exp(i\omega t)$$

This solution is then replaced in the equation of motion and an eigenvalue Boundary Value Problem (EBVP) is obtained. It is a fourth-order differential equation with respect to space function $W(x)$. The solutions of $W(x)$ of the EBVP are called eigenfunction. The frequency can only take values in such a way the following reduced equation is satisfied:

$$\frac{\partial^4 W(x)}{\partial x^4} + \beta^4 W(x) = 0$$

with:

$$\beta^4 = \frac{\rho A \omega^2}{EJ}$$

The final solution is:

$$w(x) = \sum_{k=1}^4 C_k \exp(\lambda_k x)$$

λ_k are the four roots of the characteristic equation:

$$\sum_{k=1}^4 C_k (\lambda_k^4 - \beta^4) \exp(\lambda_k x) = 0$$
$$\lambda_k^4 - \beta^4 = 0; \lambda_1 = \beta, \lambda_2 = -\beta, \lambda_3 = i\beta, \lambda_4 = -i\beta$$

Finally:

$$W(x) = C_1 \exp(\beta x) + C_2 \exp(-\beta x) + C_3 \exp(i\beta x) + C_4 \exp(-i\beta x)$$

that can be re-written as:

$$W(x) = A \cosh(\beta x) + B \sinh(-\beta x) + C \cos(\beta x) + D \sin(\beta x)$$

The constants A , B , C , D and β depend on the boundary conditions of the beam. β is related to natural frequency ω and therefore the natural frequencies depend on boundary conditions.

CHAPTER 6: CASE STUDY

6.1. METHODOLOGY

The jumper response against slugging loads has been assessed performing ABAQUS FE analysis. A FE model of jumper has been developed with ABAQUS to evaluate the dynamic response during the passage of slug.

The jumper configuration of the case study is the following:

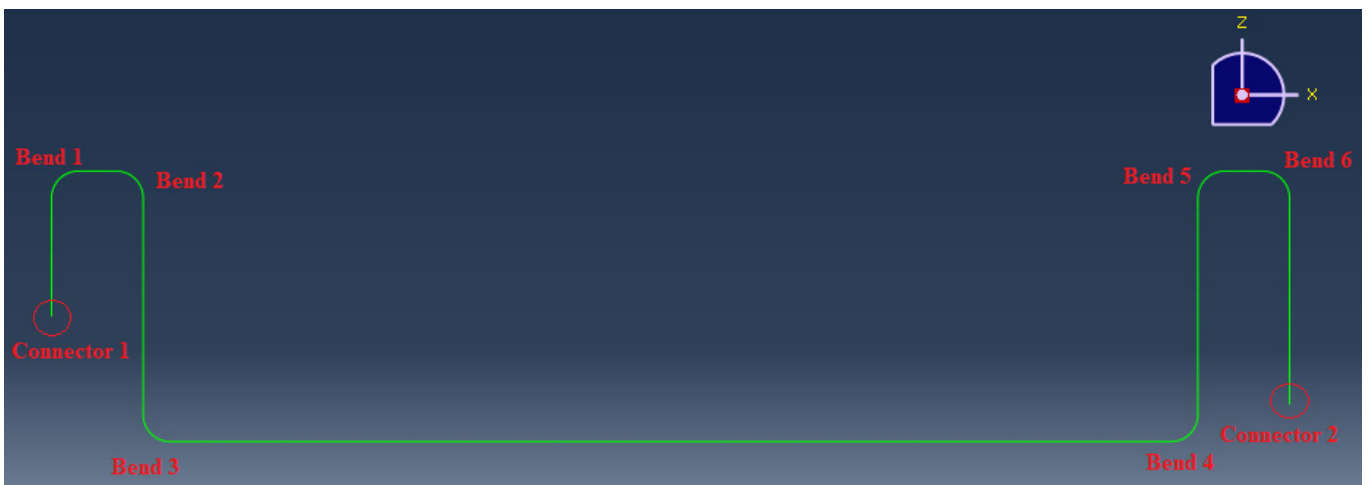


Figure 50 - Jumper configuration: ABAQUS FE Model

Jumper Data	
Outside Diameter	0,32385m 12,75 inch
Internal Diameter	0,24765 m
Wall Thickness	0,0381 m
Steel Density	7850 kg/m ³
Mass per linear m	377,93kg/m
Material	X65

Table 3 - Jumper Data

Connector Data	
Outside Diameter	0,32385m 12,75 inch
Internal Diameter	0,17145 m
Wall Thickness	0,0762 m
Steel Density	7850 kg/m ³
Material	X65

Table 4 - Connector Data

Input Data	
Water Depth	-1826 m
Water Density	1025 kg/m ³
Sea Temperature	3,8 °C
Operative Temperature	121 °C

*Table 5 - Input Data***Water Depth**

Distance between sea level and seabed. This input data, with the **water density**, serves to define the external pressure applied over the jumper.

The jumper model is built up of nodes and three-dimensional pipe elements (PIPE31H, § APPENDIX A) able to predict global pipeline behaviour.

In addition to the study of the slug step effects, the analysis takes into account all the life phases of the jumper (installation, operation, etc.). In particular, a modal analysis is carried out, in order to verify the possible occurrence of **resonance**.

6.2. MODAL ANALYSIS

Modal analysis is the first step of every dynamic study, because identify the elementary *natural* frequencies and their associated mode of vibration of the structural system.

The dynamics is characterized by the mass, stiffness and damping distribution along the structure and allow the structural identification, with the aim to predict its behavior when exposed to operational loads.

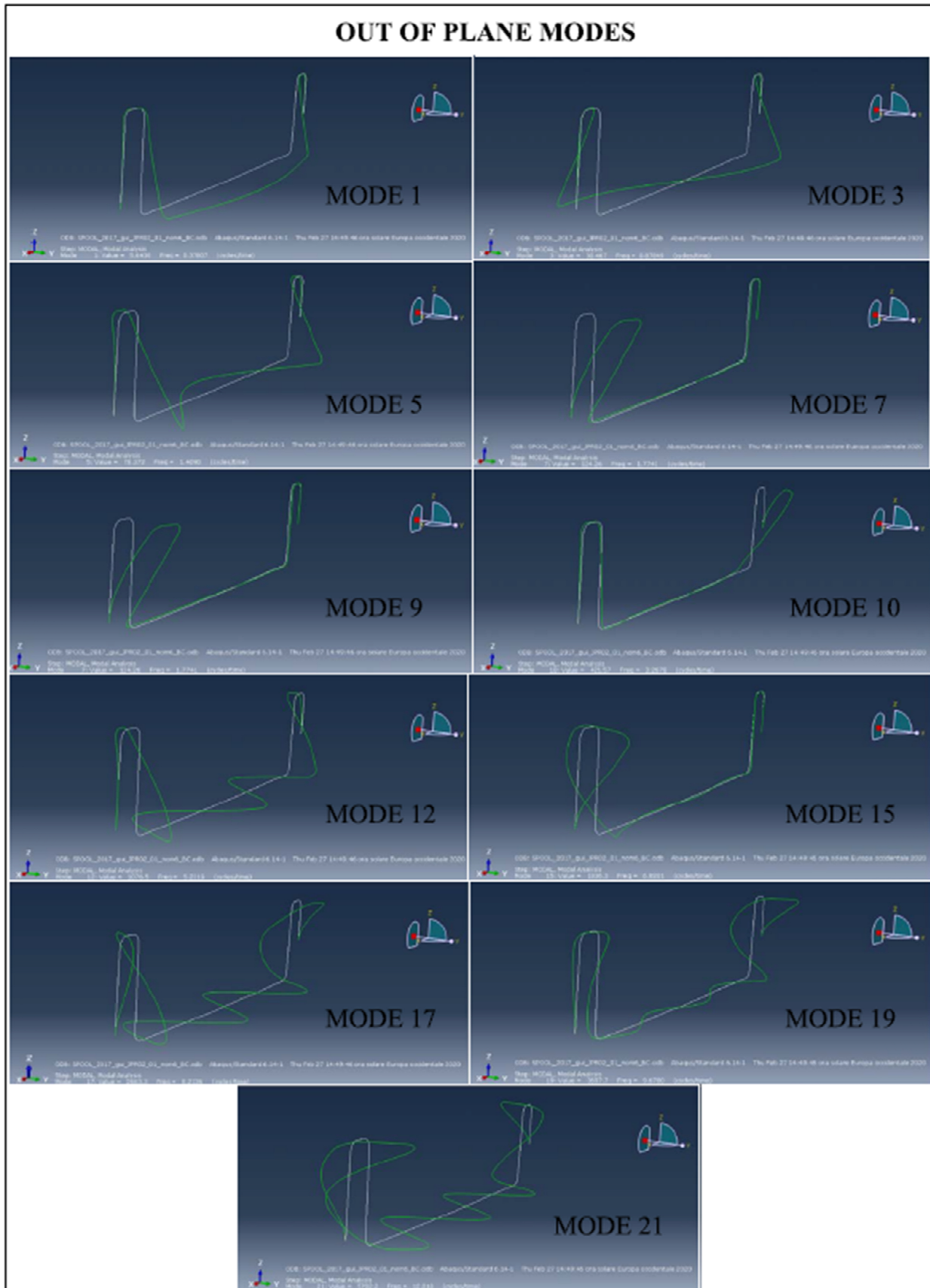


Figure 51 - Out-of-Plane Modes

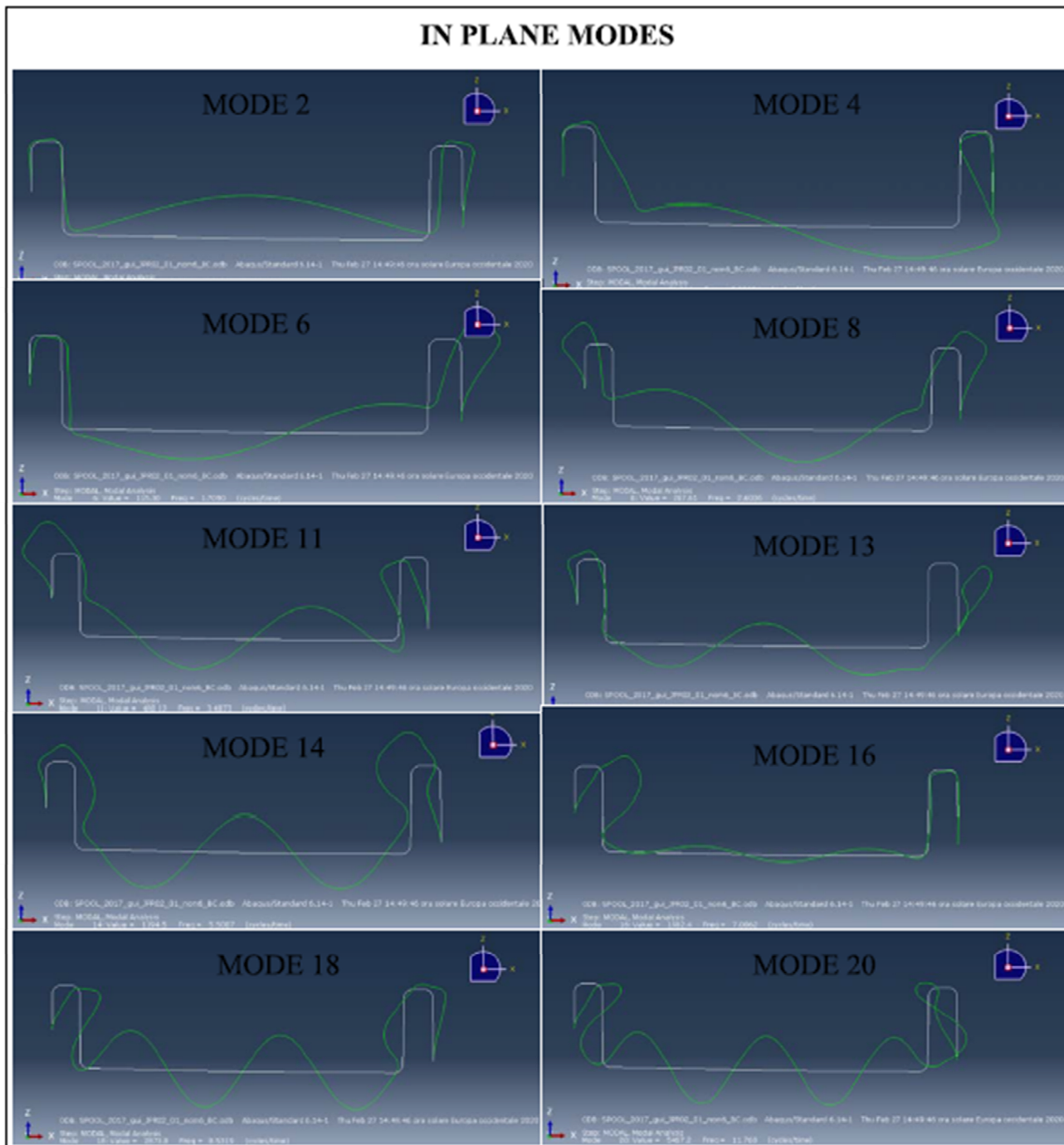


Figure 52 - In-Plane Modes

MODAL ANALYSIS		
MODE	FREQ [Hz]	In/Out of Plane
1	0,37807	Out
2	0,77329	In
3	0,87849	Out
4	0,88634	In
5	1,409	Out
6	1,709	In
7	1,7741	Out
8	2,6036	In
9	2,9116	Out
10	3,2678	Out
11	3,4873	In
12	5,2219	Out
13	5,2844	In
14	5,5007	In
15	6,8201	Out
16	7,0862	In
17	8,2136	Out
18	8,5319	In
19	9,678	Out
20	11,768	In
21	12,018	Out

Table 6 - Modal Analysis Results

Table 6 shown that mode 4, characterized by a frequency of 0.88634 Hz, could be cause of resonance.

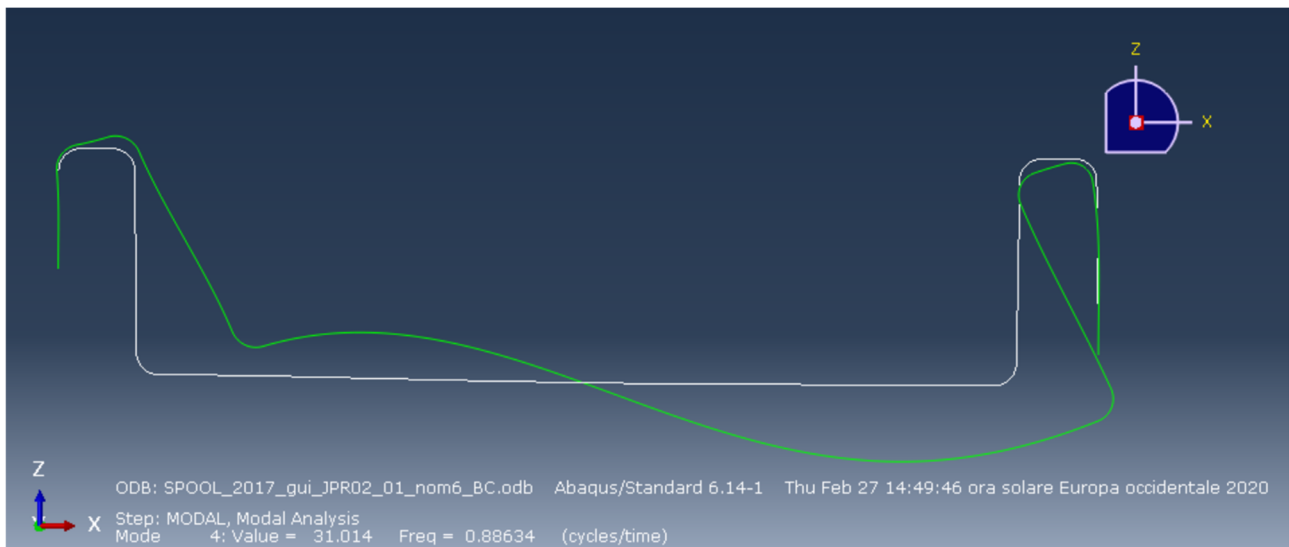


Figure 53 - In-Plane Mode 4

6.3. SLUG ANALYSIS

Structural damping is not considered to result in a conservative solution.

6.3.1. INPUT DATA

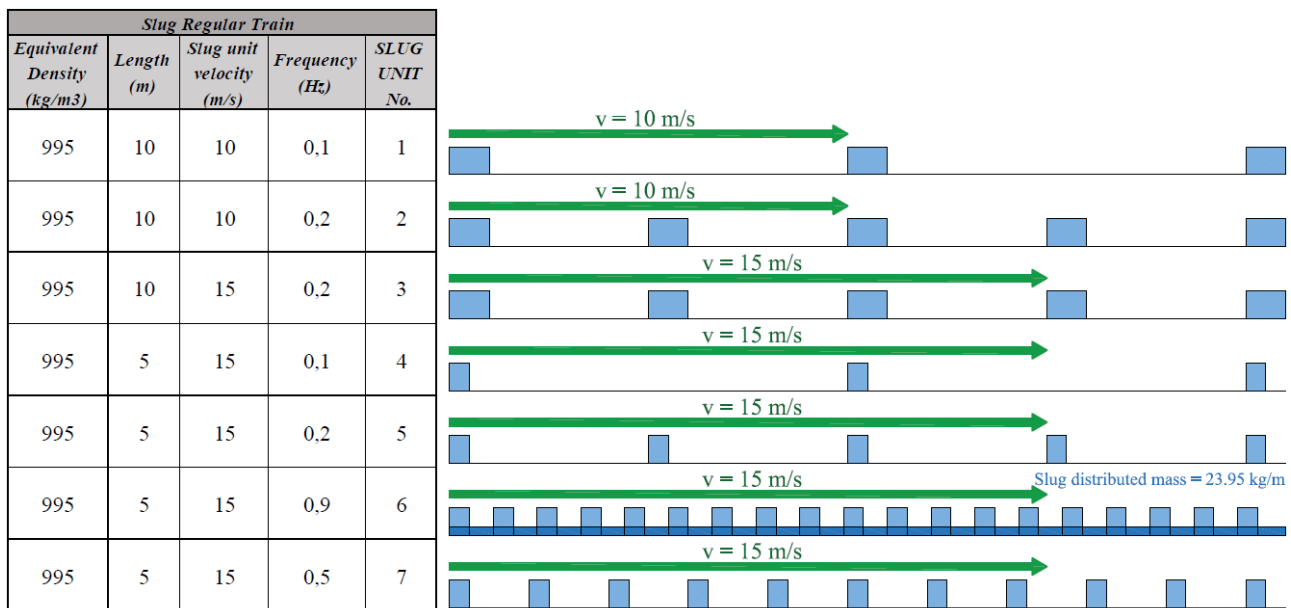


Figure 54 - Slug Input Data

The mass of the slug per linear meter is **47,90 kg/m**; the jumper mass per linear meter is **377,93 kg/m**.

In case 6+slug mass an analysis is made considering a distributed mass equivalent to **23,95kg/m**.

Case 6 is an **extreme condition**, considered to test the behavior of the system.



Figure 55 - Example: Slug unit in Bend 1

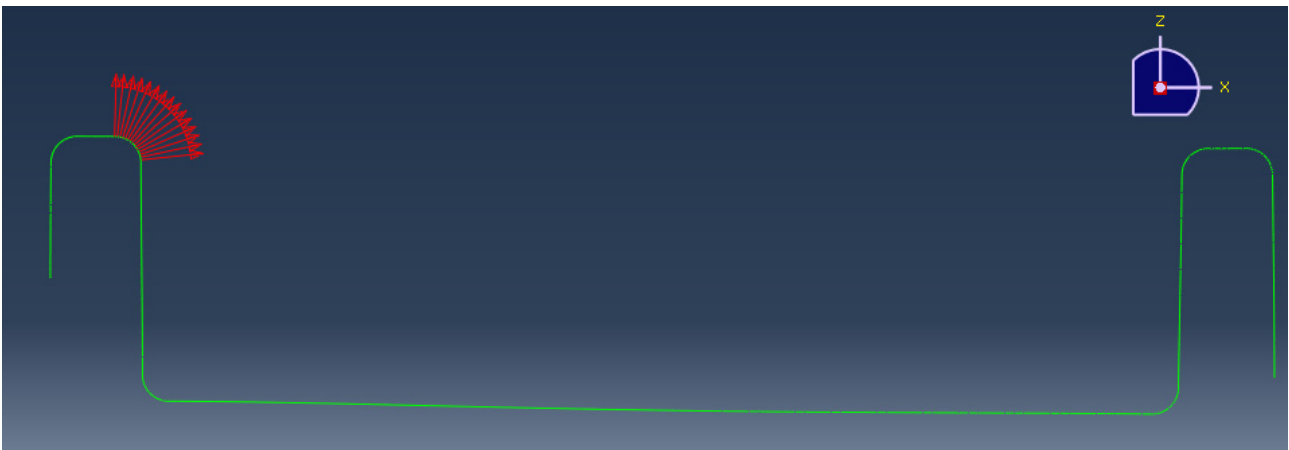


Figure 56 - Example: Slug unit in Bend 2

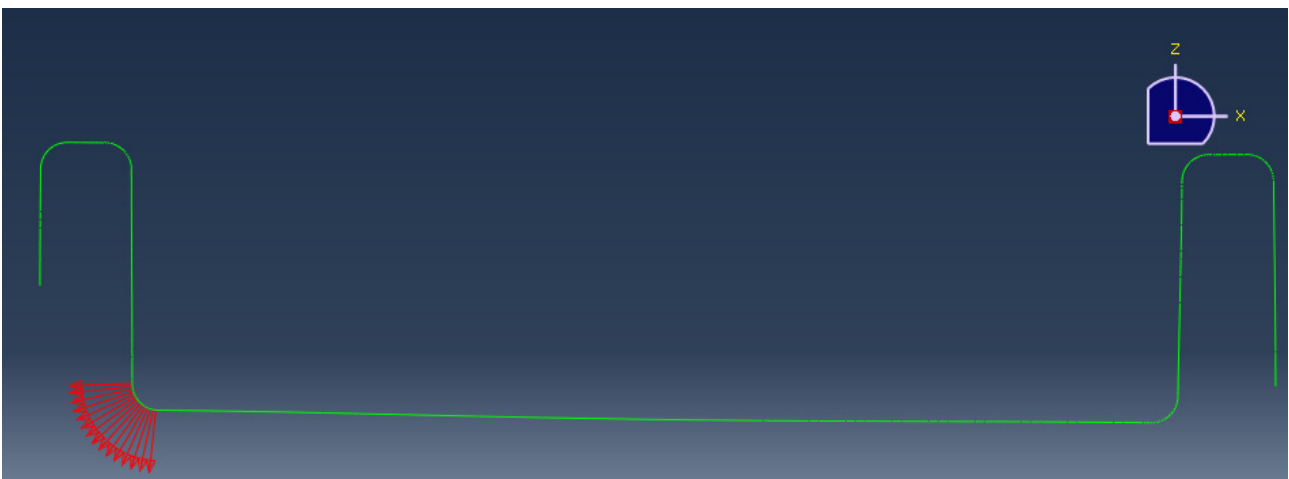


Figure 57 - Example: Slug unit in Bend 3

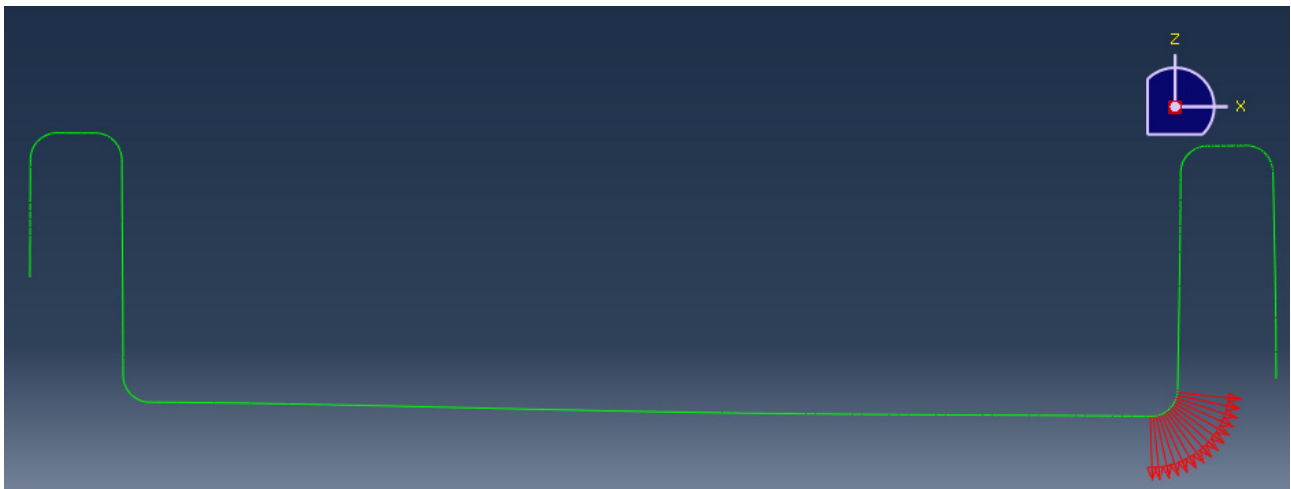


Figure 58 - Example: Slug unit in Bend 4

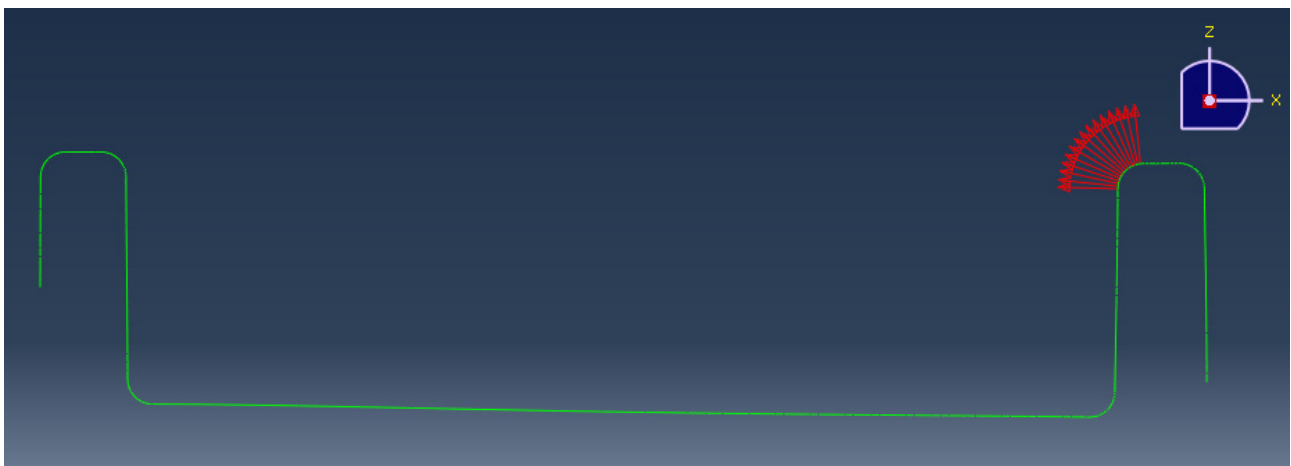


Figure 59 - Example: Slug unit in Bend 5

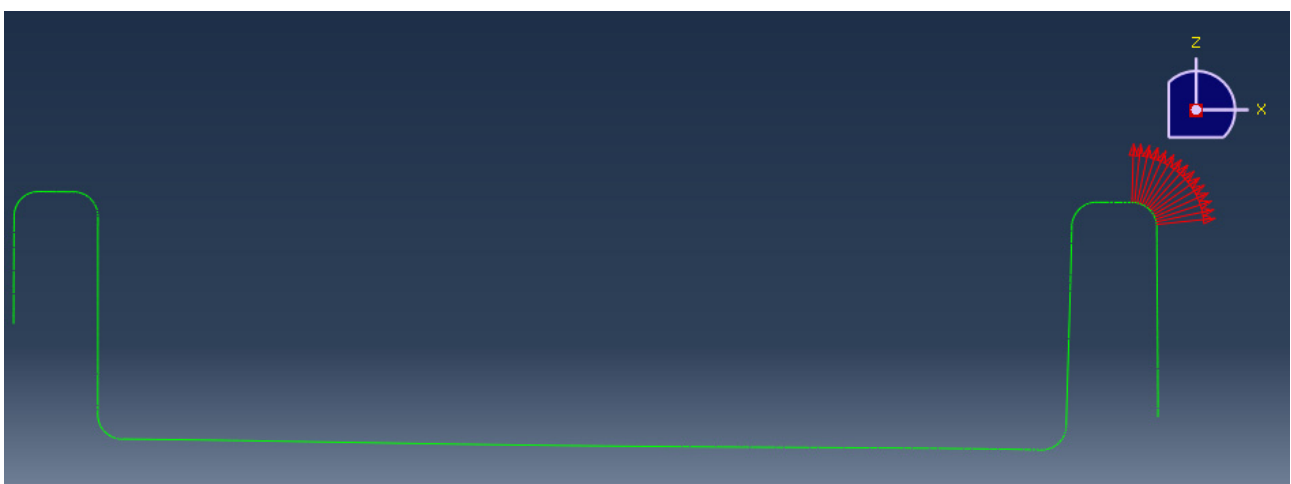


Figure 60 - Example: Slug unit in Bend 6

The slug units enter and exit from the different bends; the **time-dependent forces** that are generated grow and decrease following the trapezoidal path in time already expressed in Figure 45:

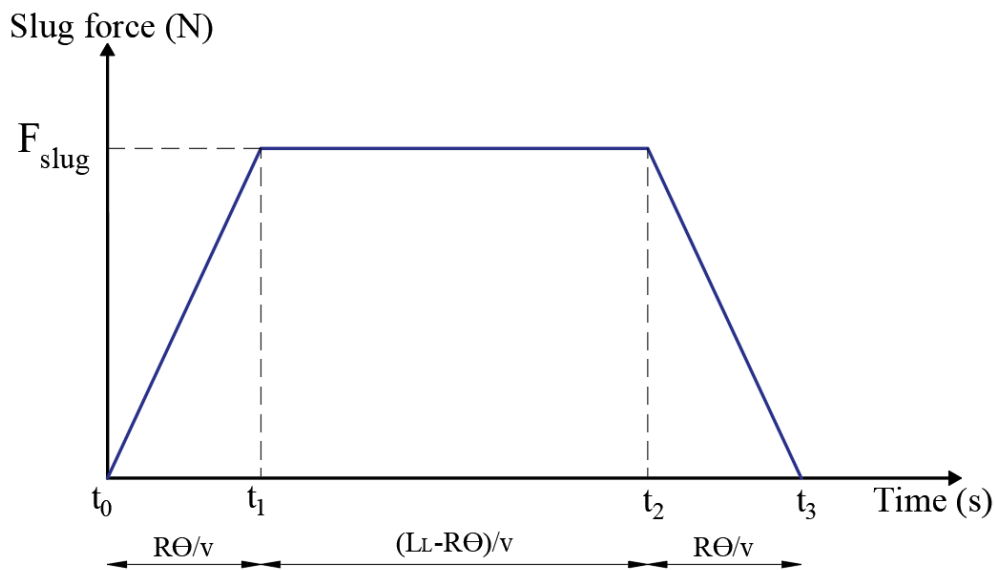


Figure 61 - Slug Force with time

With:

$$F_{slug} = F_{centrifugal} = \rho_{slug} A v_{slug}^2$$

6.3.2. RESULTS

The following diagrams show the result of the time history of the forces and the displacement in two representative node of the two upper curves:

Bend 3 (from 91 to 105): **Node 97**

Bend 4 (from 220 to 234): **Node 228.**

Displacement starts at time $t = 5$ s, discarding the effect of the previous static load conditions (adjustment, gravitation loads, etc), generating initial nonzero offset.

SLUG UNIT No. 1

Length **10 m**
 Frequency **0,1 Hz**
 Velocity **10 m/s**

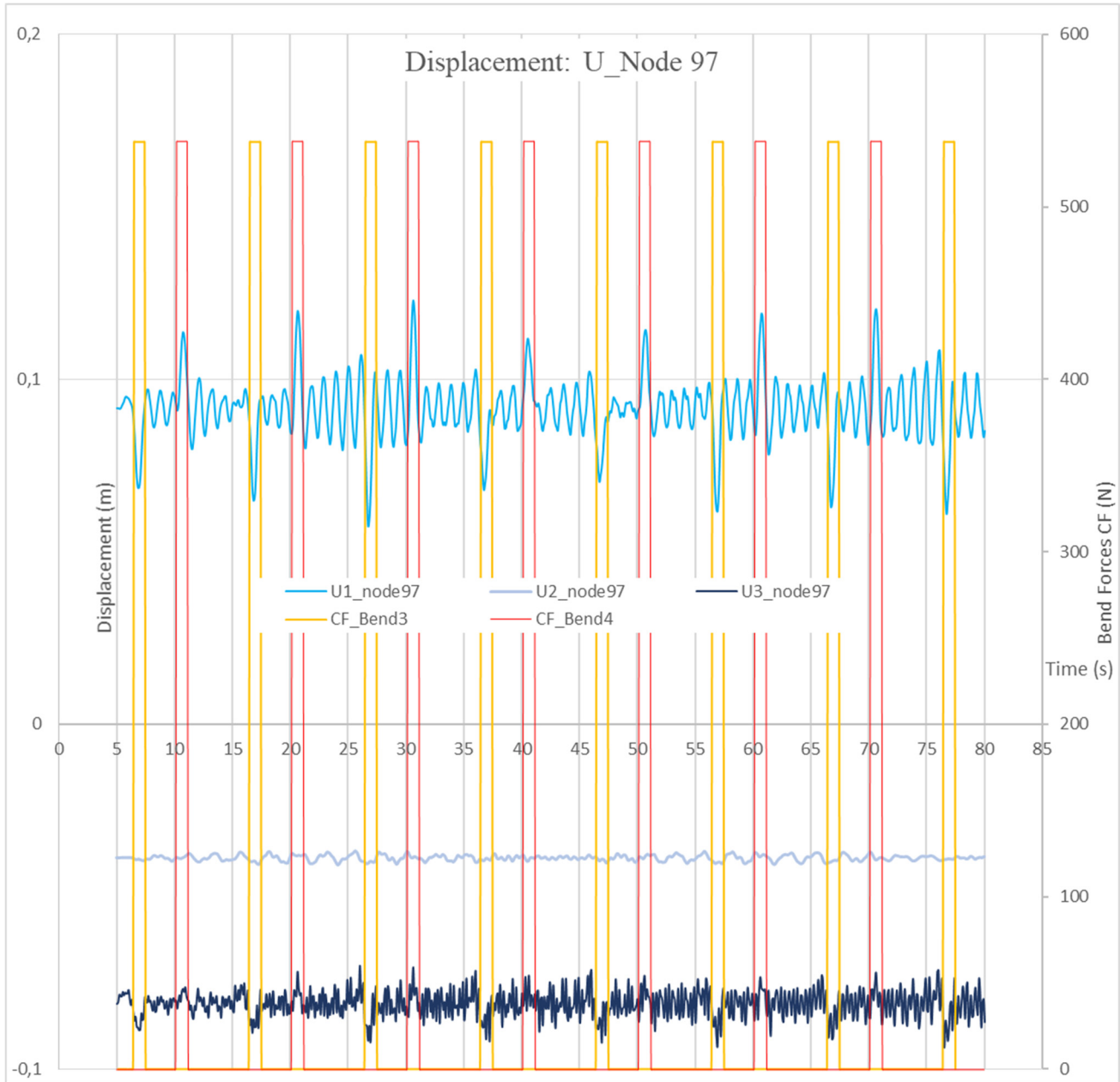


Figure 62 - Total Displacement Node 97: U1=longitudinal displacement, U2=transversal displacement, U3=vertical displacement. CF_Bend 3 = Slug Forces (In-Phase) in bend 3 that are characterized by the trapezoidal path (see figure 61), CF_Bend 4 = Slug Forces (Out-of-Phase) in bend 4 that are characterized by the trapezoidal path (see figure 61).

SLUG UNIT No. 1

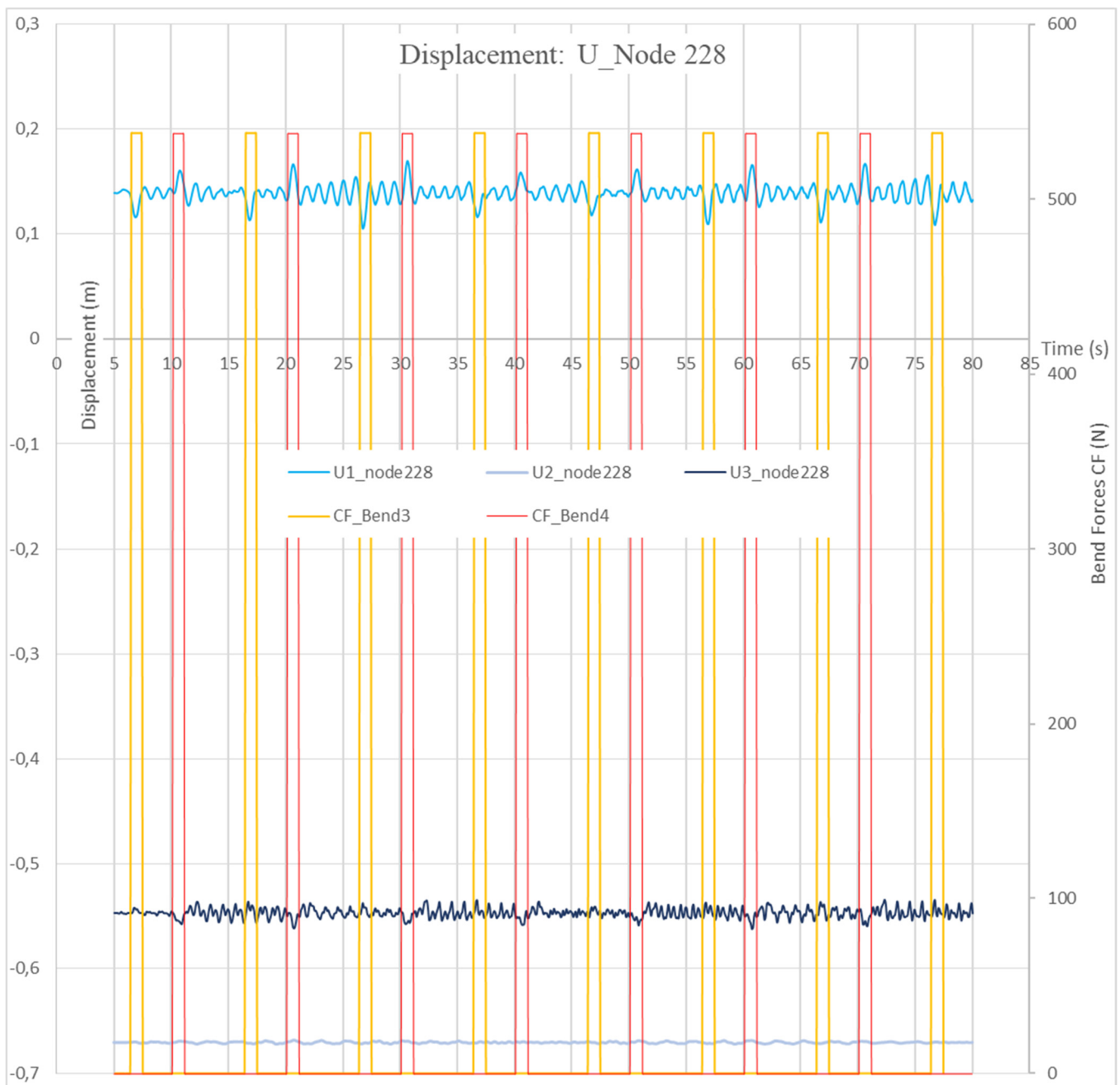


Figure 63 - Total Displacement Node 228: U1=longitudinal displacement, U2=transversal displacement, U3=vertical displacement. CF_Bend 3 = Slug Forces (Out-of-Phase) in bend 3, CF_Bend 4 = Slug Forces (In-Phase) in bend 4.

SLUG UNIT No. 2

Length **10 m**
Frequency **0,2 Hz**
Velocity **10 m/s**

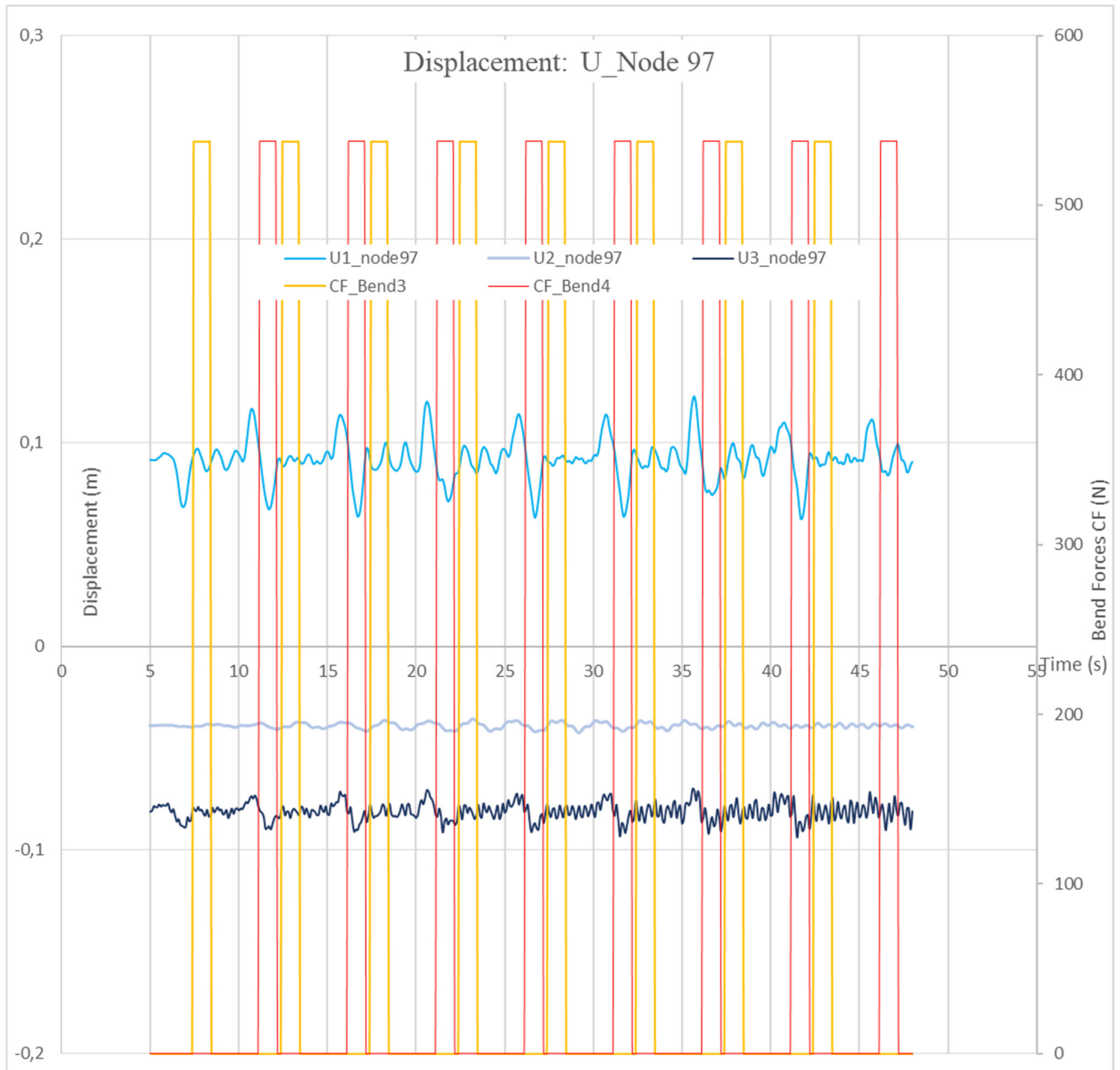


Figure 64 - Total Displacement Node 97: U1=longitudinal displacement, U2=transversal displacement, U3=vertical displacement. CF_Bend 3 = Slug Forces (In-Phase) in bend 3, CF_Bend 4 = Slug Forces (Out-of-Phase) in bend 4.

SLUG UNIT No. 2

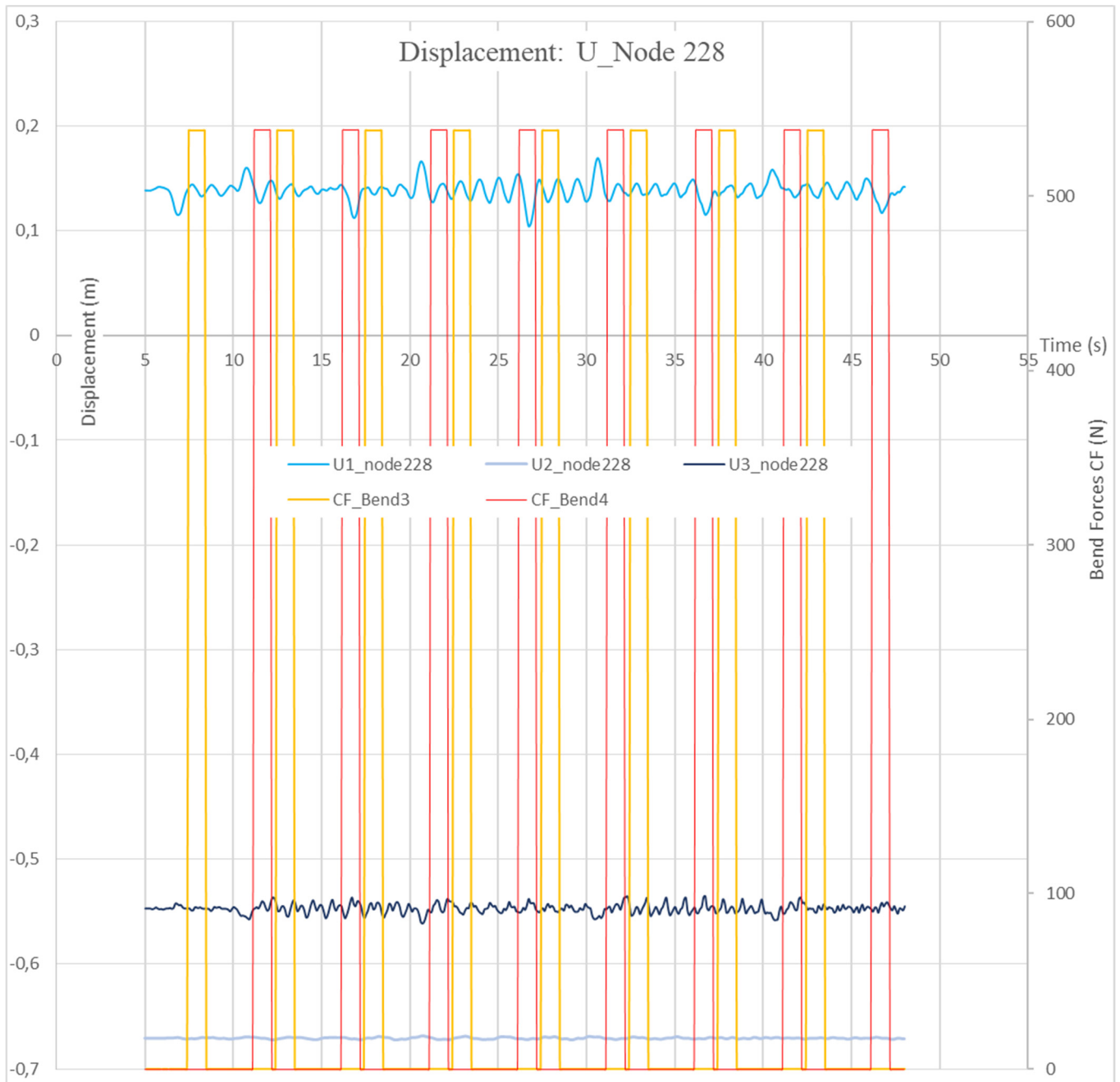


Figure 65 - Total Displacement Node 228: U1=longitudinal displacement, U2=transversal displacement, U3=vertical displacement. CF_Bend 3 = Slug Forces (Out-of-Phase) in bend 3, CF_Bend 4 = Slug Forces (In-Phase) in bend 4.

SLUG UNIT No. 3

Length **10 m**
Frequency **0,2 Hz**
Velocity **15 m/s**

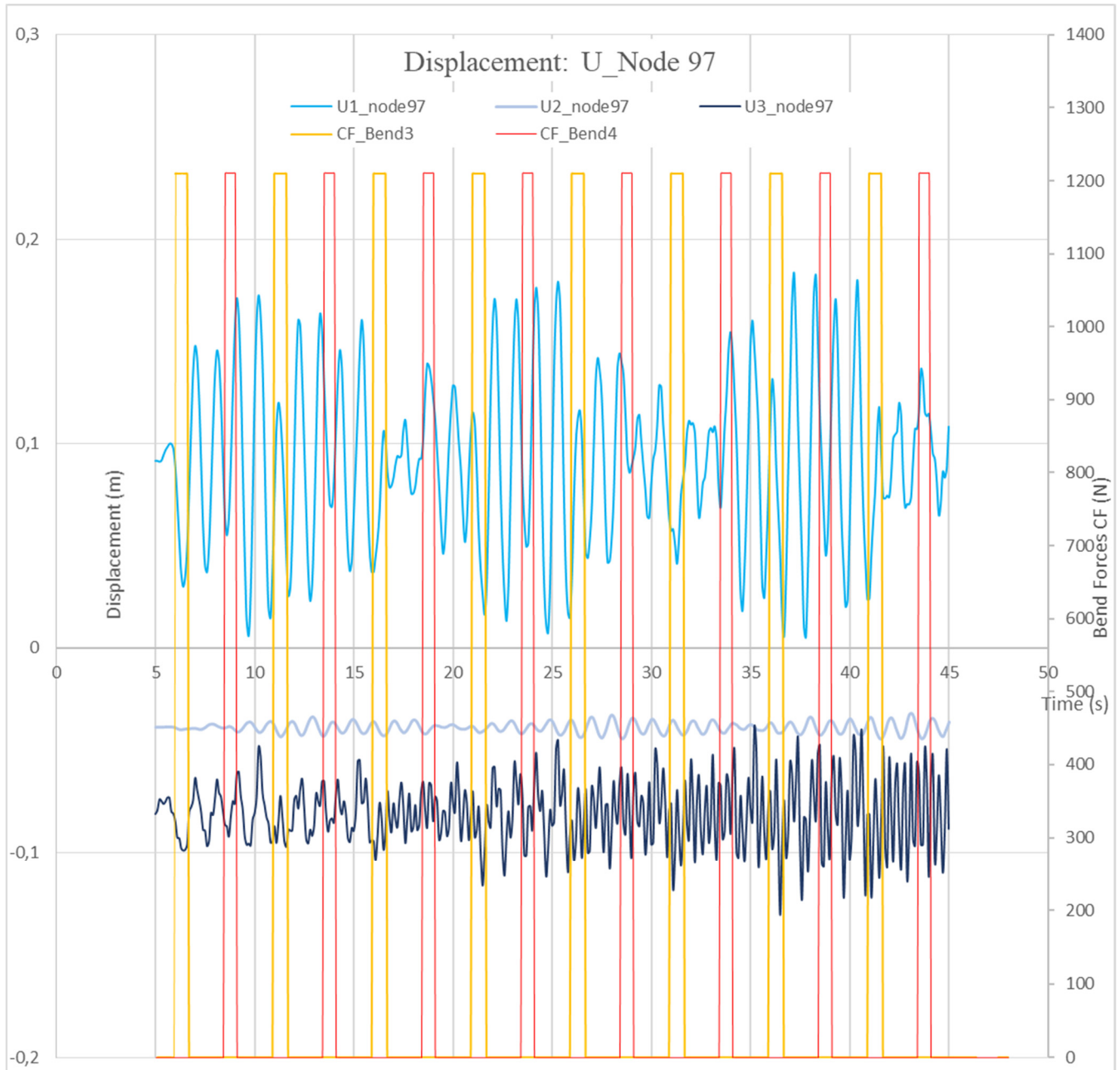


Figure 66 - Total Displacement Node 97: U1=longitudinal displacement, U2=transversal displacement, U3=vertical displacement. CF_Bend 3 = Slug Forces (In-Phase) in bend 3, CF_Bend 4 = Slug Forces (Out-of-Phase) in bend 4.

SLUG UNIT No. 3

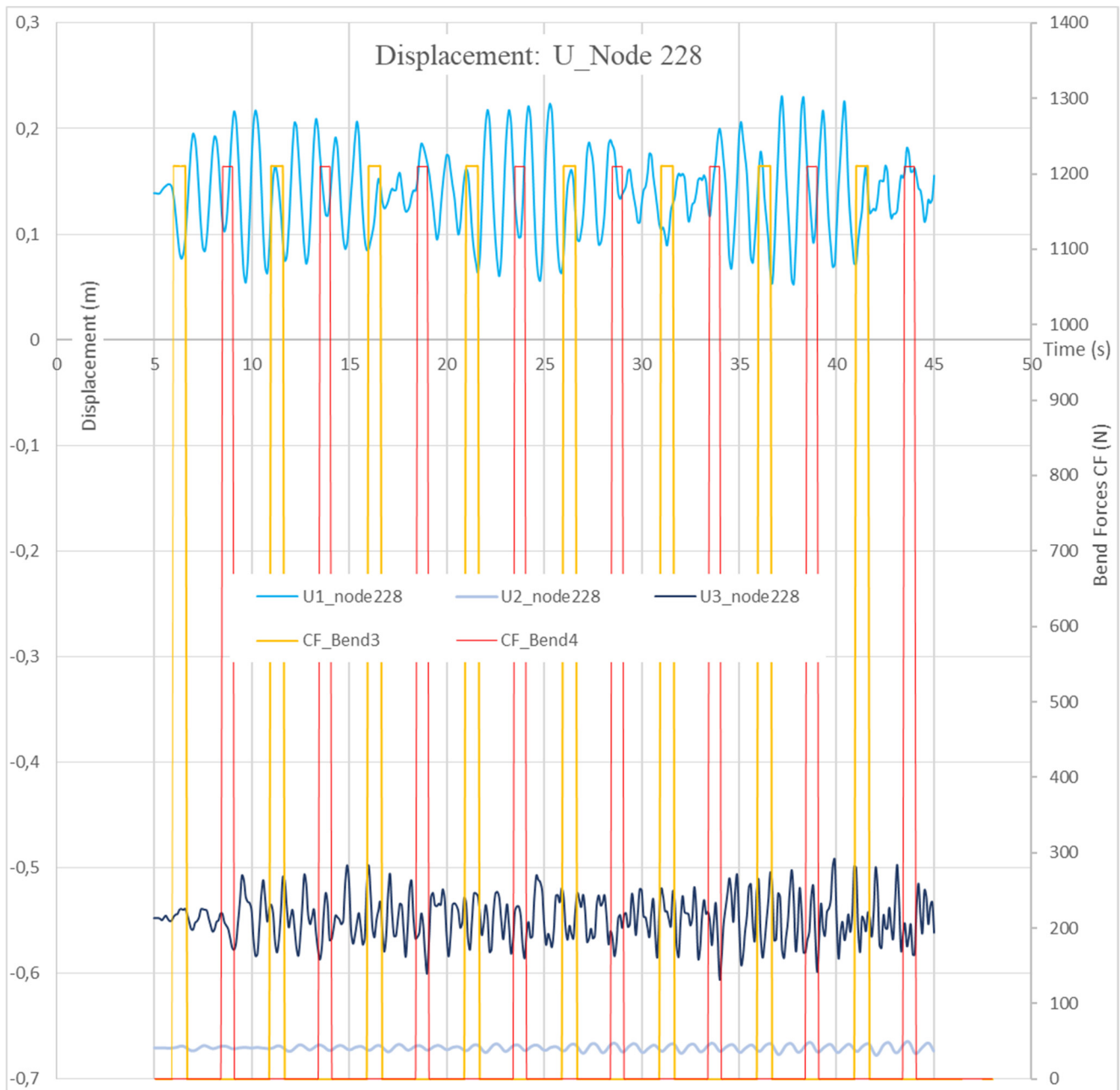


Figure 67 - Total Displacement Node 228: U1=longitudinal displacement, U2=transversal displacement, U3=vertical displacement. CF_Bend 3 = Slug Forces (Out-of-Phase) in bend 3, CF_Bend 4 = Slug Forces (In-Phase) in bend 4.

SLUG UNIT No. 4

Length **5 m**
Frequency **0,1 Hz**
Velocity **15 m/s**

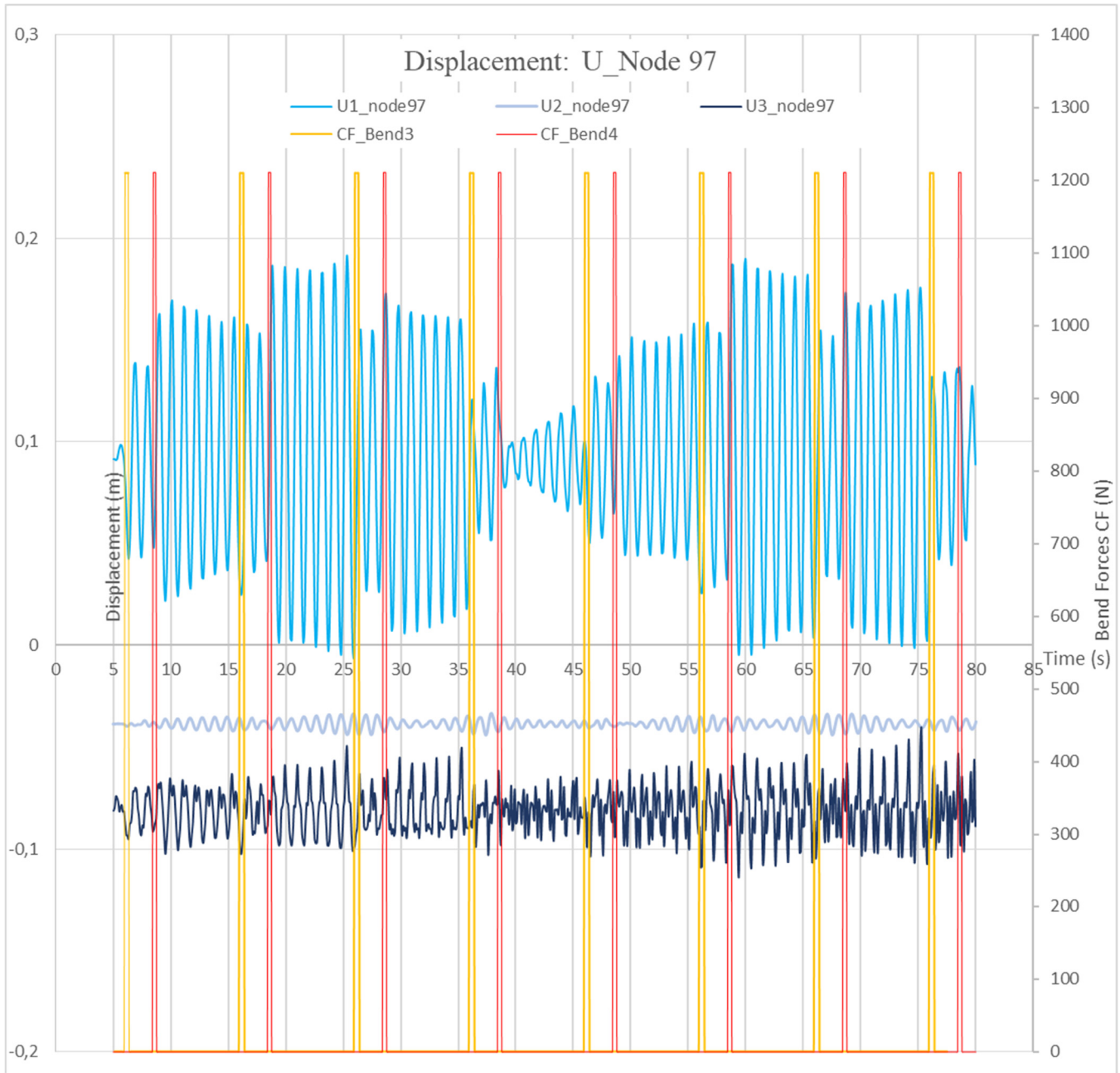


Figure 68 - Total Displacement Node 97: U1=longitudinal displacement, U2=transversal displacement, U3=vertical displacement. CF_Bend 3 = Slug Forces (In-Phase) in bend 3, CF_Bend 4 = Slug Forces (Out-of-Phase) in bend 4.

SLUG UNIT No. 4

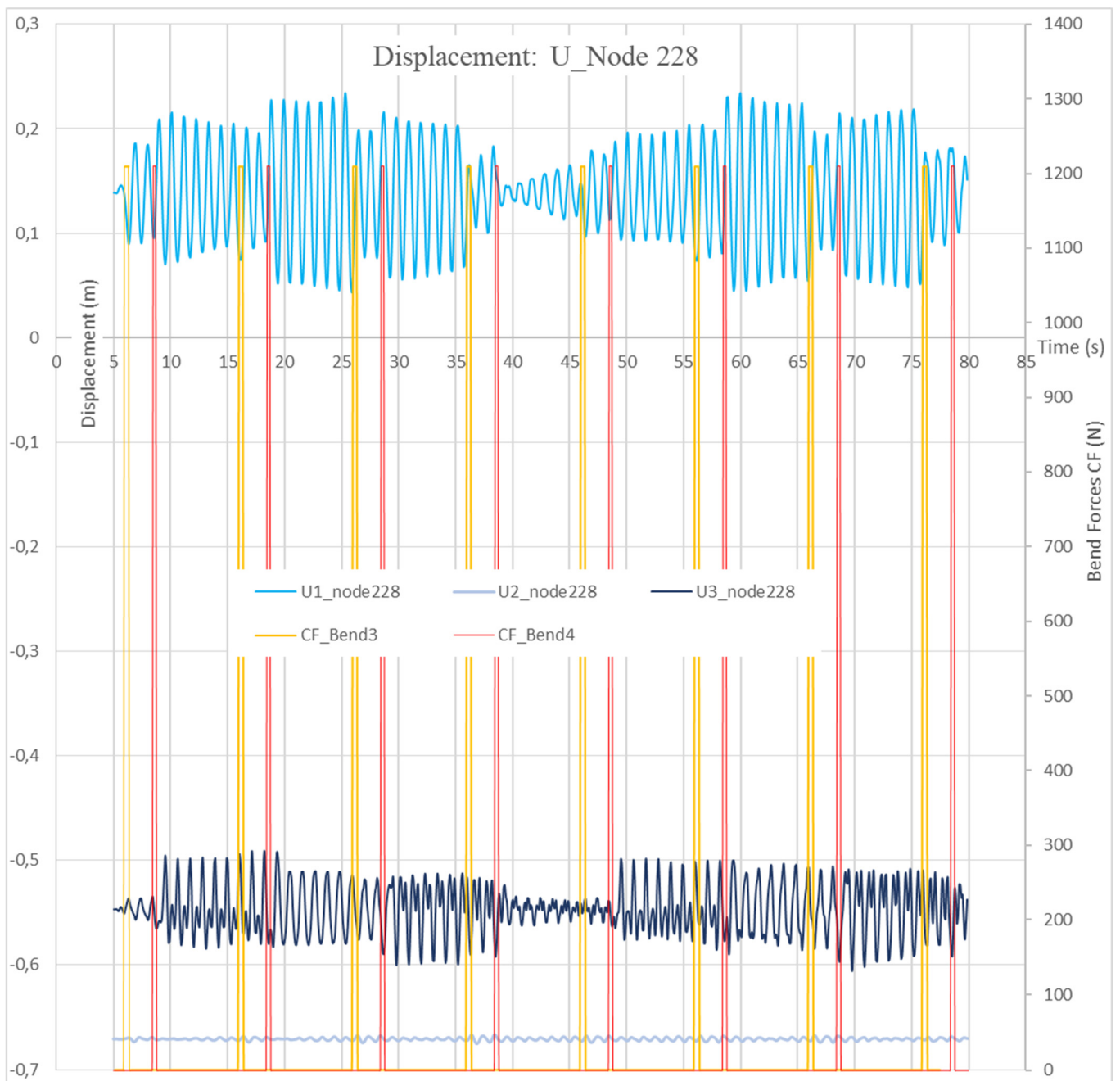


Figure 69 - Total Displacement Node 228: U1=longitudinal displacement, U2=transversal displacement, U3=vertical displacement. CF_Bend 3 = Slug Forces (Out-of-Phase) in bend 3, CF_Bend 4 = Slug Forces (In-Phase) in bend 4.

SLUG UNIT No. 5

Length **5 m**
Frequency **0,2 Hz**
Velocity **15 m/s**

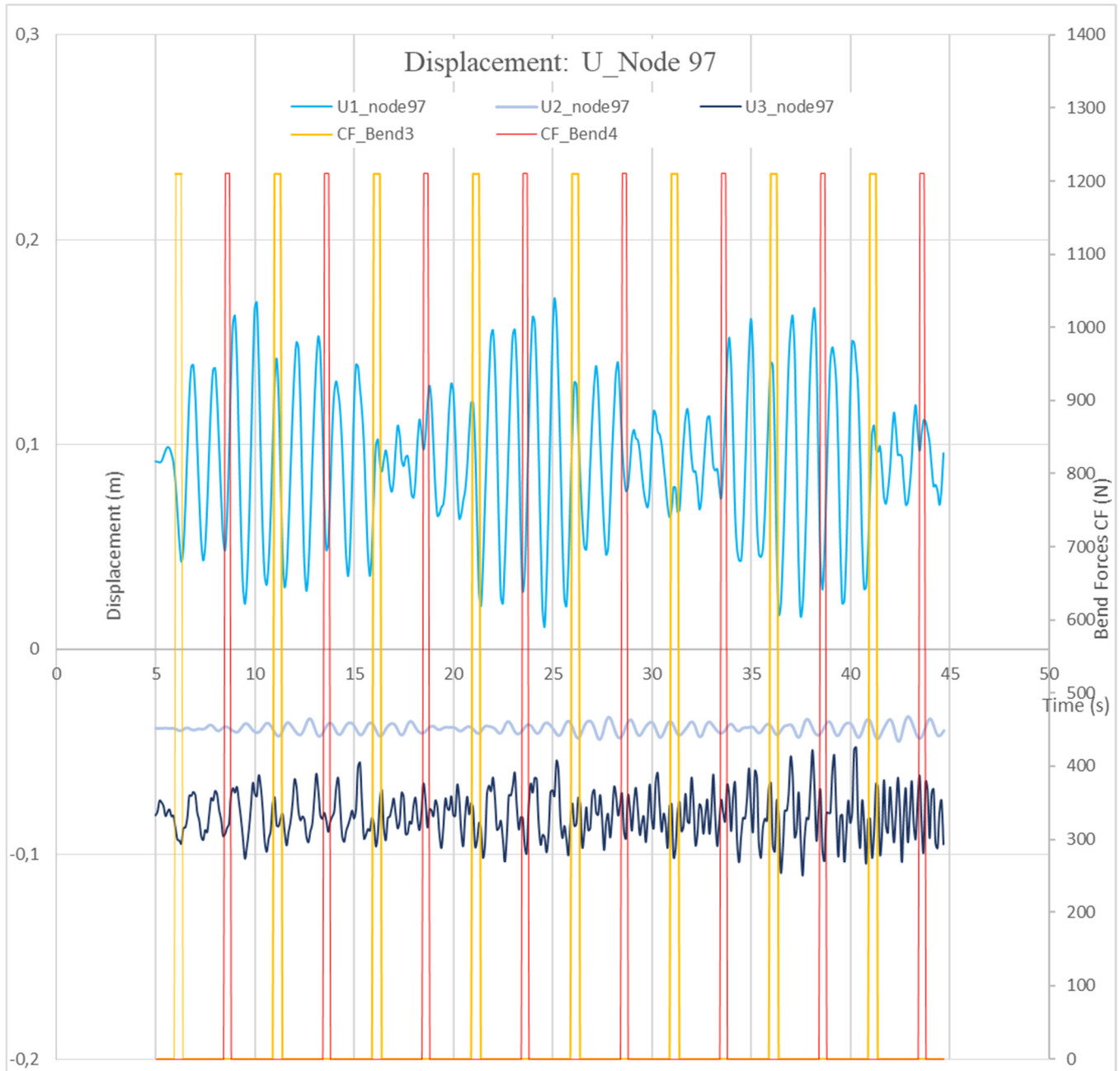


Figure 70 - Total Displacement Node 97: U1=longitudinal displacement, U2=transversal displacement, U3=vertical displacement. CF_Bend 3 = Slug Forces (In-Phase) in bend 3, CF_Bend 4 = Slug Forces (Out-of-Phase) in bend 4.

SLUG UNIT No. 5

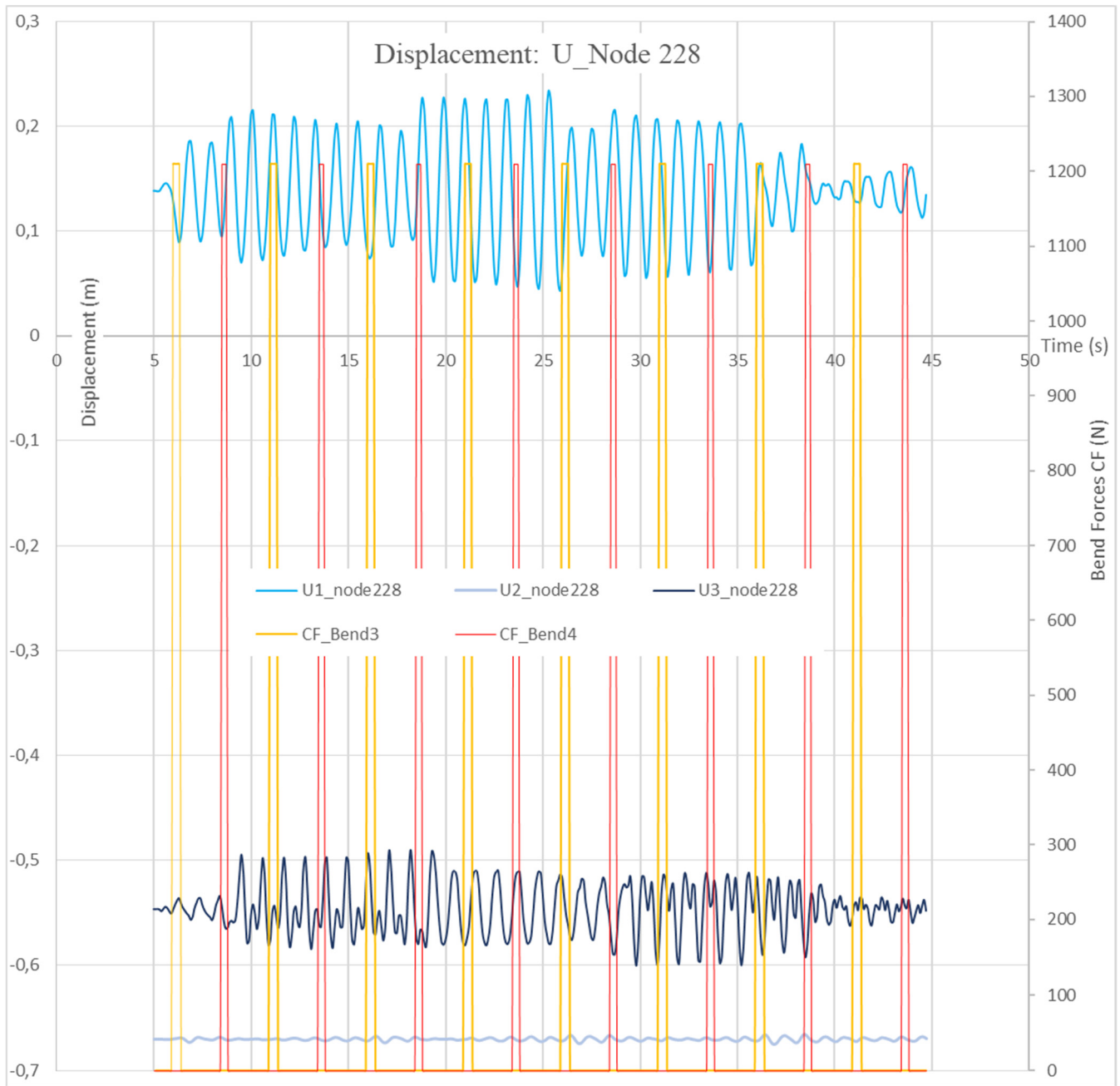


Figure 71 - Total Displacement Node 228: U1=longitudinal displacement, U2=transversal displacement, U3=vertical displacement. CF_Bend 3 = Slug Forces (Out-of-Phase) in bend 3, CF_Bend 4 = Slug Forces (In-Phase) in bend 4.

SLUG UNIT No. 6

Length **5 m**
Frequency **0,9 Hz**
Velocity **15 m/s**

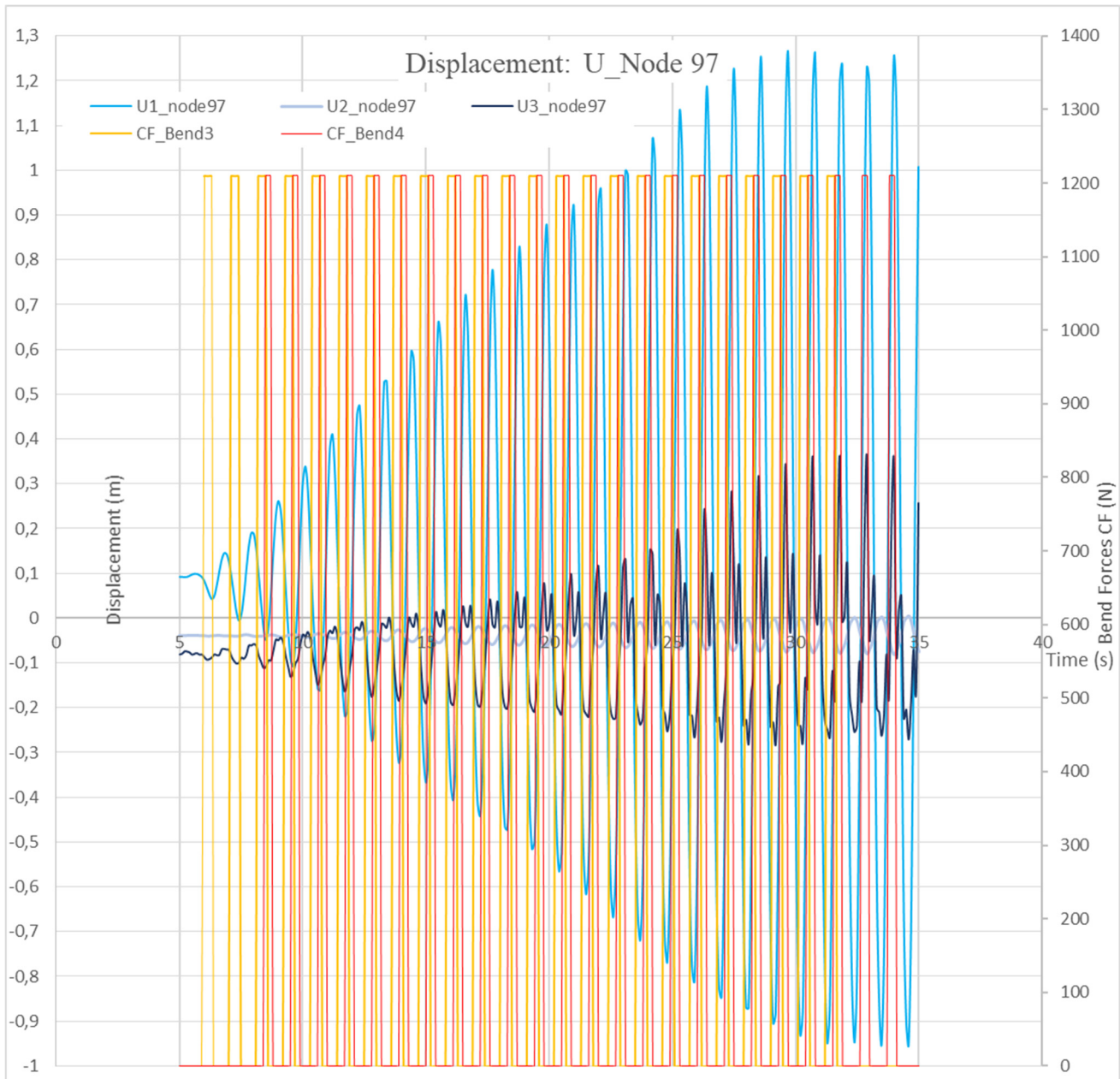


Figure 72 - Total Displacement Node 97: U1=longitudinal displacement, U2=transversal displacement, U3=vertical displacement. CF_Bend 3 = Slug Forces (In-Phase) in bend 3, CF_Bend 4 = Slug Forces (Out-of-Phase) in bend 4.

SLUG UNIT No. 6

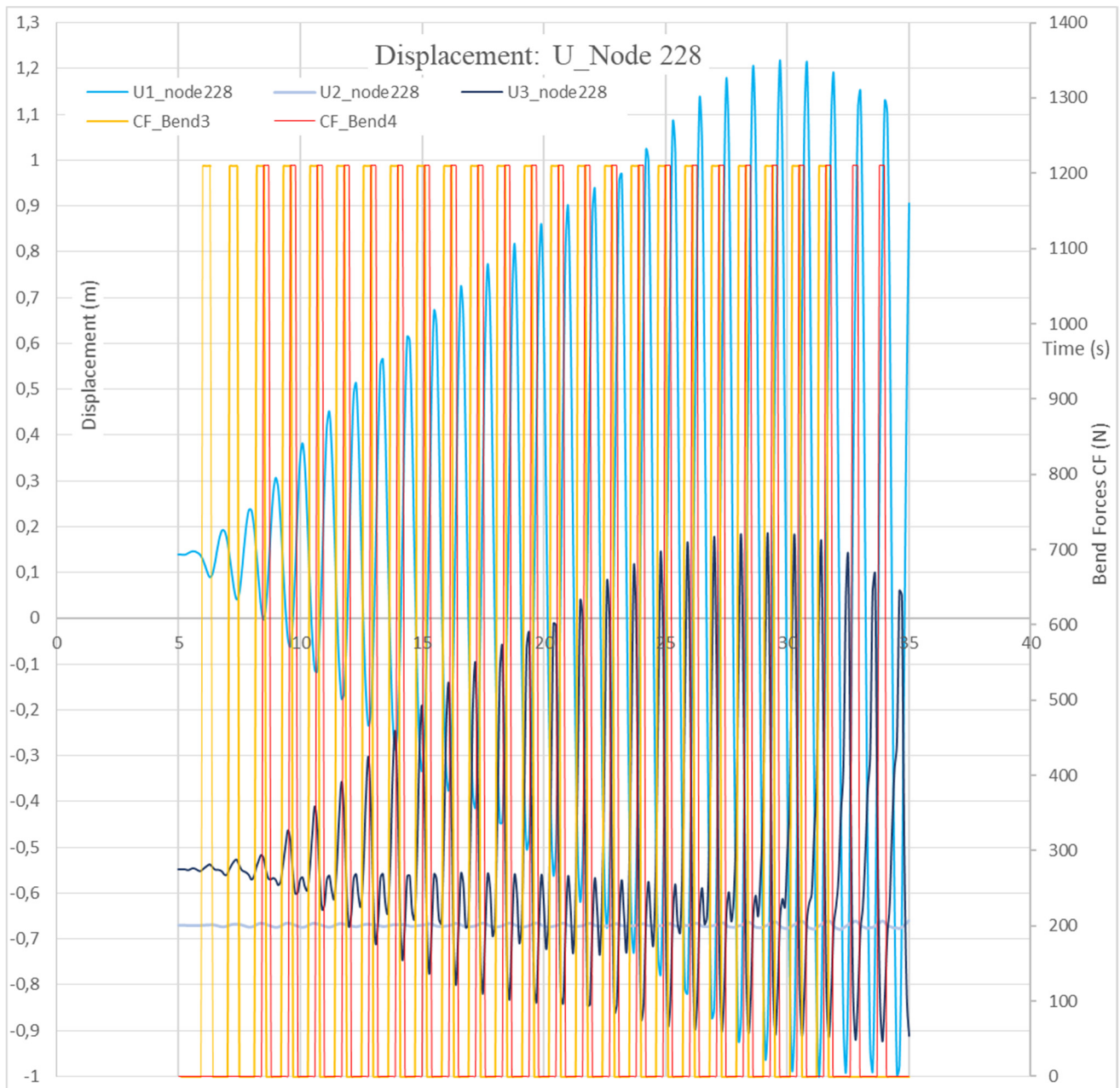


Figure 73 - Total Displacement Node 228: U1=longitudinal displacement, U2=transversal displacement, U3=vertical displacement. CF_Bend 3 = Slug Forces (Out-of-Phase) in bend 3, CF_Bend 4 = Slug Forces (In-Phase) in bend 4.

SLUG UNIT No. 7

Length **5 m**
Frequency **0,5 Hz**
Velocity **15 m/s**

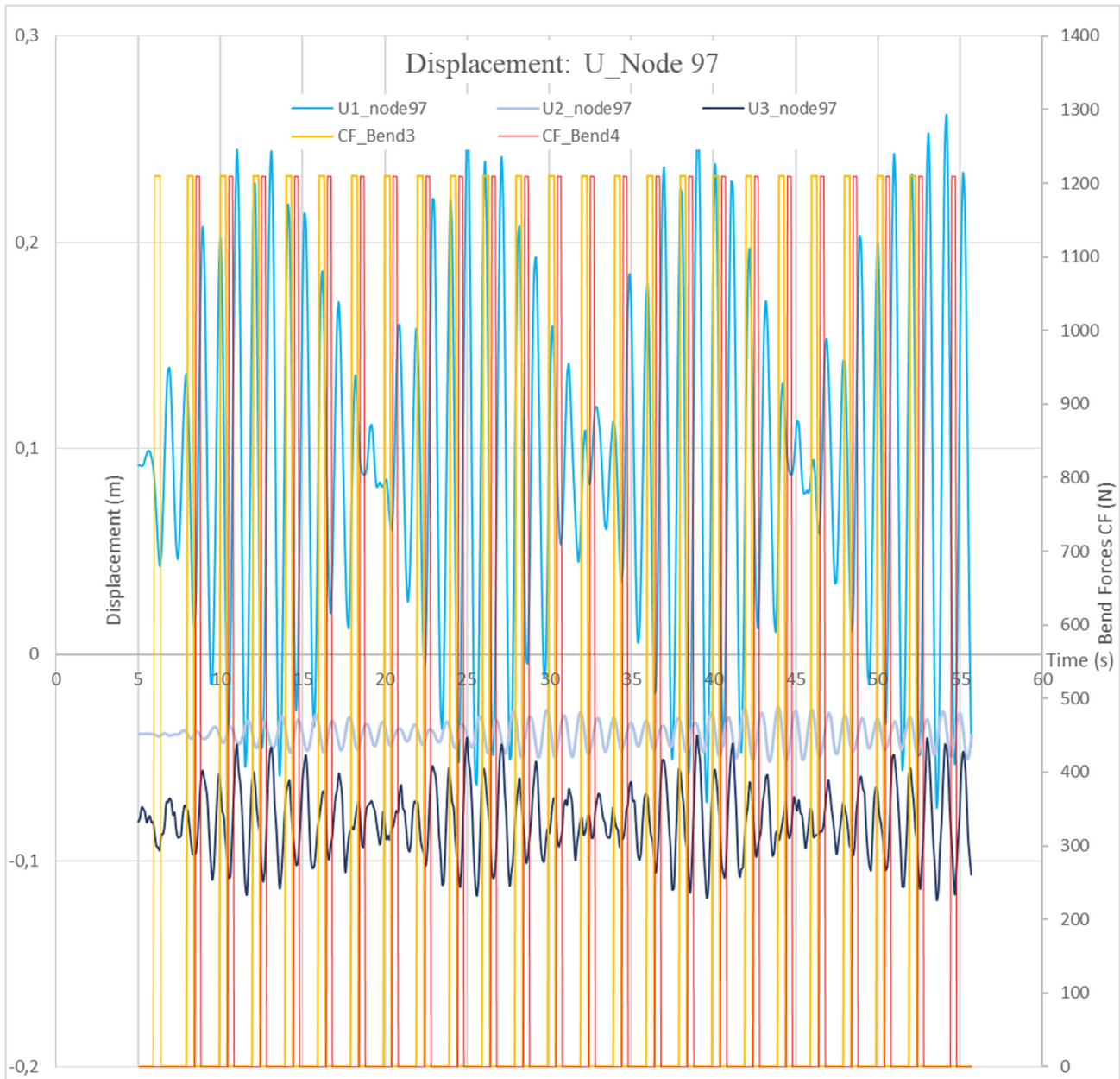


Figure 74 - Total Displacement Node 97: U1=longitudinal displacement, U2=transversal displacement, U3=vertical displacement. CF_Bend 3 = Slug Forces (In-Phase) in bend 3, CF_Bend 4 = Slug Forces (Out-of-Phase) in bend 4.

SLUG UNIT No. 7

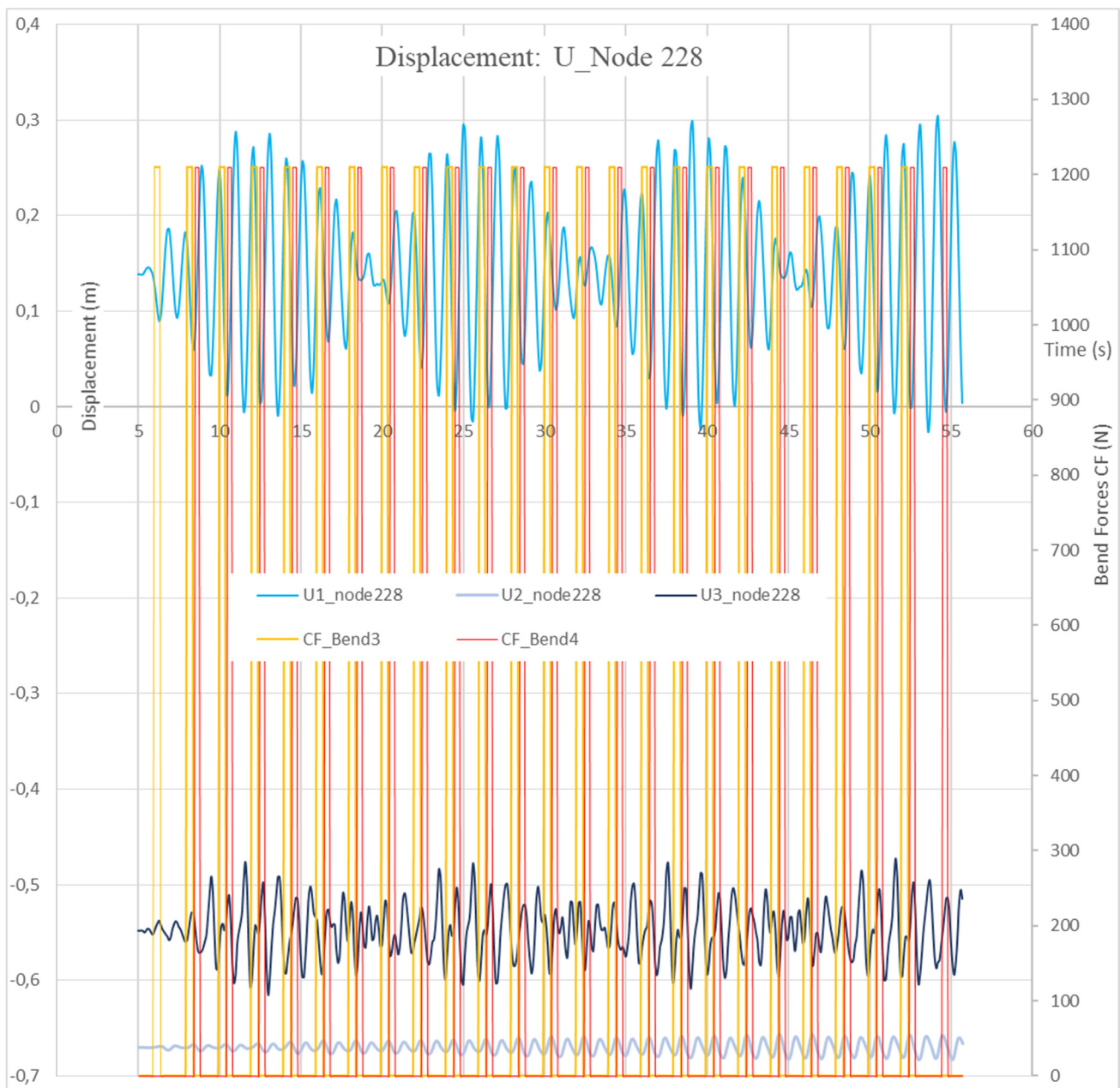


Figure 75 - Total Displacement Node 228: U1=longitudinal displacement, U2=transversal displacement, U3=vertical displacement. CF_Bend 3 = Slug Forces (Out-of-Phase) in bend 3, CF_Bend 4 = Slug Forces (In-Phase) in bend 4.

COMPARISON DISPLACEMENT U1

Node 97

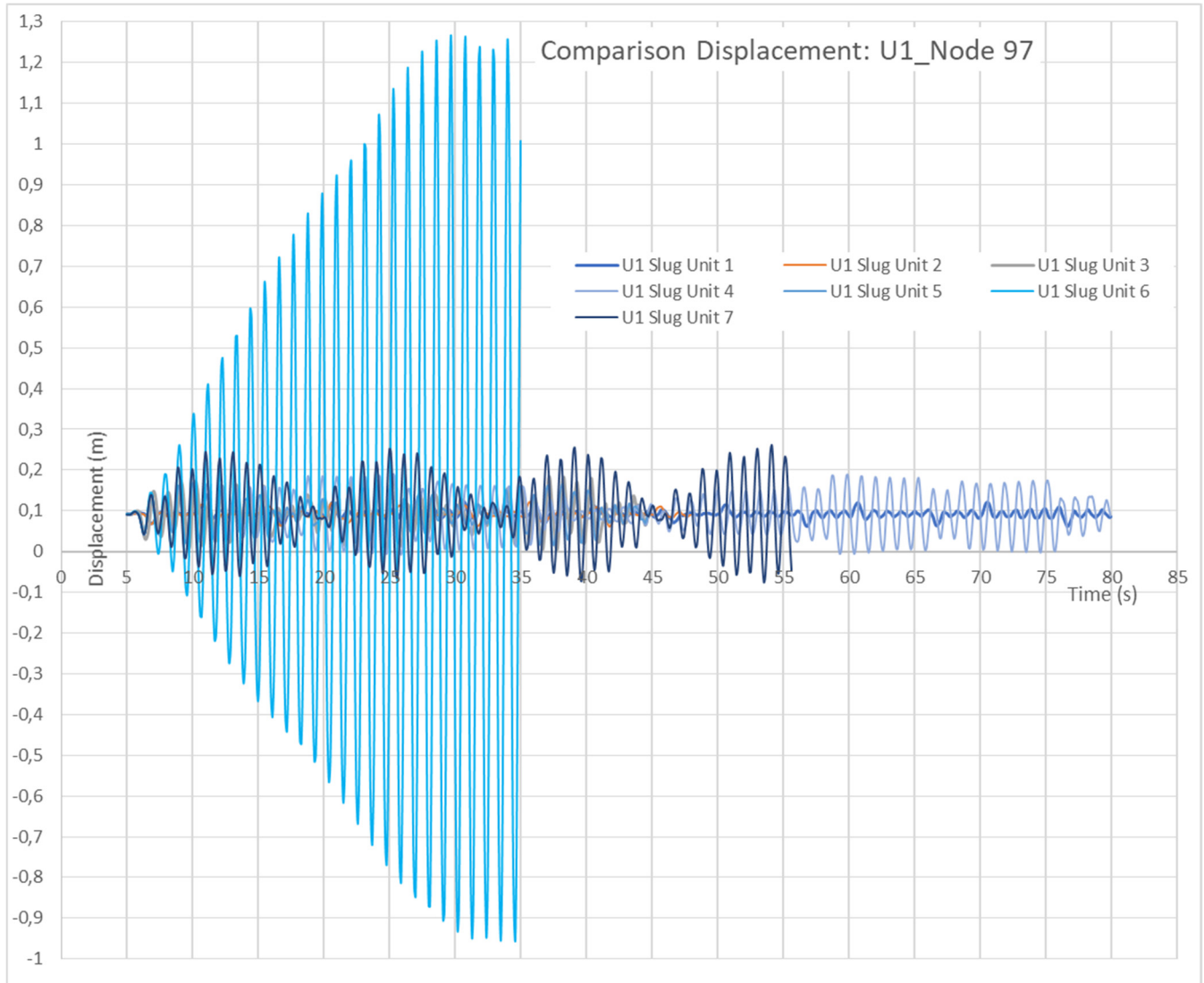


Figure 76 – Comparison Displacement (U1) Node 97 (the time history for the Slug Unit 6 is limited to the first 35 s)

Node 228

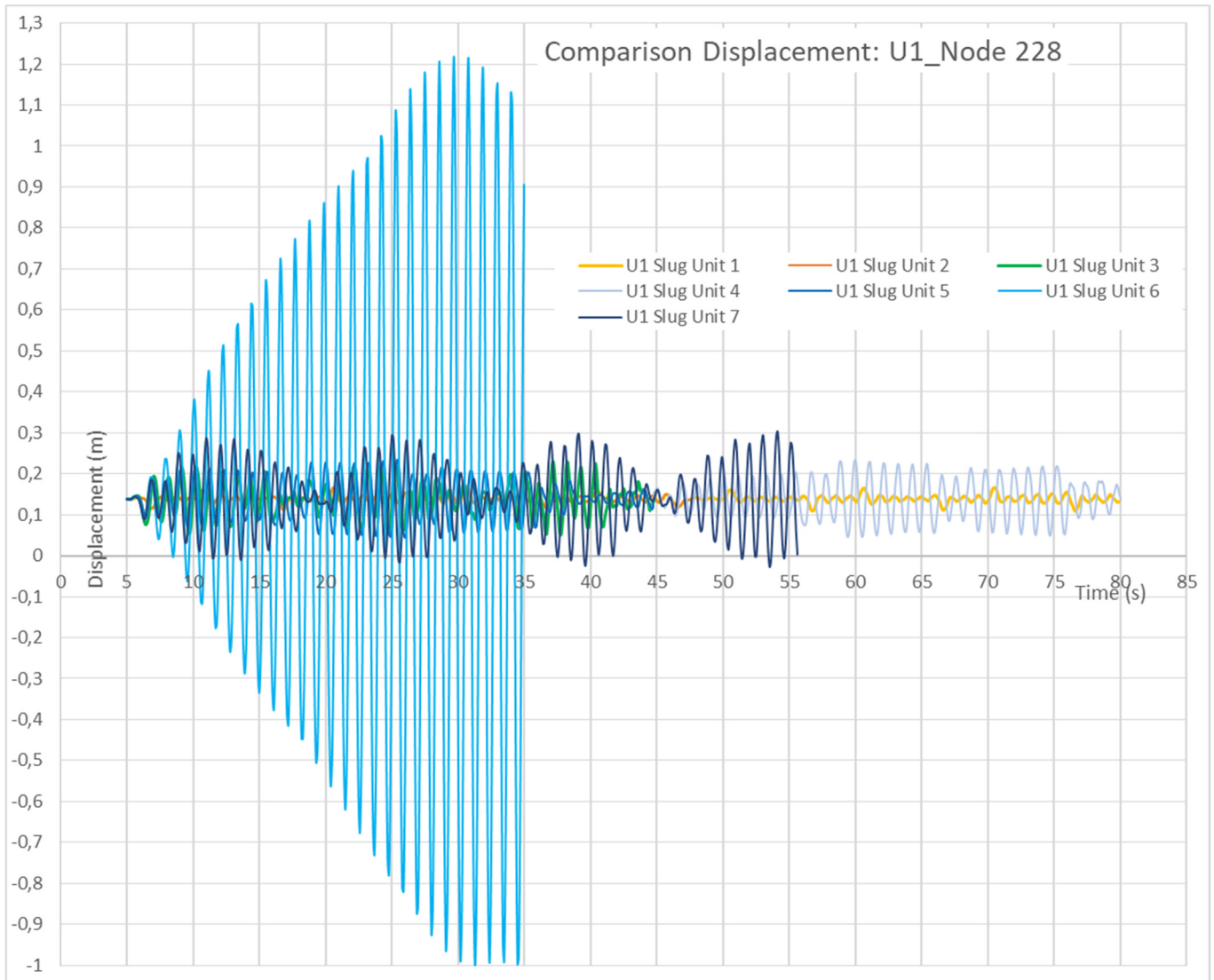


Figure 77 – Comparison Displacement (U1) Node 228 (the time history for the Slug Unit 6 is limited to the first 35 s)

This graph clearly shows that the slug with the frequency 0.9 Hz causes very high displacements.

In this case the slug mass assumes a fundamental importance. On the other hand, the mass this slug adds to the system, cannot be considered irrelevant: the moving mass cannot be ignored.

So, it is clear that the modal response assumed at the beginning of the analysis is not perfectly true and a correction of the process is required.

SLUG UNIT No. 6+slug: mass added fixed mass (and same frequency).

Length = 5 m,

Frequency = 0,9 Hz,

Velocity = 15 m/s,

Equivalent Distributed Slug Mass = 23,95 kg/m]

The modal analysis should be re-done and the frequency table updated.

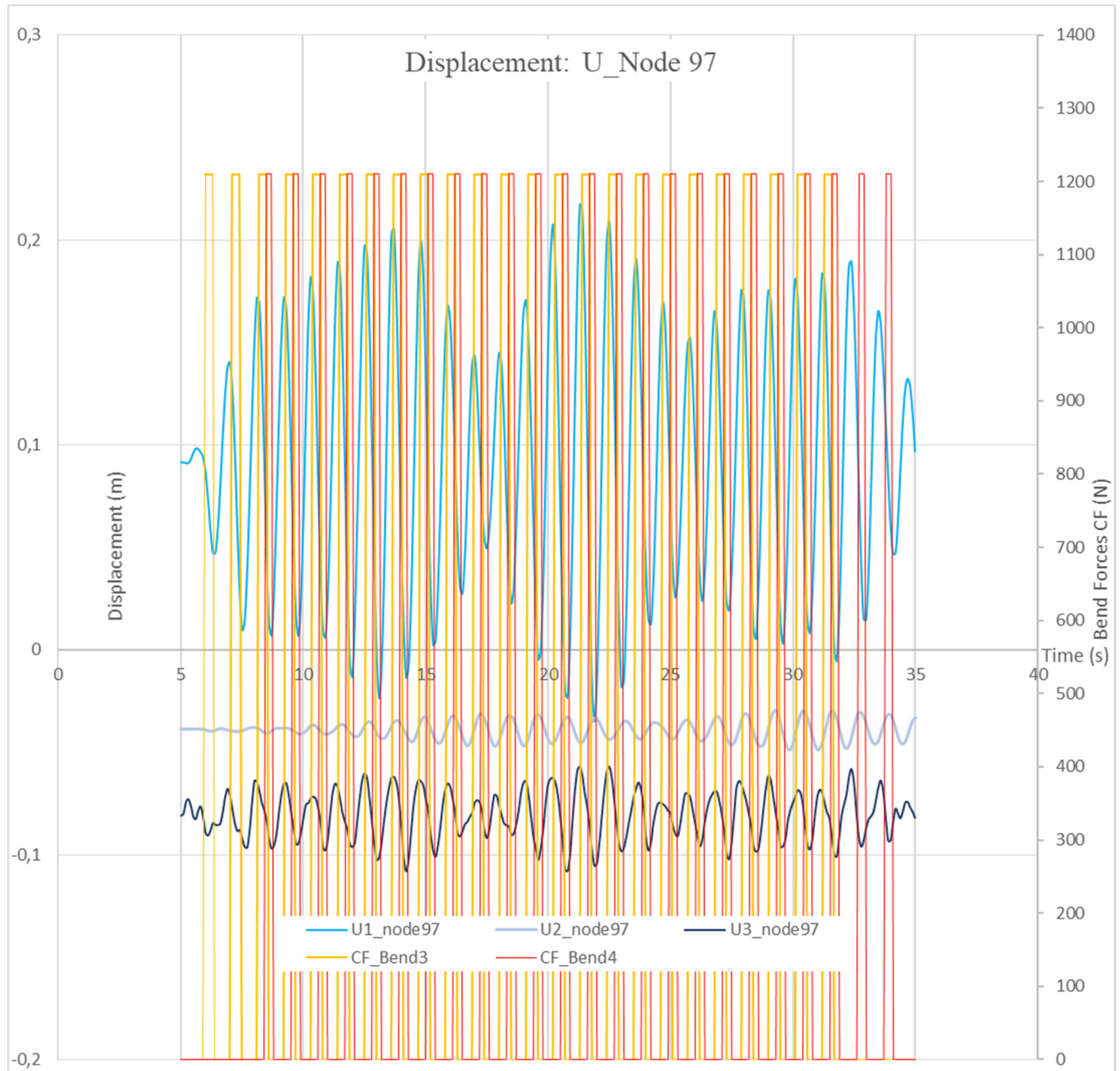


Figure 78 - Total Displacement Node 97: U1=longitudinal displacement, U2=transversal displacement, U3=vertical displacement. CF_Bend 3 = Slug Forces (In-Phase) in bend 3, CF_Bend 4 = Slug Forces (Out-of-Phase) in bend 4.

SLUG UNIT No. 6+slug: mass added fixed mass (and same frequency).

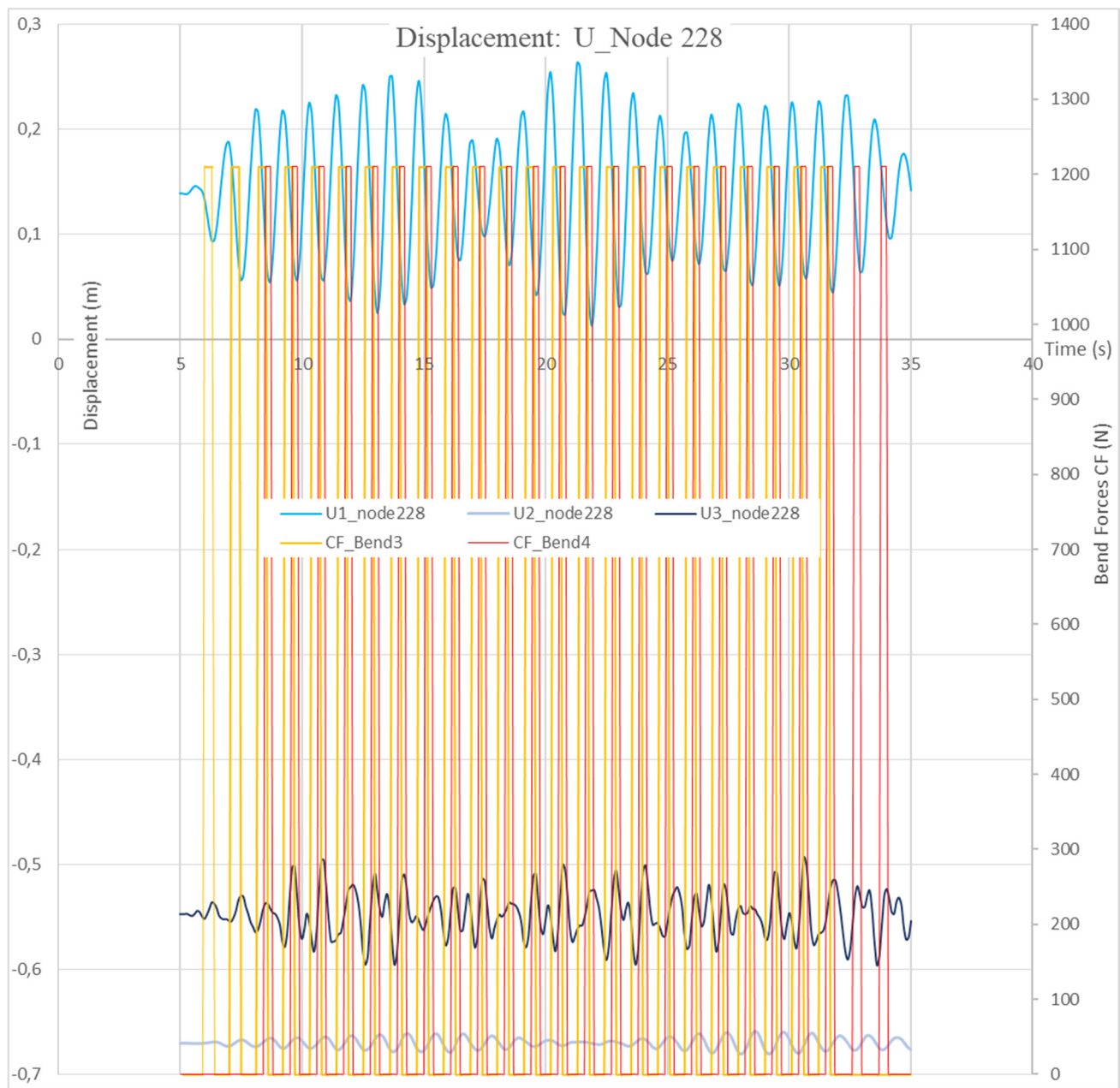


Figure 79 - Total Displacement Node 228: U1=longitudinal displacement, U2=transversal displacement, U3=vertical displacement. CF_Bend 3 = Slug Forces (Out-of-Phase) in bend 3, CF_Bend 4 = Slug Forces (In-Phase) in bend 4.

COMPARISON DISPLACEMENT U1 (with Slug Unit No. 6+Slug Mass)

Node 97

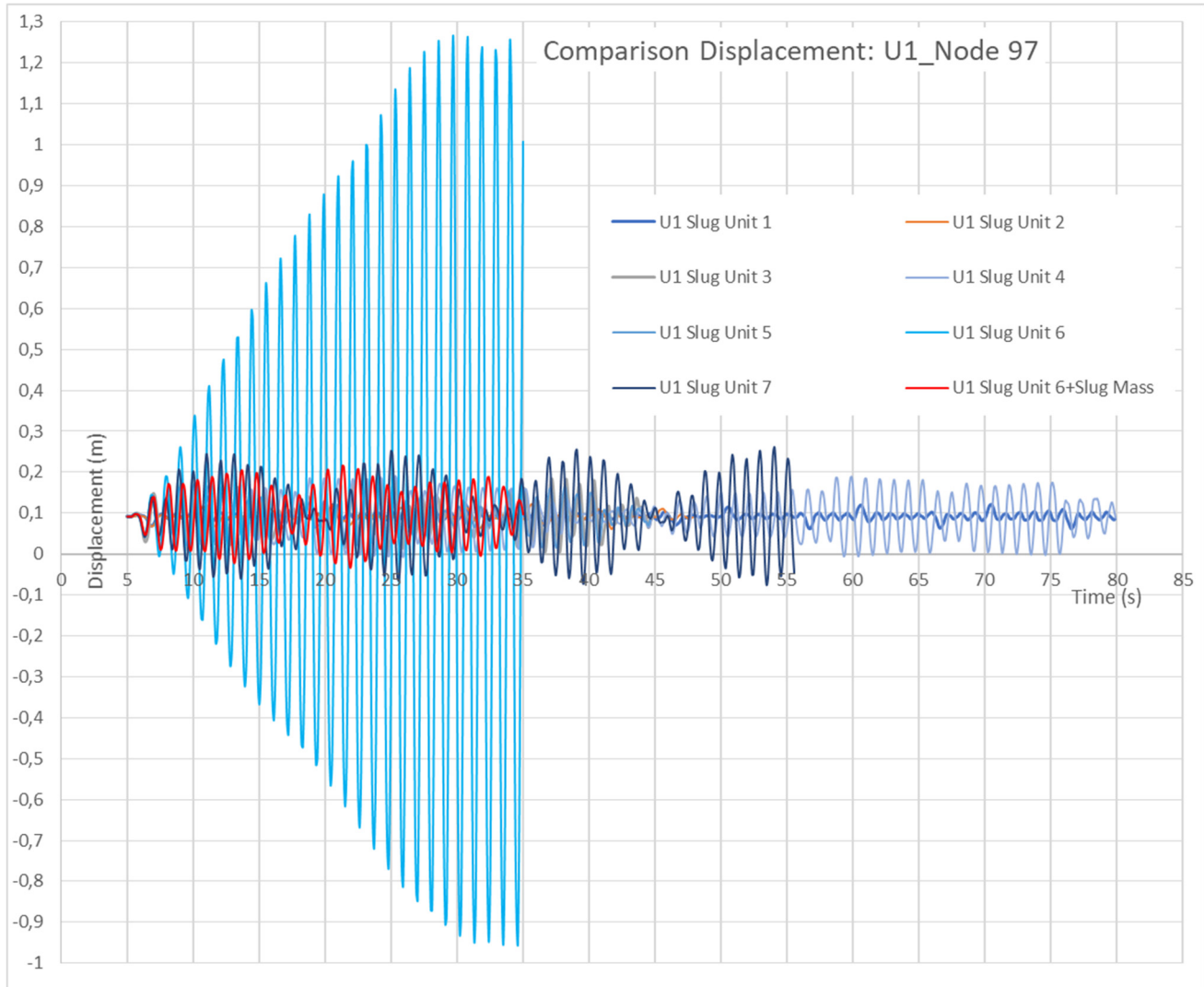


Figure 80 – Comparison Displacement (U1) Node 97 (the time history for the Slug Unit 6 is limited to the first 35 s)

Node 228

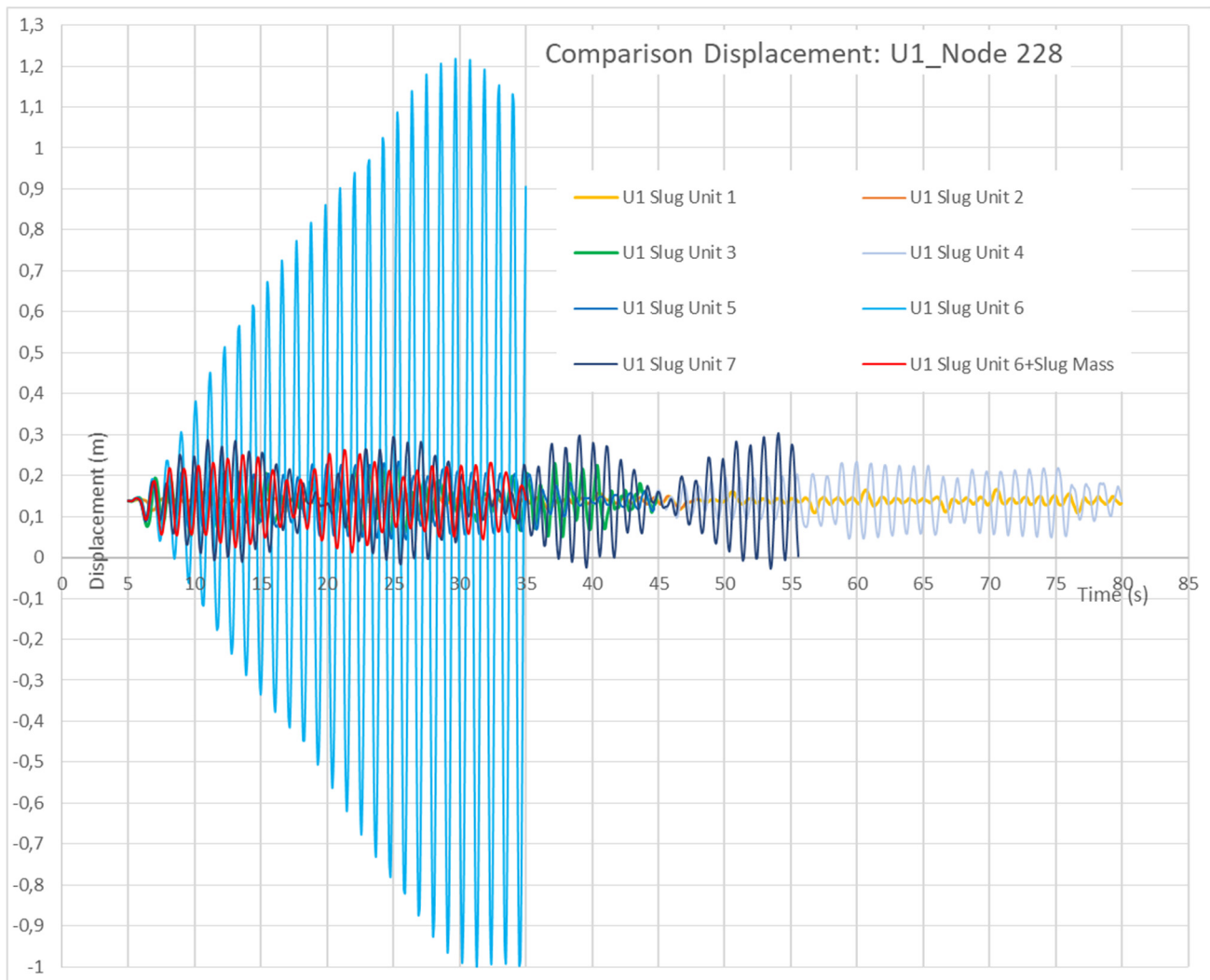


Figure 81 – Comparison Displacement (U1) Node 97 (the time history for the Slug Unit 6 is limited to the first 35 s)

The above graphs clearly show that the out-of-plane behavior (transverse displacements U2, U3) is irrelevant compared to the in-plane behavior (U1). In addition, there is an evident synchrony between the displacement peaks and the passage of force in the curves.

The investigation of the various cases of slug regimes shows the sensitivity of the system near the modal frequencies. In fact, when the slug frequency is 0.9 Hz, very close to the mode 4 natural frequency, the displacements become of the order of 1 m.

On the other hand, these slugs are spatially very close, so that the hypothesis of **massless load seems to be inaccurate**. Therefore, the model can be improved, by adding an equivalent *fixed uniform distributed mass* along the pipes. The result is that the displacements are drastically reduced, because the increase of the total mass of the jumper by 5-10 %, moves away the forcing loads from the new natural frequency.

Finally, an approximated global procedure is devised to exploit the information obtained from a specific designed *sequence* of modal analysis, correlated by *different* slug regimes, for the identification of the more severe loading condition, as follows.

6.3.3. CRITICAL CASES IDENTIFICATION PROTOCOL

At this stage, the real question is to avoid a *vicious circle*: the structure is excited near a modal frequency resonance, depending on the frequency of the slug train; on the other hand, the mass of the slug train (that should be considered belonging to the structure) influences the modes of the structure.

The problem can be coped with the following reducing procedure:

1. **Identify** the fundamental **frequency**, $\nu_1[St_i]$, of each type of **slug train**, St_i ; together with the possible more significant subsequent harmonics, via Fourier analysis.
2. **Assign**, to each St_i , a value of its distributed **equivalent mass** in the classes, M_k , obtained by a discretization of the possible masses.
3. **Add** these distributed masses to the basic structure, obtaining a **sequence of Modal Analysis**, MA_k , for each classes of the mass-structure association.
4. **Intersect** the frequencies $\nu_1[St_i]$ of the slug trains St_i (and, possibly, its harmonics) with the frequency in MA_k , taking into account the **pertinence of the association** Slug-train \leftrightarrow Modal Analysis.

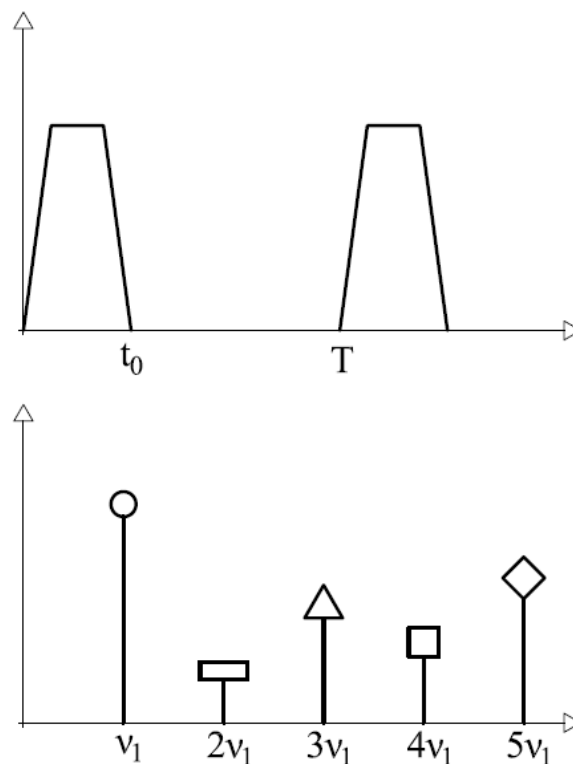


Figure 82 – Step 1a: Fourier harmonics of the periodic slug train

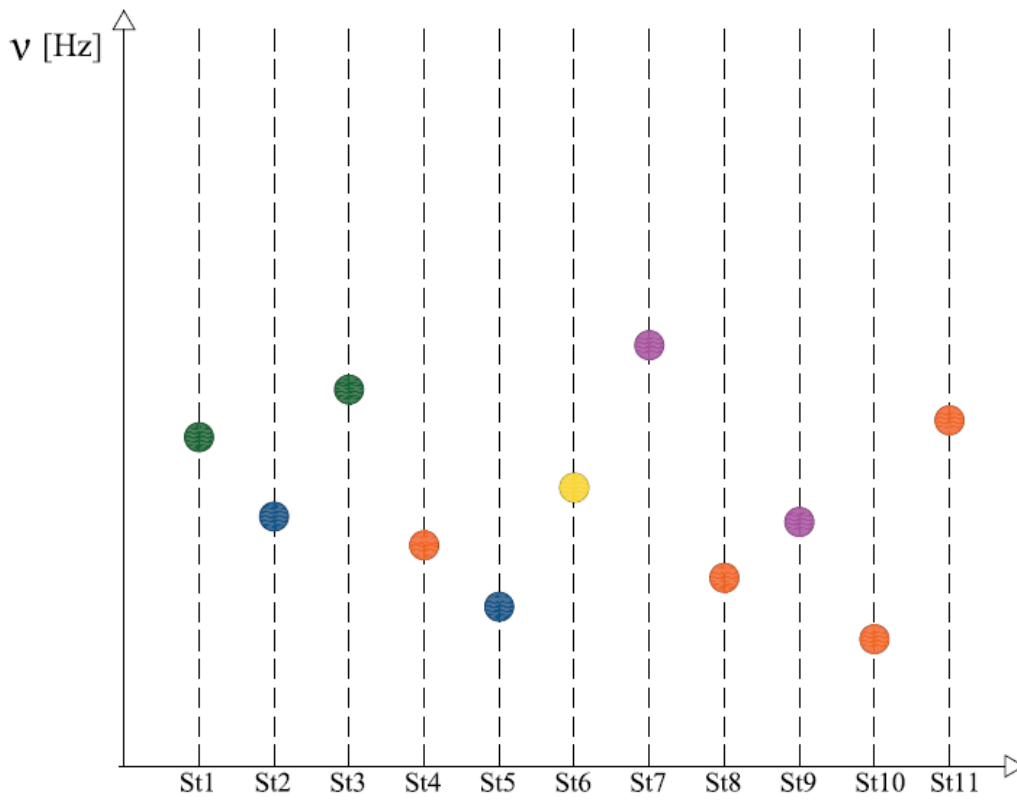


Figure 83 - **Step 1b**: First (fundamental) **harmonic frequency** of each Slug Train

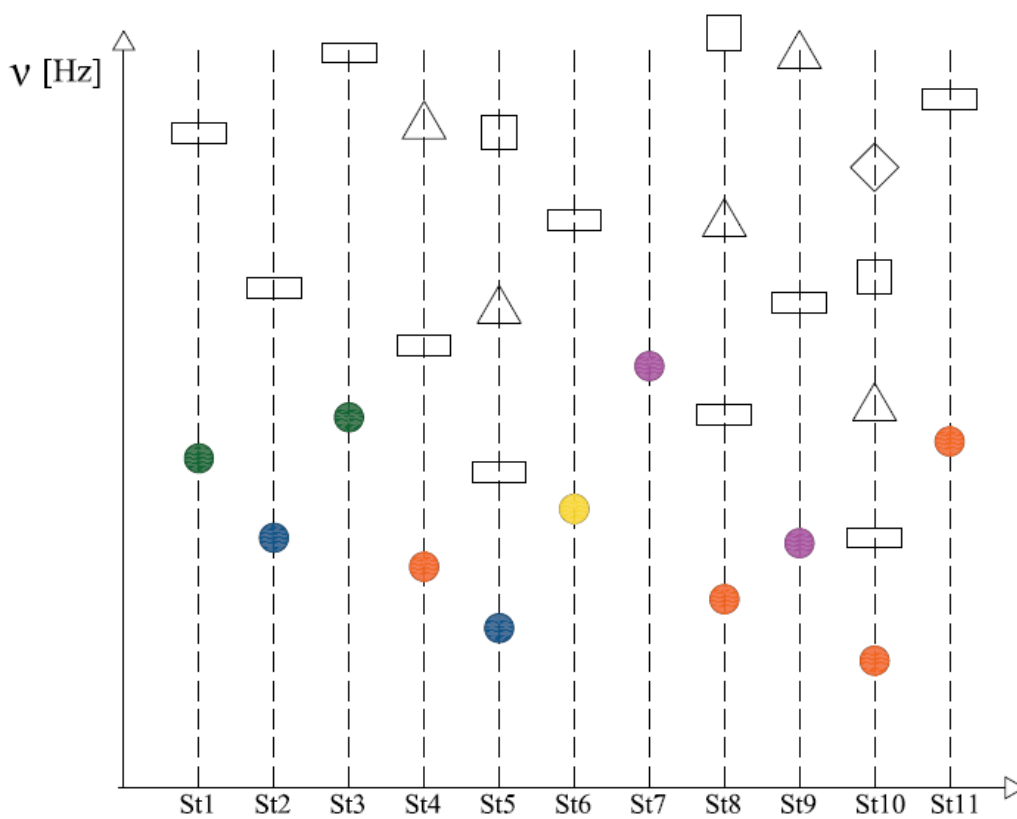


Figure 84 - **Step 1b**: First five **harmonics** of each Slug Train

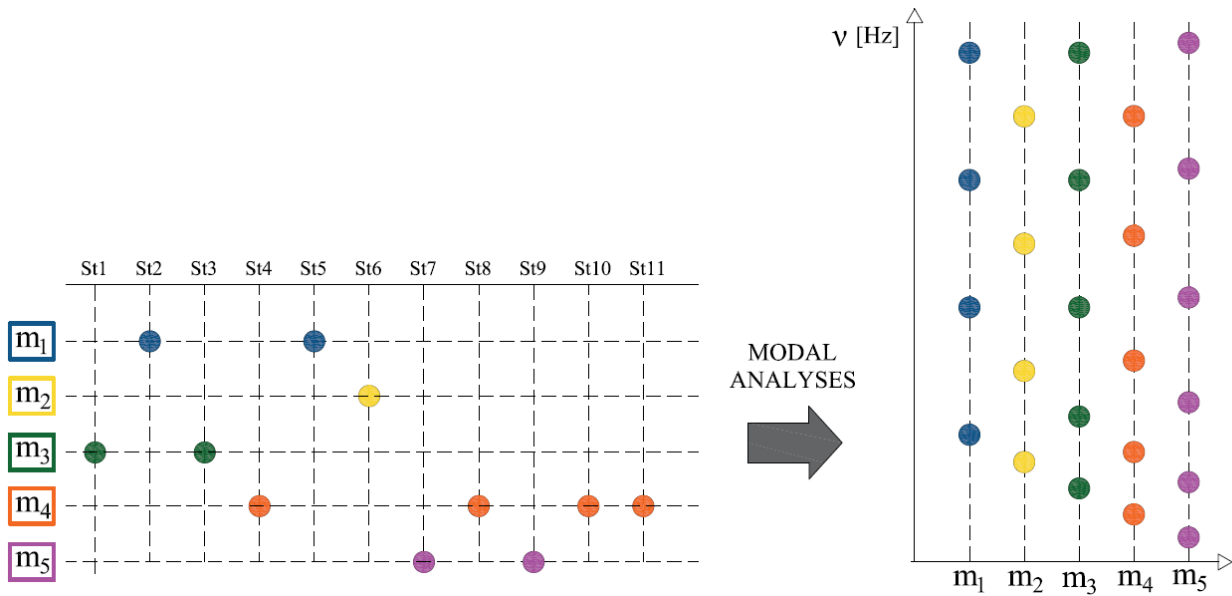


Figure 85 – **Step 2:** Assignment of a mass-class of each Slug Train, $m_1 < m_2 < m_3 < m_4 < m_5$ (left);

Step 3: Modal Analyses of the mass-class structures (right)

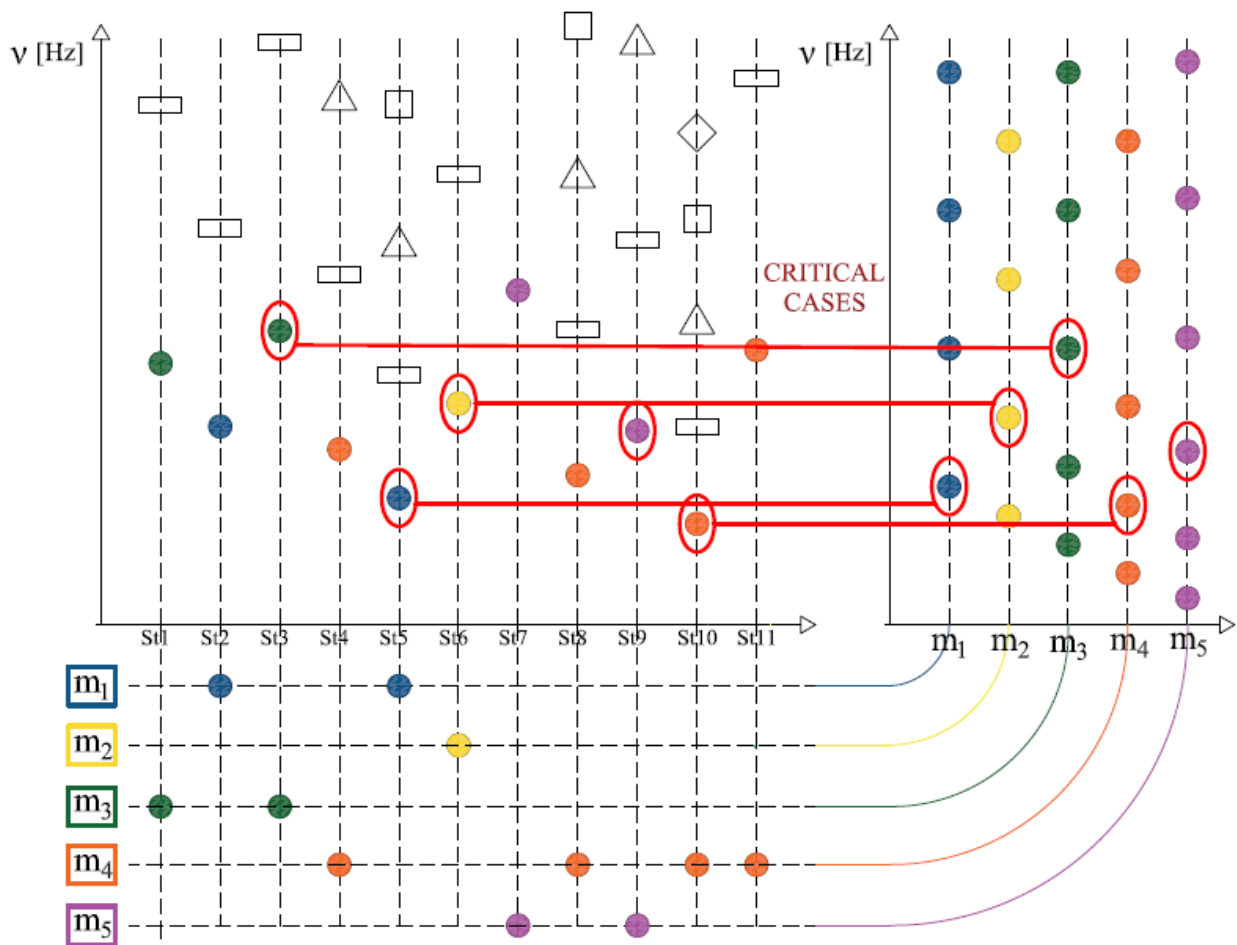


Figure 86 – **Step 4:** Identification of **Critical Cases**: association of Slug Train frequencies with the natural frequencies of the appropriate mass-class structures

CHAPTER 7: CONCLUSIONS AND FUTURE STUDIES

An important and increasingly required aspect to take into account in the project of the jumpers is the effects of the slug flow.

The study of this regime is currently done by decoupling the definition of loads from the dynamic response of the structure. In this way, the interaction of the structure with the internal fluid is reduced to the forces it exerts on structure.

For instance, a dynamic modal analysis of the studied structure shows that mode 4, characterized by a frequency of 0.88634 Hz, causes a resonance, with an order of magnitude of the displacement of 1 m. Nevertheless, the slug mass influences the modal response of the jumper. The results, show also that the out-of-plane behavior (transverse displacements U2, U3) is irrelevant compared to the in-plane behavior (U1). In addition, there is an evident synchrony between the displacement peaks and the passage of force in the curves.

Notwithstanding case 6 is an **extreme condition**, it clearly shows the paramount importance of considering the mass that generated the resonance, hither to ignored in the structural analysis. So, it is clear that the modal response assumed at the beginning is not correct altogether. Strictly speaking, the modal analysis should be redone, and so on!

On the other hand, these slugs are spatially very close, so that the hypothesis of **massless load seems to be inaccurate**. Therefore, the model can be improved, by adding an equivalent *fixed uniform distributed mass* along the pipes. The result is that the displacements are drastically reduced, because the increase of the total mass of the jumper by 5-10 %, moves away the forcing loads from the new natural frequency. Finally, an approximated global procedure is devised (**Critical cases identification protocol**) to exploit the information obtained from a specific designed *sequence* of modal analysis, correlated by *different* slug regimes, for the identification of the more severe loading condition.

Future studies

A critical review of the obtained results, suggest possible future enhancements:

1. Changes of the model

An alternative to the step-by-step integration method is the *integration in modal variables*, which could significantly reduce the calculation time. Furthermore, it can be assessed whether hybrid elements can be reliably substituted by ordinary beam elements.

2. Validation of the proposed procedure

The proposed protocol can be validated by a series of non-linear analysis, of the configurations identified as severe.

3. Spectral Analysis

The steady-state response of the structure under indefinite slug trains could be described by a *Spectral characterization* of the slug regimes. If in these cases the response of the structure can be reliably assumed to be linear (in small

displacement), then a spectral analysis could greatly simplify the detection of the critical conditions. Of course, in order to make spectral analysis, one must "build" the spectrum.

4. Parametric Resonance

The approximate approach currently adopted, namely the uncoupling of the structural behavior from the moving slug mass, can be overcome using the theoretical tools discussed within the scope of the Hill and Matthieu dynamic stability problem.

APPENDIX A: ABAQUS™

A.1. BACKGROUND

ABAQUS (Simulia) is a Multiphysics suite of simulation programs based on the **finite element method** (FEA), capable of solving problems ranging from linear analysis (very simple) to the most difficult non-linear and coupled simulations. Designed as a general purpose tool, Abaqus can be used to study structural problems and obtain complete *force-displacement-acceleration response*. A complete analysis in Abaqus usually consists of three distinct phases: **pre-processing**, **simulation** and **post-processing**.

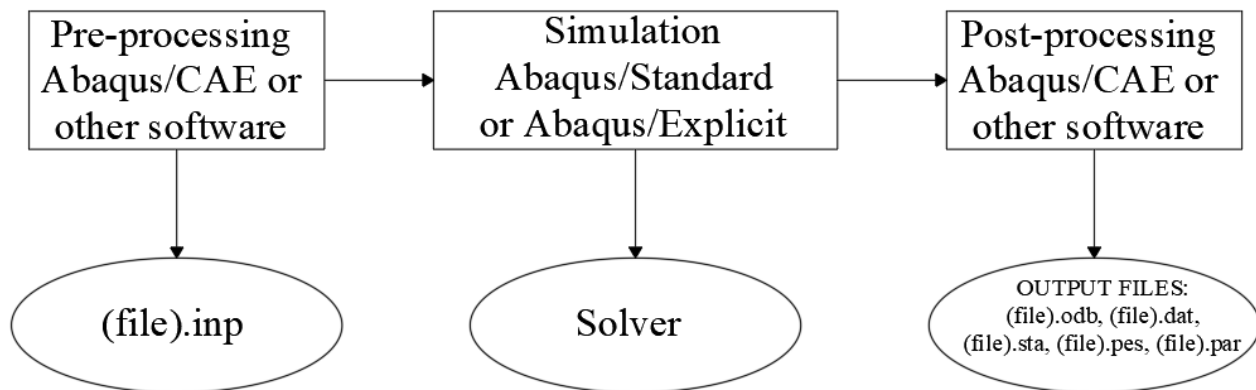


Figure A.1 - Chart: Analysis Phases with ABAQUS

With:

- **Abaqus/CAE (Pre-processing):** *Complete Abaqus Environment*. It provides a simple interface for *creating the model* and is divided into modules, which define a logical aspect of the modeling process (Part, Material, Sections ...).
- **Abaqus/CAE (Post-processing):** It reads the results of the binary output file of the database and has a variety of options for *displaying results, including animations, deformed graphs, and X-Y graphs*.

PRE-PROCESSING

At this step, you have to define the model of the physical problem and create an Abaqus input file. The information required for the model analysis are: geometry, section properties, elements and materials, loads and boundary conditions, type of analysis and output requests.

A more efficient and robust way to generate the model (of part of it) is to write the input instructions in a *script* file, with possible exploiting the facilities of an integrated environment (Matlab) of an electronic sheet (Excel).

GEOMETRY

Finite elements and **nodes** define the basic geometry of the physical structure. In this thesis, the geometry of the jumper has been defined through an excel file that is read, in a second moment, from Matlab (**GUI=Graphical User Interface**). Therefore, geometry will be built using an algorithm (vertex→nodes and lines→element).

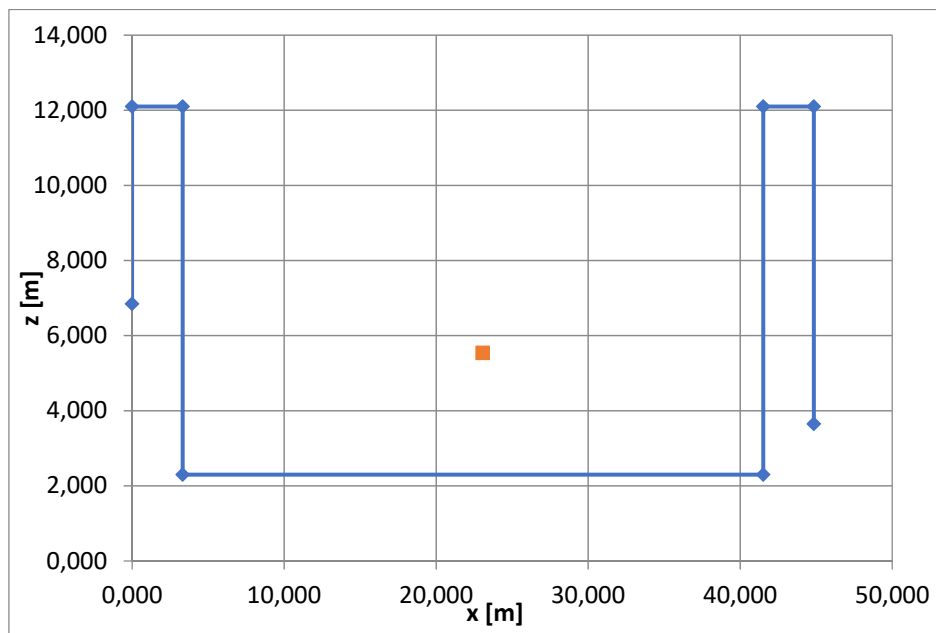
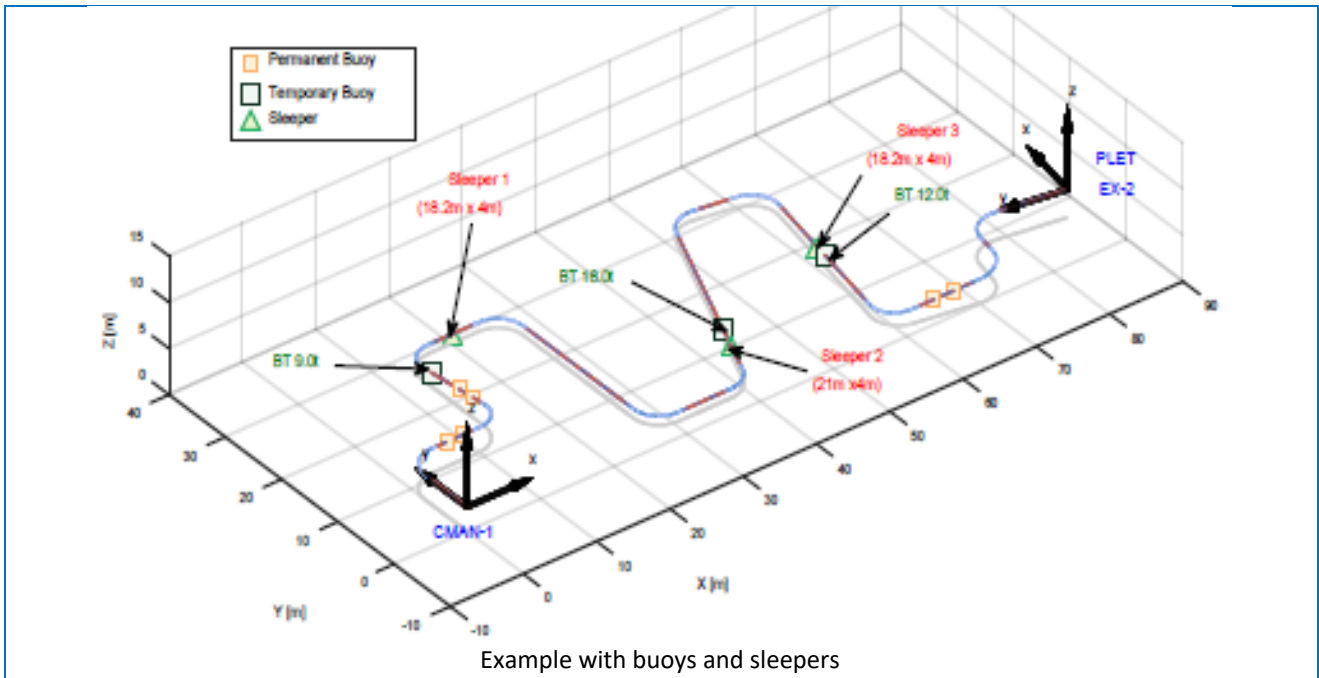
	Coordinates			Bends		Buoyancy			Length	Sleeper		
	East (x)	North (y)	z	Radius	Tangent Length	Buoy	Weight submerged	Permanent Buoy		Distance from Vertex	Sleeper Height from Seabed	Sleeper Width
	[m]	[m]	[m]	[m]	[m]	[m]	[kg]	[-]		[m]	[m]	[m]
V1	0,000	0,000	6,847	0	0				5,25			
V2	0,000	0,000	12,100	0,972	0,323				3,32			
V3	3,320	0,000	12,100	0,972	0,323				9,80			
V4	3,320	0,000	2,300	0,972	0,323				38,20			
V5	41,520	0,000	2,300	0,972	0,323				9,80			
V6	41,520	0,000	12,100	0,972	0,323				3,32			
V7	44,840	0,000	12,100	0,972	0,323				8,45			
V8	44,840	0,000	3,650	0	0							

Buoyancy data

Buoyancy modules are modelled as uplift forces with net buoyancy during the static analysis. For modal and seismic analysis also the mass of the buoyancy is considered with the relative drag load and added mass coefficients.

Sleepers data

The data to be entered are: sleeper position, sleeper bearing capacity and stability and eccentricity and spool displacements on the sleeper.



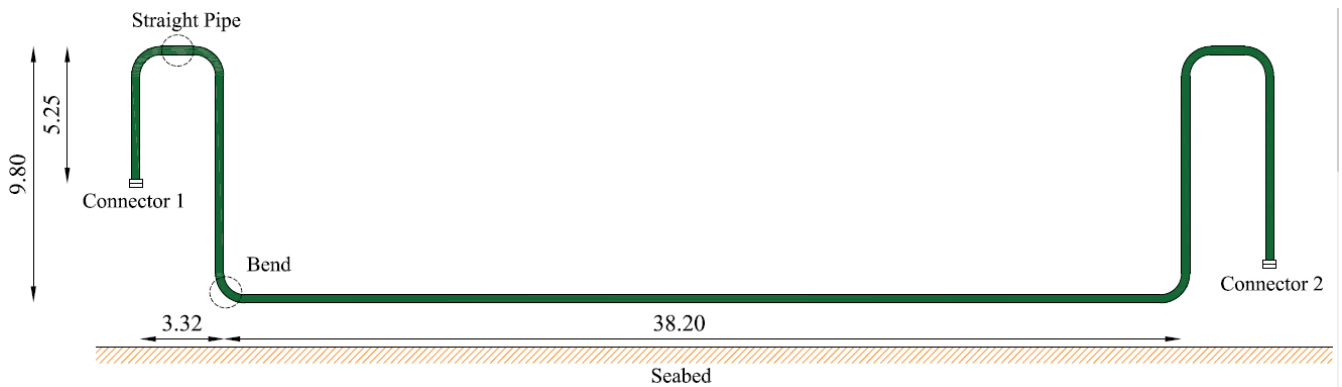


Figure A.2 - Jumper Geometry

Shared nodes connect the elements to each other. The set of all elements and nodes is the **mesh**. Generally, the mesh will only approximate the real structure geometry. The type of element, shape and position, as well as the total number of elements used, influence the results obtained from the simulation. The higher density of the mesh (i.e., the greater the number of elements), the more accurate the results. As the mesh density increases, the analysis results converge to one solution and the time required to process an analysis increases.

Usually a good way to define the mesh is to do a **sensitivity analysis**, i.e. do the same analyses with the same configuration but going to reduce the mesh and look at the results behaviour.

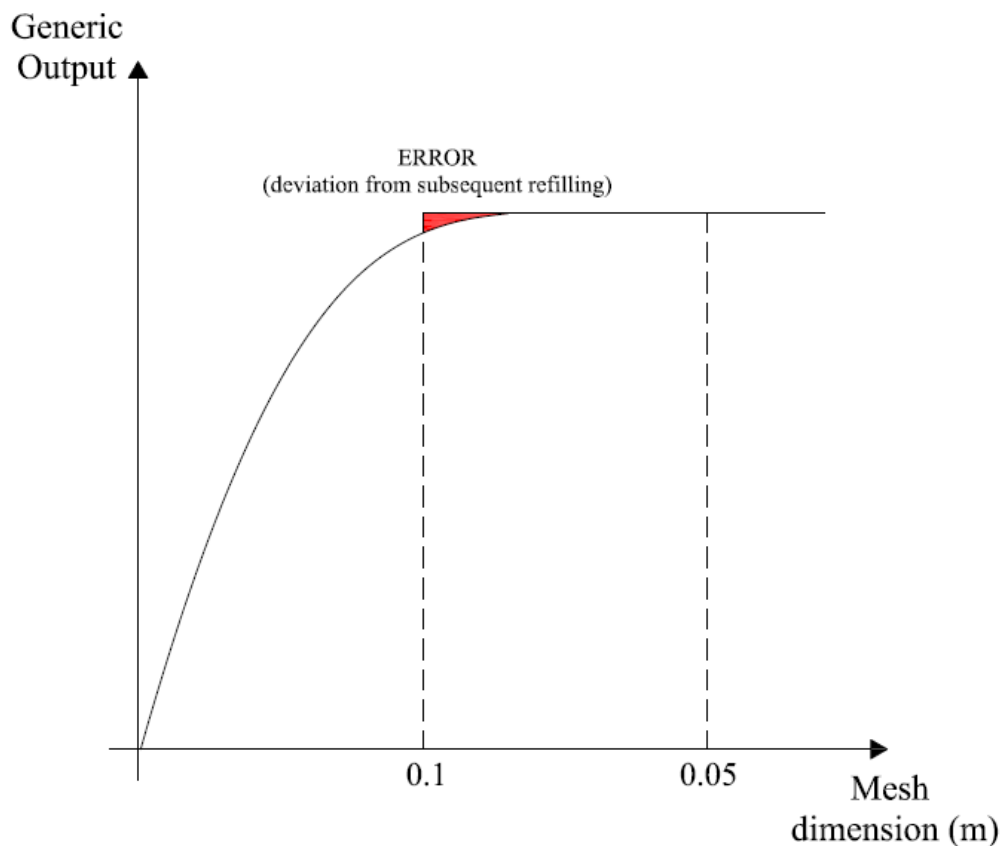


Figure A.3 - Results Behaviour

Between 0.1 and 0.05 there is a minimum error so that the exact result can be considered attained. It is important to emphasize that passing, from instance, from the 0.1 to 0.05 mesh the cost of the analysis (time, resources) will be much increased. The right compromise must be found between a dense mesh and an approximate result (i.e., if the mesh is reduced, the results are refined but the computational times are too high).

Jumpers and spools are defined through the elements that are divided into *three subsets*: **connectors**, **straight pipe** and **bend**.

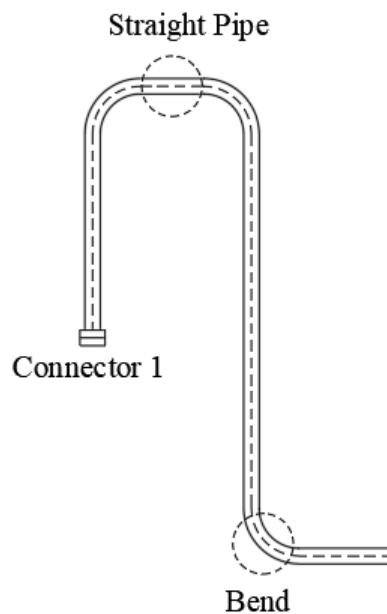


Figure A.4 - Detail of Jumper Subsets

The reason is that, from a structural point of view, these are not the same element but have different deformation capacity, stiffness and strength.

For the jumper (OD=12,75 inch) studied in this thesis, the mesh used is:

Mesh_bend	0,11	m
Mesh_straight	0,34	m

Moreover, the **type of element** used must also be defined. In this case it is **PIPE31H**.

PIPE31H

The PIPE31H element is a 3D hybrid pipe element with six degrees of freedom at each node. It is a classic element used to model jumper. The element uses linear interpolation and therefore has a lumped mass distribution. It is a single-row element that does not have the ability to oval but always remains circular.

HYBRID BEAMS

Hybrid beam element types (B21H, B33H, etc.) are provided in Abaqus/Standard for use in cases where it is numerically difficult to compute the axial and shear forces in the beam by the usual finite element displacement method. This problem arises most commonly in geometrically nonlinear analysis when the beam undergoes large rotations and is very rigid in axial and transverse shear deformation, such as in flexing long pipe or cable. The hybrid elements uses a more general formulation in which the axial and transverse shear forces in the elements are included, along with the nodal displacements and rotations, as primary variables. Although this formulation makes these elements more expensive, they generally converge much faster when the beam's rotations are large and, therefore, are more efficient overall in such cases.

A.2. ABAQUS INPUT FILES

```
*PARAMETER
gravity = 9.806650           # m/s^2
Water_density = 1025.000000 # kg/m^3
WD_ref = 1826.000000        # m - Water depth from medium sea level
ro_inst = 1100.000000       # kg/m^3 - Content density during System Test
ro_op = 882.000000          # kg/m^3 - Content density during Operating
OD = 0.323900               # m - Outside Diameter
R=OD/2                       # m - Pipe Section Radius
WT = 0.038100               # m - Wall Thickness
ID=OD-2*WT                   # m - Inner Pipe Diameter
steel_eq_dens = 7850.000000 # kg/m^3 - Steel Equivalent Density
mesh_straight = 0.340000    # mesh straight elements
Nnodes = 335                 # number of SPOOL nodes
Deployment = -0.000000       # Deployment for Spool/Jumper
```

```
*****
**
**      LOAD STEPS DEFINITION
**      SPOOL_2017_gui_JPR02_01_nom6_BC
**
*****
**      STEP 1
**      **Spool Landed water filled and rigging is removed
**STEP, NAME=GRAVITY, INC=200, NLGEOM, UNSYMM=YES, EXTRAPOLATION=LINEAR
STEP 1:GRAVITY
*STATIC
0.02, 1.0, ,0.5
*CONTROLS, ANALYSIS=DISCONTINUOUS
*DLOAD
aSPOOL.STRAIGHT,      GRAV, 9.8065, 0.0, 0.0, -1.0
aSPOOL.BENDS_TANGENTS, GRAV, 9.8065, 0.0, 0.0, -1.0
aSPOOL.CONNECTOR1,    GRAV, 9.8065, 0.0, 0.0, -1.0
aSPOOL.CONNECTOR2,    GRAV, 9.8065, 0.0, 0.0, -1.0
aSPOOL.CONN1_MASS,    GRAV, 9.8065, 0.0, 0.0, -1.0
aSPOOL.CONN2_MASS,    GRAV, 9.8065, 0.0, 0.0, -1.0
**
** Weight of Coating
aSPOOL.STRAIGHT, PZ, -0.000000
**
aSPOOL.STRAIGHT, HPE, <p_ext>, <WD_ref>, 0.000000, 0.323900
aSPOOL.CONNECTOR1, HPE, <p_ext>, <WD_ref>, 0.000000, 0.323850
aSPOOL.CONNECTOR2, HPE, <p_ext>, <WD_ref>, 0.000000, 0.323850
aSPOOL.STRAIGHT, HPI, 18354335.725000, 1701.473974, 0.000000, 0.247700
aSPOOL.CONNECTOR1, HPI, 18354335.725000, 1701.473974, 0.000000, 0.171450
aSPOOL.CONNECTOR2, HPI, 18354335.725000, 1701.473974, 0.000000, 0.171450
aSPOOL.BENDS_TANGENTS, HPE, 18354335.725000, 1826.000000, 0.000000, 0.323900
aSPOOL.BENDS_TANGENTS, HPI, 18354335.725000, 1701.473974, 0.000000, 0.247700
** Weight of Coating
aSPOOL.BENDS_TANGENTS, PZ, -0.000000
**

*BOUNDARY
aSPOOL.conn_NODE_f, 4, 6
FIRST_NODE, 1, 1, 0.0
FIRST_NODE, 2, 2, 0.0
FIRST_NODE, 3, 3, <Deployment>
aSPOOL.conn_NODE_l, 4, 6
LAST_NODE, 1, 1, 0.0
LAST_NODE, 2, 2, 0.0
LAST_NODE, 3, 3, <Deployment>
**
*****
*OUTPUT, FIELD, FREQUENCY=15
*ELEMENT OUTPUT
SF, ESF1
*ELEMENT OUTPUT
1, 2, 3, 4, 5, 6, 7, 8
S, MISES
*ELEMENT OUTPUT, ELSET=Conn_Primary_ALL
CTF, CTM, CU, CUR
*NODE OUTPUT
U, COORD, RF, CF
*CONTACT OUTPUT
CSTRESS, CDISP
*****
*EL PRINT, FREQ=9999, SUMMARY=NO, ELSET=aSPOOL.MODEL_ELEMENTS
1,2,3,4,5,6,7,8
S, MISES
*EL PRINT, FREQ=9999, SUMMARY=NO, ELSET=aSPOOL.STRAIGHT0
SF, ESF1
*EL PRINT, FREQ=9999, SUMMARY=NO, ELSET=BENDS_TANGENTS
SF, ESF1
*NODE PRINT, FREQ=9999, GLOBAL=YES, SUMMARY=NO, NSET=NO_ALL
U
*NODE PRINT, FREQ=9999, NSET=FIRST_NODE, SUMMARY=YES, GLOBAL=NO
RF
*NODE PRINT, FREQ=9999, NSET=LAST_NODE, SUMMARY=YES, GLOBAL=NO
```

```
*NODE PRINT, FREQ=9999, NSET=LAST_NODE, SUMMARY=YES, GLOBAL=NO
RF
*NODE PRINT, FREQ=9999, NSET=conn_NODE, SUMMARY=YES, GLOBAL=NO
RF
*NODE PRINT, FREQ=9999, NSET=FIRST_NODE, SUMMARY=YES, GLOBAL=NO
U
*NODE PRINT, FREQ=9999, NSET=LAST_NODE, SUMMARY=YES, GLOBAL=NO
U
*NODE PRINT, FREQ=9999, GLOBAL=YES, SUMMARY=NO, NSET=NO_ALL
COORD
*ENDSTEP
*****
**          STEP 2          **
*STEP, NAME=Linear_Tolerances, INC=200, NLGEOM, UNSYMM=YES, EXTRAPOLATION=LINEAR
STEP 2:Apply Only Linear Tolerances on both Ends
*STATIC
0.48, 1.0, ,0.5
*BOUNDARY
FIRST_NODE, 1, 1, <endl_U1>
FIRST_NODE, 2, 2, <endl_U2>
FIRST_NODE, 3, 3, <endl_U3>
LAST_NODE, 1, 1, <end2_U1>
LAST_NODE, 2, 2, <end2_U2>
LAST_NODE, 3, 3, <end2_U3>
*CONNECTOR MOTION, FIXED
connf1, 4,
connl1, 4,
**
*ENDSTEP
*****
**          STEP 3          **
*STEP, NAME=Connection, INC=200, NLGEOM, UNSYMM=YES, EXTRAPOLATION=LINEAR
STEP 3:Apply Linear and Angular Tolerances at both ends
*STATIC
1.2E-1, 1.0, SE-11,0.5

*CONTROLS, RESET
*CONTROLS, ANALYSIS=DISCONTINUOUS
*CONTROLS, PARAMETERS=FIELD, FIELD=DISPLACEMENT
0.01, 1.0
*CONTROLS, PARAMETERS=FIELD, FIELD=ROTATION
0.01, 1.0
*CONNECTOR MOTION
connf1, 4, <endl_UR1>
connf2, 4, <endl_UR2>
connl1, 4, <end2_UR1>
connl2, 4, <end2_UR2>
*CONNECTOR MOTION, FIXED
connf3, 4,
connl3, 4,
**
*ENDSTEP
*****
**          STEP 4          **
**STEP: OPERATION
*STEP, NAME=OPERATION, INC=250, NLGEOM, UNSYMM=YES, EXTRAPOLATION=LINEAR
STEP 4:Apply Design Pressure, Expansion and Temperature
*STATIC
0.3, 1.0, 1E-7, 0.5
*DLOAD
aSPOOL.STRAIGHT, HPI, <p_design>, <zero_pressure_operative>, 0.0, 0.247700
aSPOOL.CONNECTOR1, HPI, <p_design>, <zero_pressure_operative>, 0.0, 0.171450
aSPOOL.CONNECTOR2, HPI, <p_design>, <zero_pressure_operative>, 0.0, 0.171450
aSPOOL.BENDS_TANGENTS, HPI, <p_design>, <zero_pressure_operative>, 0.0, 0.247700
**
*TEMPERATURE
NO_ALL, 121.000000
*BOUNDARY
FIRST_NODE, 1, 1, <endl_OPE_u1>
FIRST_NODE, 2, 2, <endl_OPE_u2>
LAST_NODE, 1, 1, <end2_OPE_u1>
LAST_NODE, 2, 2, <end2_OPE_u2>
```

```
**RESTART, WRITE, FREQUENCY=9999, OVERLAY
*ENDSTEP
*****
**      STEP 5
**STEP: OPERATING + SETTLEMENT
*STEP, NAME=OPERATING_SETTLEMENT, INC=200, NLGEOM, UNSYMM=YES, EXTRAPOLATION=LINEAR
STEP 5:Apply Structure Settlement
*STATIC
0.5, 1.0, ,0.5
*BOUNDARY
FIRST_NODE, 3, 3, <endl SETT>
*BOUNDARY
LAST_NODE, 3, 3, <end2 SETT>
***
*DLOAD
aSPOOL.STRAIGHT, FI, 0.323900, 1.0
aSPOOL.CONNECTOR1, FI, 0.323850, 1.0
aSPOOL.CONNECTOR2, FI, 0.323850, 1.0
aSPOOL.BENDS_TANGENTS, FI, 0.323900, 1.0
**
*ENDSTEP
*****
**
**      STEP 6: DYNAMIC SLUG
**
*****
**
*STEP, NAME=DYNAMIC_SLUG, NLGEOM, UNSYMM=YES, INC=7800
STEP 6: DYNAMIC_SLUG
**
*DYNAMIC, SINGULAR MASS=ERROR
0.01, 78.0, 1E-10, 0.01
**
*CONTROLS, RESET

***CONTROLS, PARAMETERS= TIME INCREMENTATION
**      / / / / / / / / 20
**
*CONTROLS, ANALYSIS=DISCONTINUOUS
**
**CONTROLS, PARAMETERS=CONSTRAINTS
**      , , , 1.0, 1.0
**
***CONTROLS, PARAMETERS=FIELD, FIELD=DISPLACEMENT
** 0.01, 1.0
**
***CONTROLS, PARAMETERS=FIELD, FIELD=ROTATION
** 0.01, 1.0
**
**CONTACT CONTROLS, STABILIZE=1e06
**
**
*INCLUDE, INPUT=SLUG_Amplitude_1.txt
**
*INCLUDE, INPUT=SLUG_Amplitude_2.txt
**
*INCLUDE, INPUT=SLUG_Amplitude_3.txt
**
*INCLUDE, INPUT=SLUG_Amplitude_4.txt
**
*INCLUDE, INPUT=SLUG_Amplitude_5.txt
**
*INCLUDE, INPUT=SLUG_Amplitude_6.txt
**
*INCLUDE, INPUT=SLUG_Cload_1.txt
**
*INCLUDE, INPUT=SLUG_Cload_2.txt
**
*INCLUDE, INPUT=SLUG_Cload_3.txt
**
```

```
*INCLUDE, INPUT=SLUG_Cload_4.txt
**
*INCLUDE, INPUT=SLUG_Cload_5.txt
**
*INCLUDE, INPUT=SLUG_Cload_6.txt
**
***
*OUTPUT, FIELD, VARIABLE=PRESELECT
*NODE OUTPUT
  U, COORD, RF, CF,
*ELEMENT OUTPUT
  S, E, SF, SE,
***
*EL PRINT, FREQ=9999, SUMMARY=NO, ELSET=aSPOOL.MODEL_ELEMENTS
  1,2,3,4,5,6,7,8
  S, MISES
*NODE PRINT, GLOBAL=YES, SUMMARY=NO, NSET=NO_ALL
  U
*NODE PRINT, GLOBAL=YES, SUMMARY=NO, NSET=NO_ALL
  COORD
*ENDSTEP

*AMPLITUDE, NAME=SLUG_18, DEFINITION=TABULAR, VALUE=RELATIVE
  0.0000, 0.0000, 0.0073, 1.0000, 0.3333, 1.0000, 0.3406, 0.0000
  10.0000, 0.0000, 10.0073, 1.0000, 10.3333, 1.0000, 10.3406, 0.0000
  20.0000, 0.0000, 20.0073, 1.0000, 20.3333, 1.0000, 20.3406, 0.0000
  30.0000, 0.0000, 30.0073, 1.0000, 30.3333, 1.0000, 30.3406, 0.0000
  40.0000, 0.0000, 40.0073, 1.0000, 40.3333, 1.0000, 40.3406, 0.0000
  50.0000, 0.0000, 50.0073, 1.0000, 50.3333, 1.0000, 50.3406, 0.0000
  60.0000, 0.0000, 60.0073, 1.0000, 60.3333, 1.0000, 60.3406, 0.0000
  70.0000, 0.0000, 70.0073, 1.0000, 70.3333, 1.0000, 70.3406, 0.0000
*AMPLITUDE, NAME=SLUG_19, DEFINITION=TABULAR, VALUE=RELATIVE
  0.0073, 0.0000, 0.0145, 1.0000, 0.3406, 1.0000, 0.3478, 0.0000
  10.0073, 0.0000, 10.0145, 1.0000, 10.3406, 1.0000, 10.3478, 0.0000
  20.0073, 0.0000, 20.0145, 1.0000, 20.3406, 1.0000, 20.3478, 0.0000
  30.0073, 0.0000, 30.0145, 1.0000, 30.3406, 1.0000, 30.3478, 0.0000
  40.0073, 0.0000, 40.0145, 1.0000, 40.3406, 1.0000, 40.3478, 0.0000
  50.0073, 0.0000, 50.0145, 1.0000, 50.3406, 1.0000, 50.3478, 0.0000
  60.0073, 0.0000, 60.0145, 1.0000, 60.3406, 1.0000, 60.3478, 0.0000
  70.0073, 0.0000, 70.0145, 1.0000, 70.3406, 1.0000, 70.3478, 0.0000
*AMPLITUDE, NAME=SLUG_20, DEFINITION=TABULAR, VALUE=RELATIVE
  0.0145, 0.0000, 0.0218, 1.0000, 0.3478, 1.0000, 0.3551, 0.0000
  10.0145, 0.0000, 10.0218, 1.0000, 10.3478, 1.0000, 10.3551, 0.0000
  20.0145, 0.0000, 20.0218, 1.0000, 20.3478, 1.0000, 20.3551, 0.0000
  30.0145, 0.0000, 30.0218, 1.0000, 30.3478, 1.0000, 30.3551, 0.0000
  40.0145, 0.0000, 40.0218, 1.0000, 40.3478, 1.0000, 40.3551, 0.0000
  50.0145, 0.0000, 50.0218, 1.0000, 50.3478, 1.0000, 50.3551, 0.0000
  60.0145, 0.0000, 60.0218, 1.0000, 60.3478, 1.0000, 60.3551, 0.0000
  70.0145, 0.0000, 70.0218, 1.0000, 70.3478, 1.0000, 70.3551, 0.0000
*AMPLITUDE, NAME=SLUG_21, DEFINITION=TABULAR, VALUE=RELATIVE
  0.0218, 0.0000, 0.0290, 1.0000, 0.3551, 1.0000, 0.3624, 0.0000
  10.0218, 0.0000, 10.0290, 1.0000, 10.3551, 1.0000, 10.3624, 0.0000
  20.0218, 0.0000, 20.0290, 1.0000, 20.3551, 1.0000, 20.3624, 0.0000
  30.0218, 0.0000, 30.0290, 1.0000, 30.3551, 1.0000, 30.3624, 0.0000
  40.0218, 0.0000, 40.0290, 1.0000, 40.3551, 1.0000, 40.3624, 0.0000
  50.0218, 0.0000, 50.0290, 1.0000, 50.3551, 1.0000, 50.3624, 0.0000
  60.0218, 0.0000, 60.0290, 1.0000, 60.3551, 1.0000, 60.3624, 0.0000
  70.0218, 0.0000, 70.0290, 1.0000, 70.3551, 1.0000, 70.3624, 0.0000
```

```
*CLOAD, AMPLITUDE=SLUG_18
aSPOOL.18, 1, -1209.2771
aSPOOL.18, 2, 0.0000
aSPOOL.18, 3, 35.3687
*CLOAD, AMPLITUDE=SLUG_19
aSPOOL.19, 1, -1203.1650
aSPOOL.19, 2, 0.0000
aSPOOL.19, 3, 126.4753
*CLOAD, AMPLITUDE=SLUG_20
aSPOOL.20, 1, -1183.4345
aSPOOL.20, 2, 0.0000
aSPOOL.20, 3, 251.1670
*CLOAD, AMPLITUDE=SLUG_21
aSPOOL.21, 1, -1151.0359
aSPOOL.21, 2, 0.0000
aSPOOL.21, 3, 372.4491
*CLOAD, AMPLITUDE=SLUG_22
aSPOOL.22, 1, -1104.6362
aSPOOL.22, 2, 0.0000
aSPOOL.22, 3, 493.3365
*CLOAD, AMPLITUDE=SLUG_23
aSPOOL.23, 1, -1046.3229
aSPOOL.23, 2, 0.0000
aSPOOL.23, 3, 607.2977
*CLOAD, AMPLITUDE=SLUG_24
aSPOOL.24, 1, -978.0147
aSPOOL.24, 2, 0.0000
aSPOOL.24, 3, 712.1020
*CLOAD, AMPLITUDE=SLUG_25
aSPOOL.25, 1, -899.1441
aSPOOL.25, 2, 0.0000
aSPOOL.25, 3, 809.4084
*CLOAD, AMPLITUDE=SLUG_26
aSPOOL.26, 1, -809.7570
aSPOOL.26, 2, 0.0000
aSPOOL.26, 3, 898.8302
```

```
** STEP 20 - MODAL **
**Modal Analysis
**STEP, NAME=MODAL, INC=150, NLGEOM, UNSYMM=YES, EXTRAPOLATION=LINEAR
Modal Analysis
**FREQUENCY
21
**CONTROLS, RESET
**CONTROLS, ANALYSIS=DISCONTINUOUS
**CONTROLS, PARAMETERS=FIELD, FIELD=DISPLACEMENT
0.01, 1.0
**CONTROLS, PARAMETERS=FIELD, FIELD=ROTATION
0.01, 1.0
**
**D ADDED MASS
aSPOOL.STRAIGHT, FI, 0.323900, 1.0, 2.0
aSPOOL.CONNECTOR1, FI, 0.323850, 1.0, 2.0
aSPOOL.CONNECTOR2, FI, 0.323850, 1.0, 2.0
aSPOOL.BENDS_TANGENTS, FI, 0.323900, 1.0, 2.0
**
***
***
**OUTPUT, FIELD, VARIABLE=PRESELECT
**NODE OUTPUT
U, COORD, RF, CF,
**ELEMENT OUTPUT
S, E, SF, SE,
***
**EL PRINT, FREQ=9999, SUMMARY=NO, ELSET=aSPOOL.MODEL_ELEMENTS
1,2,3,4,5,6,7,8
S, MISES
**NODE PRINT, GLOBAL=YES, SUMMARY=NO, NSET=NO_ALL
U
**NODE PRINT, GLOBAL=YES, SUMMARY=NO, NSET=NO_ALL
COORD
**ENDSTEP
```


APPENDIX B: REACTION ON A CURVED PIPE DUE TO STEADY-STATE FLOW

This Appendix briefly presents the computation of the reaction on a curved pipe (bend) due to the inside steady-state flow, under the following simplifying hypotheses:

1. Steady-state;
2. Pressure (p) constant at the cross section;
3. p, A, ρ, v , constant with the abscissa s ;
4. R , constant;
5. gravity (g) contributions neglected;

(vector symbols are boldface).

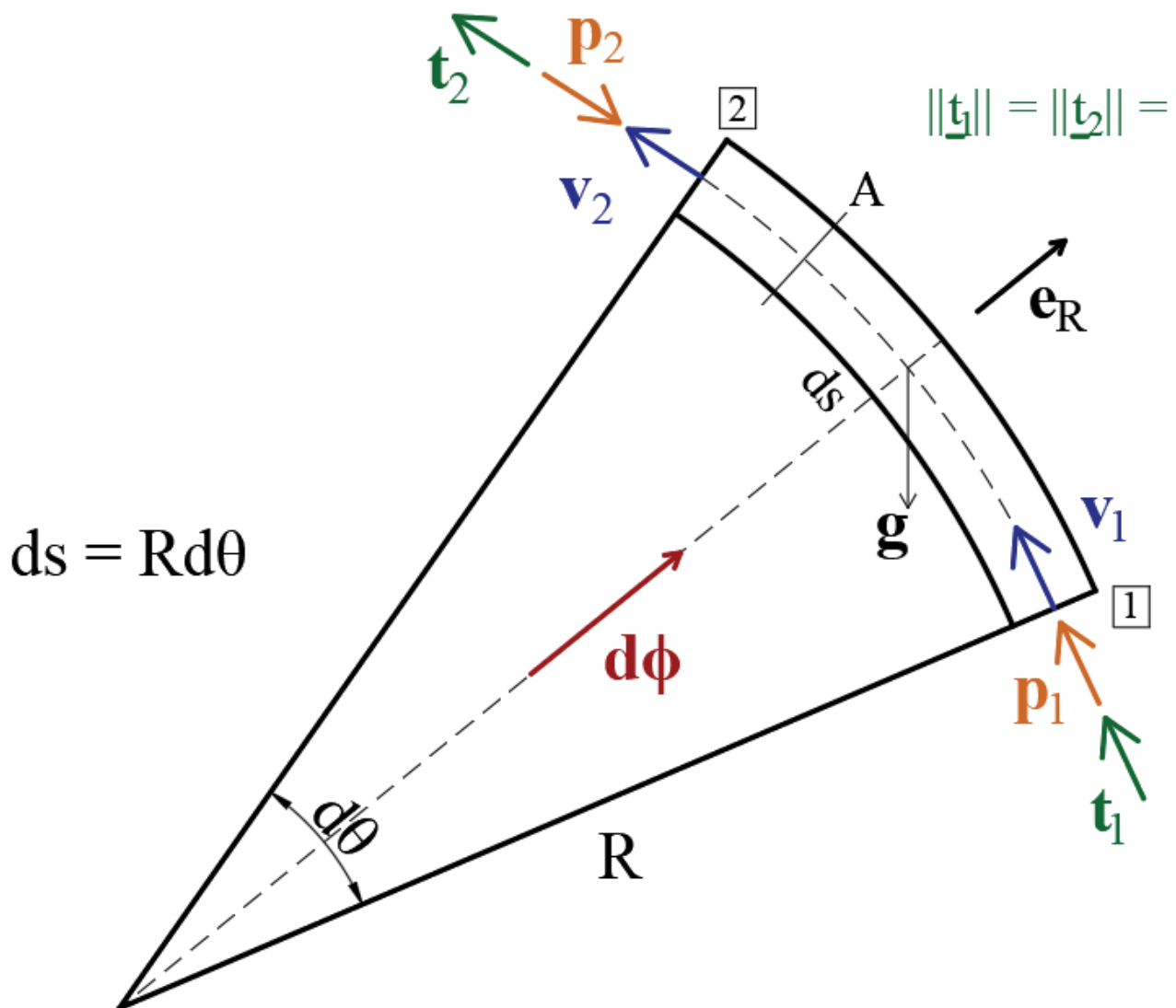


Figure B.1: Forces and Fluxes

BALANCE OF MOMENTUM

Variation of the Momentum = Σ Forces:

$$\frac{dQ}{dt} = r \quad (\text{B.1})$$

namely (Figure B.1)

$$\rho A v_2 v - \rho A v_1 v = p_1 A + p_2 A + \rho A R d\theta g + \phi' ds \quad (\text{B.2})$$

being,

$$\phi' = \frac{\Delta\phi}{\Delta s} \quad (\text{B.3})$$

the force per unit length *on the fluid*.

The projections of Eq. (B.2):

$$\rho A v^2 (t_2 - t_1) = p A (t_1 - t_2) + \phi' ds \quad (\text{B.4})$$

give:

- direction $(\mathbf{e}_R)^\perp$ = trivial (steady state).
- direction \mathbf{e}_R (Fig. B.2)

$$\rho A v^2 d\theta = p A d\theta + \phi' ds \quad (\text{B.5})$$

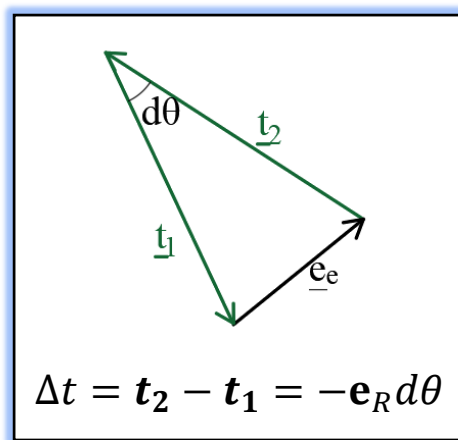


Figure B.2: $t_2 - t_1$

Therefore the **radial Reaction** on the pipe, *per unit length*, is

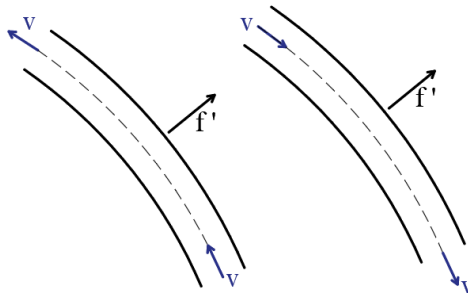
$$f' = -\phi' = A(p + \rho v^2) \frac{d\theta}{ds} \quad (\text{B.6})$$

or, being $\frac{d\theta}{ds} = \frac{1}{R}$, finally

$$f' = \frac{A}{R} (p + \rho v^2). \quad (\text{B.7})$$

Remark

f' is independent of the direction of v .



RESULTANT ON A FINITE PART OF THE BEND PIPE

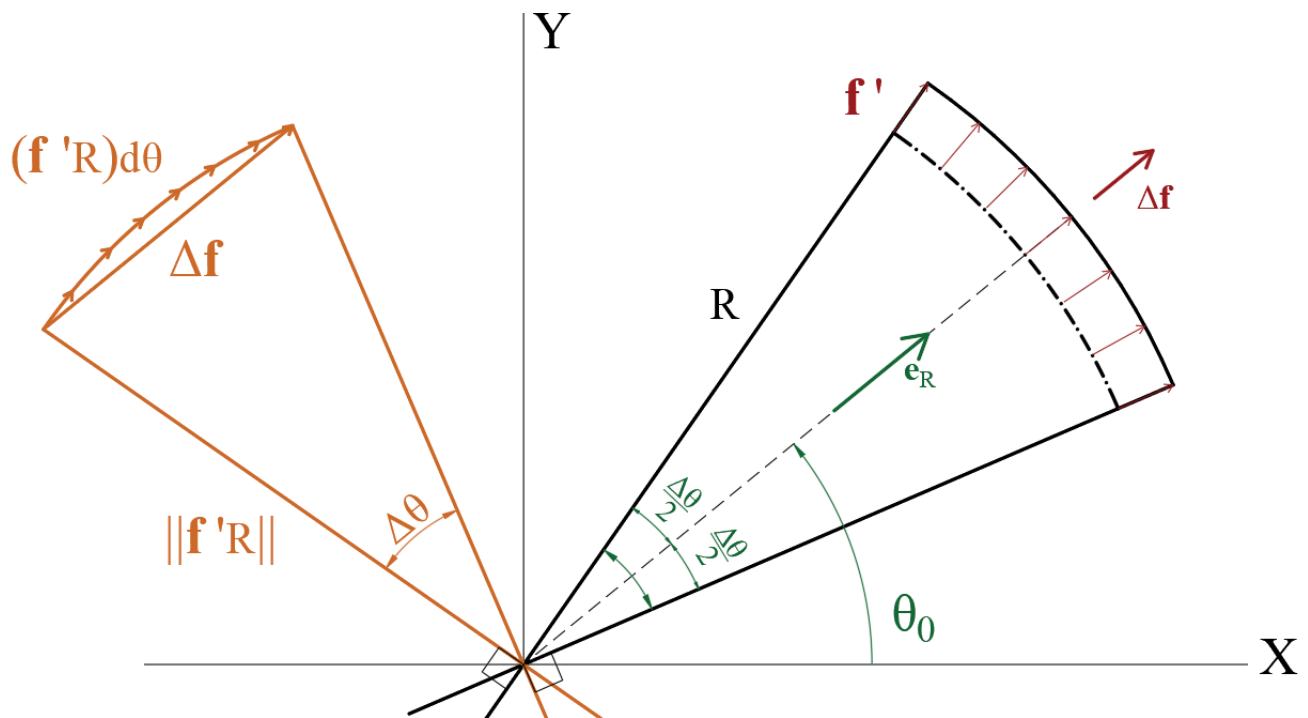
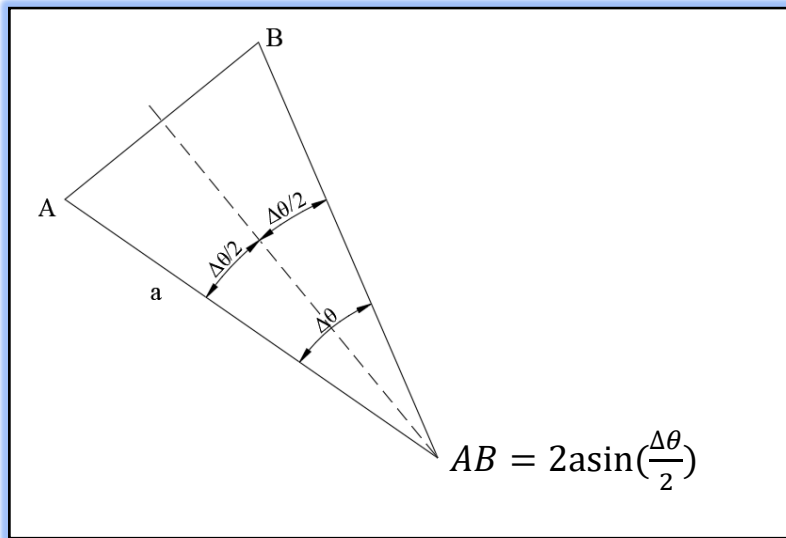


Figure B.3: Typical section of a bend. Right: geometry (aperture $\Delta\theta$, inclination θ_0).
Left: polygon of the forces.

By applying the result (B.7) on the scheme in Figure B.3

$$\Delta \mathbf{f} = \int_{\theta_0 - \frac{\Delta\theta}{2}}^{\theta_0 + \frac{\Delta\theta}{2}} \mathbf{f}' R d\theta \quad (\text{B.8})$$

$$\|\mathbf{f}' R\| = A(p + \rho v^2) \quad (\text{B.9})$$



$$\Delta f = f' R 2 \sin \frac{\Delta \theta}{2} \quad (\text{B.10})$$

$$\Delta f = e_R A (p + \rho v^2) 2 \sin \frac{\Delta \theta}{2} \quad (\text{B.11})$$

Remark: The total reaction, Δf is independent of R.

CARTESIAN COMPONENT (to use in ABAQUS)

$$\Delta f_X = A (p + \rho v^2) 2 \sin \frac{\Delta \theta}{2} \cos \theta_0 \quad (\text{B.12})$$

$$\Delta f_Y = A (p + \rho v^2) 2 \sin \frac{\Delta \theta}{2} \sin \theta_0$$

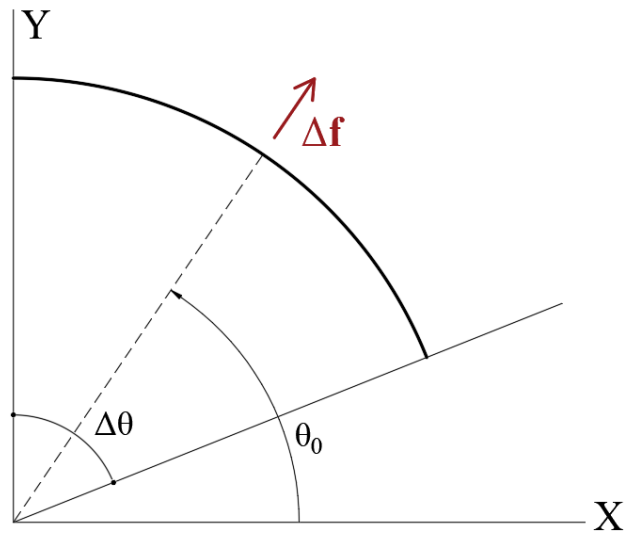
By posing

$$f_0 = A (p + \rho v^2) \quad (\text{B.13})$$

$$\frac{\Delta f_X}{f_0} = 2 \sin \frac{\Delta \theta}{2} \cos \theta_0 \quad (\text{B.14})$$

$$\frac{\Delta f_Y}{f_0} = 2 \sin \frac{\Delta \theta}{2} \sin \theta_0$$

Example 1. Generic bend, starting horizontally.



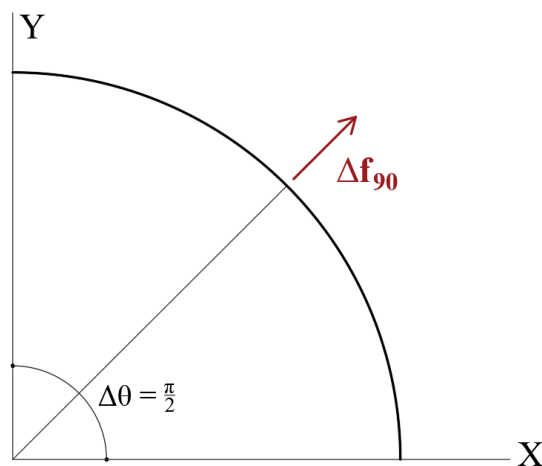
$$\theta_0 = \frac{\pi}{2} - \frac{\Delta\theta}{2}$$

Cartesian components:

$$\frac{\Delta f_X}{f_0} = 2 \sin \frac{\Delta\theta}{2} \cos \left(\frac{\pi}{2} - \frac{\Delta\theta}{2} \right) = 2 \sin \frac{\Delta\theta}{2} \sin \frac{\Delta\theta}{2} = 1 - \cos \Delta\theta$$

$$\frac{\Delta f_Y}{f_0} = 2 \sin \frac{\Delta\theta}{2} \sin \left(\frac{\pi}{2} - \frac{\Delta\theta}{2} \right) = 2 \sin \frac{\Delta\theta}{2} \cos \frac{\Delta\theta}{2} = \sin \Delta\theta,$$

Example 2. A quarter bend

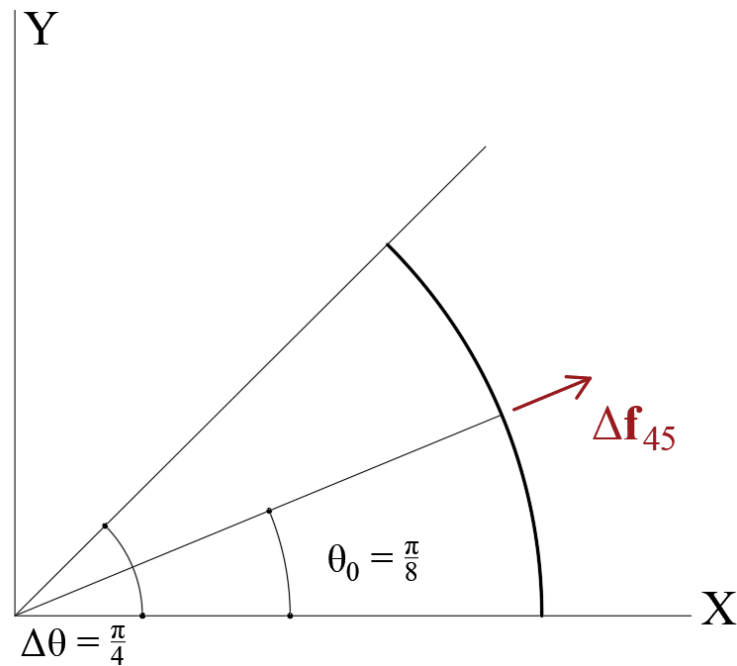


Cartesian components:

$$\frac{\Delta f_X}{f_0} = 1, \frac{\Delta f_Y}{f_0} = 1, \text{ so that the resultant is}$$

$$\frac{\Delta f}{f_0} = \sqrt{2} = 0.4142$$

Example 3. A half-quarter bend



Cartesian components:

$$\frac{\Delta f_X}{f_0} = \sin \frac{\pi}{4} = \frac{1}{\sqrt{2}}$$

$$\frac{\Delta f_Y}{f_0} = 1 - \cos \frac{\pi}{4} = 1 - \frac{1}{\sqrt{2}}$$

Resultant:

$$\frac{\Delta f}{f_0} = \sqrt{\left(1 - \frac{1}{\sqrt{2}}\right)^2 + \left(\frac{1}{\sqrt{2}}\right)^2} = \sqrt{2 - \sqrt{2}} = 0.7654$$

List of FIGURE

Figure 1 - Subsea Pipeline and Associated Infrastructure.....	10
Figure 2 - Subsea Production System	11
Figure 3 - Relationship among the major components of a Subsea Production Systems	12
Figure 4 - Pipeline End Termination (PLET)	13
Figure 5 - Subsea Manifold and ROV	14
Figure 6 - Typical Subsea Umbilicals (Cross-Section)	15
Figure 7 - Subsea Production Risers	16
Figure 8 - Steel Catenary Riser configuration	17
Figure 9 - Top Tensioned Riser Configurations.....	18
Figure 10 - Typical Cross Section of Flexible Pipe.....	19
Figure 11 - Flexible Risers Configurations	20
Figure 12 - Subsea Rigid Jumper.....	21
Figure 13 - Main Components.....	21
Figure 14 - Subsea Rigid and Flexible Jumpers	23
Figure 15 - Configurations of Vertical SRJs	23
Figure 16 - Jumper configurations	25
Figure 17 - Step 1: Pick up the Jumper.....	26
Figure 18 - Step 2: Deploy through splash zone.....	27
Figure 19 - Step 3: Jumper landing	27
Figure 20 - Typical compositions of pipeline steels (Palmer & King, 2008).....	30
Figure 21 - Pipe Components	31
Figure 22 - Geometric characteristics of the pipe.....	32
Figure 23 - Pipe Parameters	32
Figure 24 - Stratified Smooth Flow	36
Figure 25 - Stratified Wavy Flow	36
Figure 26 - Slug Flow.....	36
Figure 27 - Annular Flow	37
Figure 28 - Dispersed Bubble Flow.....	37
Figure 29 - Gas-liquid flow regimes in horizontal pipe.....	37
Figure 30 - Bubble Flow.....	38
Figure 31 - Slug Flow.....	39
Figure 32 - Churn Flow.....	39
Figure 33 - Annular Flow	40
Figure 34 - Generalized flow map for multiphase flow in a horizontal pipe (Taitel, Barnea, & Duckler, 1980)	42
Figure 35 - Generalized flow map for multiphase flow in a vertical pipe (Taitel, Barnea, & Duckler, 1980)	42
<i>Figure 36 - Pigging Operation</i>	<i>44</i>
Figure 37 - Example of Severe Slugging.....	46
Figure 38 - Example of Hydrodynamic Slug Initiation	46
Figure 39 - Kelvin Helmholtz Instability	47
Figure 40 - Vessel Type.....	48
Figure 41 - Finger Type.....	48

Figure 42 - Representation of SLUG UNIT	51
Figure 43 - Gravitational Effects	53
Figure 44 - Centrifugal Force.....	54
Figure 45 - Bend Impact Force history due to Slug Flow	55
Figure 46 - Position of liquid slug with time.....	56
Figure 47 - Bend impact forces.....	57
Figure 48 - Slug "Trains".....	67
Figure 49 - Cross section of an infinitely long slender cylinder (H.E.J. van der Heijden, 2013).....	69
Figure 50 - Jumper configuration: ABAQUS FE Model	72
Figure 51 - Out-of-Plane Modes.....	74
Figure 52 - In-Plane Modes	75
Figure 53 - In-Plane Mode 4.....	77
Figure 54 - Slug Input Data.....	77
Figure 55 - Example: Slug unit in Bend 1	78
Figure 56 - Example: Slug unit in Bend 2	78
Figure 57 - Example: Slug unit in Bend 3	78
Figure 58 - Example: Slug unit in Bend 4	79
Figure 59 - Example: Slug unit in Bend 5	79
Figure 60 - Example: Slug unit in Bend 6	79
Figure 61 - Slug Force with time	80
Figure 62 - Total Displacement Node 97: U1=longitudinal displacement, U2=transversal displacement, U3=vertical displacement. CF_Bend 3 = Slug Forces (In-Phase) in bend 3 that are characterized by the trapezoidal path (see figure 61), CF_Bend 4 = Slug Forces (Out-of-Phase) in bend 4 that are characterized by the trapezoidal path (see figure 61).	81
Figure 63 - Total Displacement Node 228: U1=longitudinal displacement, U2=transversal displacement, U3=vertical displacement. CF_Bend 3 = Slug Forces (Out-of-Phase) in bend 3, CF_Bend 4 = Slug Forces (In-Phase) in bend 4.....	82
Figure 64 - Total Displacement Node 97: U1=longitudinal displacement, U2=transversal displacement, U3=vertical displacement. CF_Bend 3 = Slug Forces (In-Phase) in bend 3, CF_Bend 4 = Slug Forces (Out-of-Phase) in bend 4.....	83
Figure 65 - Total Displacement Node 228: U1=longitudinal displacement, U2=transversal displacement, U3=vertical displacement. CF_Bend 3 = Slug Forces (Out-of-Phase) in bend 3, CF_Bend 4 = Slug Forces (In-Phase) in bend 4.....	84
Figure 66 - Total Displacement Node 97: U1=longitudinal displacement, U2=transversal displacement, U3=vertical displacement. CF_Bend 3 = Slug Forces (In-Phase) in bend 3, CF_Bend 4 = Slug Forces (Out-of-Phase) in bend 4.....	85
Figure 67 - Total Displacement Node 228: U1=longitudinal displacement, U2=transversal displacement, U3=vertical displacement. CF_Bend 3 = Slug Forces (Out-of-Phase) in bend 3, CF_Bend 4 = Slug Forces (In-Phase) in bend 4.....	86
Figure 68 - Total Displacement Node 97: U1=longitudinal displacement, U2=transversal displacement, U3=vertical displacement. CF_Bend 3 = Slug Forces (In-Phase) in bend 3, CF_Bend 4 = Slug Forces (Out-of-Phase) in bend 4.....	87

Figure 69 - Total Displacement Node 228: U1=longitudinal displacement, U2=transversal displacement, U3=vertical displacement. CF_Bend 3 = Slug Forces (Out-of-Phase) in bend 3, CF_Bend 4 = Slug Forces (In-Phase) in bend 4.....88

Figure 70 - Total Displacement Node 97: U1=longitudinal displacement, U2=transversal displacement, U3=vertical displacement. CF_Bend 3 = Slug Forces (In-Phase) in bend 3, CF_Bend 4 = Slug Forces (Out-of-Phase) in bend 4.....89

Figure 71 - Total Displacement Node 228: U1=longitudinal displacement, U2=transversal displacement, U3=vertical displacement. CF_Bend 3 = Slug Forces (Out-of-Phase) in bend 3, CF_Bend 4 = Slug Forces (In-Phase) in bend 4.....90

Figure 72 - Total Displacement Node 97: U1=longitudinal displacement, U2=transversal displacement, U3=vertical displacement. CF_Bend 3 = Slug Forces (In-Phase) in bend 3, CF_Bend 4 = Slug Forces (Out-of-Phase) in bend 4.....91

Figure 73 - Total Displacement Node 228: U1=longitudinal displacement, U2=transversal displacement, U3=vertical displacement. CF_Bend 3 = Slug Forces (Out-of-Phase) in bend 3, CF_Bend 4 = Slug Forces (In-Phase) in bend 4.....92

Figure 74 - Total Displacement Node 97: U1=longitudinal displacement, U2=transversal displacement, U3=vertical displacement. CF_Bend 3 = Slug Forces (In-Phase) in bend 3, CF_Bend 4 = Slug Forces (Out-of-Phase) in bend 4.....93

Figure 75 - Total Displacement Node 228: U1=longitudinal displacement, U2=transversal displacement, U3=vertical displacement. CF_Bend 3 = Slug Forces (Out-of-Phase) in bend 3, CF_Bend 4 = Slug Forces (In-Phase) in bend 4.....94

Figure 76 – Comparison Displacement (U1) Node 97 (the time history for the Slug Unit 6 is limited to the first 35 s)95

Figure 77 – Comparison Displacement (U1) Node 228 (the time history for the Slug Unit 6 is limited to the first 35 s)96

Figure 78 - Total Displacement Node 97: U1=longitudinal displacement, U2=transversal displacement, U3=vertical displacement. CF_Bend 3 = Slug Forces (In-Phase) in bend 3, CF_Bend 4 = Slug Forces (Out-of-Phase) in bend 4.....97

Figure 79 - Total Displacement Node 228: U1=longitudinal displacement, U2=transversal displacement, U3=vertical displacement. CF_Bend 3 = Slug Forces (Out-of-Phase) in bend 3, CF_Bend 4 = Slug Forces (In-Phase) in bend 4.....98

Figure 80 – Comparison Displacement (U1) Node 97 (the time history for the Slug Unit 6 is limited to the first 35 s)99

Figure 81 – Comparison Displacement (U1) Node 97 (the time history for the Slug Unit 6 is limited to the first 35 s) 100

Figure 82 – **Step 1a: Fourier harmonics** of the periodic slug train 101

Figure 83 - **Step 1b: First (fundamental) harmonic frequency** of each Slug Train 102

Figure 84 - **Step 1b: First five harmonics** of each Slug Train 102

Figure 85 – **Step 2:** Assignment of a mass-class of each Slug Train, $m_1 < m_2 < m_3 < m_4 < m_5$ (left); 103

Figure 86 – **Step 4: Identification of Critical Cases:** association of Slug Train frequencies with the natural frequencies of the appropriate mass-class structures 103



Figure A.1 - Chart: Analysis Phases with ABAQUS	106
Figure A.2 - Jumper Geometry	109
Figure A.3 - Results Behaviour.....	109
Figure A.4 - Detail of Jumper Subsets	110
Figure B.1: Forces and Fluxes.....	117
Figure B.2: $t_2 - t_1$	118
Figure B.3: Typical section of a bend. Right: geometry (aperture $\Delta\theta$, inclination θ_0). Left: polygon of the forces.....	119



List of TABLE

Table 1 - Comparison of different Jumper configurations (Sun & Kang, 2015)	24
Table 2 - Data Format (Time History Approach).....	52
Table 3 - Jumper Data	72
Table 4 - Connector Data	72
Table 5 - Input Data	73
Table 6 - Modal Analysis Results	76

ACRONYMS

1D	Mono-Dimensional or One-Dimensional
3D	Three-Dimensional
API	American Petroleum Institute
ASTM	American Society of Testing and Materials
CFD	Computational Fluid Dynamics
FE	Finite Element
FIV	Flow Induced Vibrations
FLET	Flowline End Termination
FSI	Fluid Structure Interaction
GUI	Graphical User Interface
ID	Inner Diameter
OD	Outside Diameter
PLEM	Pipeline End Manifold
PLET	Pipeline End Termination
R	Bend Radius
SCRs	Subsea Catenary Risers
SRJs	Subsea Rigid Jumpers
TL	Tangent Length
TTRs	Top Tensioned Risers
VIV	Vortex Induced Vibrations
WT	Wall Thickness

List of SYMBOLS

A	Cross-Sectional Area
A_e	External Cross-Sectional Area
A_i	Internal Cross-Sectional Area
E	Young Modulus
EJ	Bending Stiffness of the Pipe
F_x	Centrifugal Force component in the x-direction
F_y	Centrifugal Force component in the y-direction
F_{slug}	Centrifugal Force: maximum slug force
g	Gravity Acceleration
H_l	Liquid Holdup
J	Moment of Inertia
L_{bend}	Bend Length
L_L	Length of the liquid slug body for a slug unit
L_P	Length of the slug pocket body for a slug unit
m	Mass per unit length of the pipe
M_f	Moving Mass
p_e	External Pressure
p_i	Internal Pressure
Q_g	Gas volumetric flowrate
Q_l	Liquid volumetric flowrate
t_0	Time when the front of liquid slug enters the bend
t_1	Time when all the liquid slug occupies the bend length

t_2	Time when the tail of liquid slug reaches the start of the bend
t_3	Time when the liquid slug exits the bend
U_m	Mixture velocity
U_{sg}	Gas superficial velocity
U_{sl}	Liquid superficial velocity
v_{slug}	Representative Slug Unit Velocity
$w(x,t)$	Transversal Displacement
δ	Dirac delta Distribution
φ_i	Shape Form
θ	Bend Angle
ρ_L	Liquid Density
ρ_m	Gas-Liquid Mixture Density
ρ_P	Gas or Pocket Density

BIBLIOGRAPHY

- Abdul-Majeed, G. H., & Al-Mashat, A. M. (2000). A mechanistic model for vertical and inclined two-phase slug flow. *International Journal of Petroleum Science and Engineering*.
- Abramyan, A., & Vakulenko, S. (2010). Oscillations of a beam with a time-varying mass.
- Al-Tameemi, W. T., & Ricco, P. (2019). Water–air flow in straight pipes and across 90 ° sharp-angled mitre elbows. *International Journal of Multiphase Flow*.
- Azam, S. E., Mofid, M., & Khoraskani, R. A. (2012). Dynamic response of Timoshenko beam under moving mass. *Scientia Iranica*.
- Azevedo, G., Baliño, J., & Burr, K. (2017). Influence of pipeline modeling in stability analysis for severe slugging. *Chemical Engineering Science*.
- Azzopardi, B., & Hills, J. (n.d.). *Modelling and Experimentation in Two-Phase Flow*.
- Bai, Y., & Bai, Q. (2012). *Subsea Engineering Handbook-Gulf Professional Publishing*.
- Bai, Y., & Bai, Q. (2014). *Subsea Pipeline Design, Analysis, and Installation*.
- Bajer, C. I., & Dyniewicz, B. (2012). *Numerical Vibrations Structures under Moving Inertial Load*.
- Bakkouch, M., & Minguez, M. (2013). Riser Base Jumper Slugging analysis by CFD Simulations. *International Conference on Ocean, Offshore and Arctic Engineering*.
- Barbas, S., Mandke, J., Bartolini, L., & Vitali, L. (2006). Deformation Capacity of Induction Bends. *International Conference on Offshore Mechanics and Arctic Engineering*.
- Bejan, A., & Kraus, A. D. (2003). *Heat Transfer Handbook*.
- Belluzzi, O. (1994). *Scienza delle costruzioni vol. 2*.
- Bordalo, S. N., & Morooka, C. K. (2018). Slug flow induced oscillations on subsea petroleum pipelines. *Journal of Petroleum Science and Engineering*.
- Bruschi, R., Parrella, A., Vignati, G., & Vitali, L. (2017). Crucial Issues For Deep-Water Rigid Jumper Design. *Ocean Engineering*.
- Carneiro, D., Gouveia, J., Parrilha, R., & Cardoso, C. d. (2009). Buckle Initiation and Walking Mitigation for HP-HT Pipelines. *Deep Offshore Technology International*.
- Casanova, E., Pelliccioni, O., & Blanco, A. (2009). Fatigue Life Prediction due to Slug Flow in Extra Long Submarine Gas Pipelines using Fourier Expansion Series. *International Conference on Ocean, Offshore and Arctic Engineering*.
- Chai, Y., & Varyani, K. (2006). An absolute coordinate formulation for three-dimensional flexible pipe analysis. *Ocean Engineering*.
- Clarke, A., & Issa, R. I. (1996). A numerical model of slug flow in vertical tubes.
- Clarke, A., & Issa, R. I. (1997). Numerical model slug flow in vertical tubes. *Computers and Fluids*.

- Clift, R., Grace, J. R., & V, S. (1974). Continuous Slug Flow in Vertical Tubes. *Journal of Heat Transfer*.
- Cooper, P., Burnett, C., & Nash, I. (2009). Fatigue Design of Flowline Systems With Slug Flow. *International Conference on Ocean, Offshore and Arctic Engineering*.
- Deendarlianto, Rahmandhika, A., Widyatama, A., Dinaryanto, O., Widyaparaga, A., & Indarto. (2019). Experimental study on the hydrodynamic behavior of gas-liquid air-water two-phase flow near the transition to slug flow in horizontal pipes. *International Journal of Heat and Mass Transfer*.
- Deka, D., Cerkovnik, M., Panicker, N., & Vamsee, A. (2013). Subsea Jumpers vibration assessment.
- DNV-OS-F201. (2010). DYNAMIC RISERS.
- Eyo, E. N., & Lao, L. (2018). Slug flow characterization in horizontal annulus. *American Institute of Chemical Engineers*.
- Faghri, A., & Zhang, Y. (2006). *Fundamentals of Multiphase Heat Transfer and Flow*.
- Fan, Y., Pereyra, E., & Sarica, C. (2020). Experimental study of pseudo-slug flow in upward inclined pipes. *Journal of Natural Gas Science and Engineering*.
- Fernandes, R. C., Semiat, R., & Dukler, A. E. (1983). Hydrodynamic Model for Gas-Liquid Slug Flow in Vertical Tubes. *AIChE Journal*.
- Foda, M. A., & Abduljabbar, Z. (1997). A Dynamic Green Function Formulation for the Response of a Beam Structure. *Journal of Sound and Vibration*.
- Gajbhiye, B. D., Kulkarni, H. A., Tiwari, S. S., & Mathpati, C. S. (2019). Teaching turbulent flow through pipe fittings using computational fluid dynamics approach.
- Gajbhiye, B. D., Kulkarni, H. A., Tiwari, S. S., & Mathpati, C. S. (2019). Teaching turbulent flow through pipe fittings using computational fluid dynamics approach.
- Giacobbi, D. B., Semler, C., & Païdoussis, M. P. (2020). Dynamics of pipes conveying fluid of axially varying density. *Journal of Sound and Vibration*.
- Gonçalves, G., Baungartner, R., Loureiro, J., & Freire, A. S. (2018). Slug flow models: Feasible domain and sensitivity to input distributions. *Journal of Petroleum Science and Engineering*.
- Gonçalves, G., Baungartner, R., Loureiro, J., & Freire, A. S. (2018). Slug flow models: Feasible domain and sensitivity to input distributions. *Journal of Petroleum Science and Engineering*.
- Guo, B., Song, S., Chacko, J., & Ghalambor, A. (2005). *Offshore Pipelines*.
- H.E.J. van der Heijden. (2013). Fatigue Analysis of Subsea Jumpers Due to Slugging Loads.

- Harrison, G., & Brunner, M. (2003). King Flowlines - Thermal Expansion Design and Implementation. *Offshore Technology Conference*.
- Hewitt, & Yadigaroglu. (2018). *Introduction to Multiphase Flow*.
- Hewitt, G. F. (n.d.). *Gas-Liquid Flow*. Retrieved from <http://www.thermopedia.com/content/2/>
- Hou, D. Q., Tijsseling, A. S., & Bozkus, Z. (2014). Dynamic force on an elbow caused by a traveling Liquid Slug.
- Hughmark, G. A. (1966). Holdup in Vertical Upward Slug Flow. *AiChE Journal*.
- Ichikawa, M., Miyakawa, Y., & Matsuda, A. (2000). Vibration Analysis of the Continuous Beam Subjected to a Moving Mass. *Journal of Sound and Vibration*.
- Irschik, H., & Belyaev, A. K. (2014). *Dynamics of Mechanical Systems with Variable Mass*.
- Jahanshahi, E., Skogestad, S., & Helgesen, A. H. (2012). Controllability analysis of severe slugging in well-pipeline-riser systems. *Workshop on Automatic Control in Offshore Oil and Gas Production*.
- Jansen, F. E., Shoham, O., & Taitel, Y. (1995). The elimination of severe slugging-experiments and modeling. *International Journal of Multiphase Flow*.
- Kansao, R., Casanova, E., Blanco, A., Kenyery, F., & Rivero, M. (2008). Fatigue Life Prediction due to Slug Flow in extra long pipelines. *International Conference on Offshore Mechanics and Arctic Engineering*.
- Karampour, H., & Alrsai, M. (n.d.). Propagation Buckling of Subsea Pipelines and Pipe-in-Pipe Systems.
- Kazi, S. N. (2012). *An Overview of Heat Transfer Phenomena*.
- Kheiri, M. (2020). Nonlinear dynamics of imperfectly-supported pipes conveying fluid. *Journal of Fluids and Structures*.
- Krysl, P. (2017). Finite Element Modeling with Abaqus and Python for Thermal and Stress Analysis.
- Kyriakides, & Corona. (2007). *Mechanics of Offshore Pipelines*.
- Lee, J., & P.E. (2008). *Introduction to Offshore Pipelines and Risers*.
- Leffler, W. L., Pattarozzi, R., & Sterling, G. (2011). *Deepwater Petroleum Exploration and Production-A Nontechnical Guide*.
- Li, W., Guo, L., & Xie, X. (2017). Effects of a long pipeline on severe slugging in an S-shaped riser. *Chemical Engineering Science*.
- Lim, J., Lee, D., Zlotnik, V. A., & Choi, H. (2020). Analytical Interpretation of Slug Test in a Vertical Cutoff Wall.

- Liu, G., & Wang, Y. (2018). Study on the natural frequencies of pipes conveying gas-liquid two-phase slug flow. *International Journal of Mechanical Sciences*.
- Lyssand, T. (2015). Design of Subsea Spools: Investigating the Effect of Spool Shape.
- Makogon, T. Y. (2019). *Handbook of Multiphase Flow Assurance*.
- Malekzadeh, R., Belfroid, S., & Mudde, R. (2012). Transient drift flux modelling of severe slugging in pipeline-riser systems. *International Journal of Multiphase Flow*.
- Malekzadeh, R., Henkes, R., & Mudde, R. (2012). Severe slugging in a long pipeline-riser system: Experiments and predictions. *International Journal of Multiphase Flow*.
- Meher, S. (2012). Dynamic Response of a Beam Structure to a Moving Mass Using Green's Function.
- Mehmood, A., Khan, A. A., & Mehdi, H. (2014). Vibration Analysis of Beam Subjected to Moving Loads using FEM. *IOSR Journal of Engineering*.
- Mohammed, A. O., Nasif, M. S., & Al-Kayiem, H. H. (2016). A study on slug induced stresses using file-based coupling technique. *Journal of Engineering and Applied Sciences*.
- Mohammed, A. O., Nasif, M. S., Al-Kayiem, H. H., & Al-Hashimy, Z. I. (2016). Numerical Study on Fluid Structure Interaction of Slug Flow in a Horizontal Pipeline. *Applied Mechanics and Materials*.
- Mohammeda, A. O., Al-Kayiem, H. H., Nasif, M. S., & Timec, R. W. (2019). Effect of slug flow frequency on the mechanical stress behavior of pipelines. *International Journal of Pressure Vessels and Piping*.
- Mohammeda, A., Al-Kayiem, H., Nasif, M., & Mohammed, Z. (2013). Finite Element Analysis of Fatigue in Pipelines due to Slug Flow.
- Ogazi, A. I. (2011). Multiphase Severe Slug Flow Control.
- OilFieldWiki*. (n.d.). Retrieved from www.oilfieldwiki.com.
- Okerekea, N., & Omotara, O. (2018). Combining self-lift and gas-lift: A new approach to slug mitigation in deepwater pipeline-riser systems. *Journal of Petroleum Science and Engineering*.
- Onuoha, M. D., Duan, M., & Wang, Y. (2016). Dynamic Response and Stress Impact Analysis of Production Riser under Severe Slug Flow. *International Ocean and Polar Engineering Conference*.
- Ortega, A., Rivera, A., & Larsen, C. M. (2017). Slug Flow and Waves Induced Motions in Flexible Riser. *Journal of Offshore Mechanics and Arctic Engineering*.
- Palmer, & King. (2008). *Subsea Pipeline Engineering*.
- Peng, L.-C., & Peng, T.-L. (2009). *Pipe Stress Engineering*.

- Pokusaev, B. G., Kazenin, D. A., Karlov, S. P., & Ermolaev, V. S. (2011). Motion of a Gas Slug in Inclined Tubes. *Theoretical Foundations of Chemical Engineering*.
- Pourazizia, R., Mohtadi-Bonabb, M., & Szpunara, J. (2020). Investigation of different failure modes in oil and natural gas. *Engineering Failure Analysis*.
- Ragab, A. M. (2008). Simulation of Hydrodynamic Slug Formation in Multiphase Flowlines and Separation Devices.
- Rashwan, F. A., & Soliman, H. M. (1987). The Onset of Slugging in Horizontal Condensers. *The Canadian Journal of Chemical Engineering*.
- Reda, A. M., Forbes, G. L., & Sultan, I. A. (2011). Characterisation Slug Flow Pipelines for Fatigue Analysis. *International Conference on Ocean, Offshore and Arctic Engineering*.
- Reda, A. M., Forbes, G. L., & Sultan, I. A. (2012). Characterization of Dynamic Slug Flow Induced Loads in Pipelines. *International Conference on Ocean, Offshore and Arctic Engineering*.
- Reda, A., Forbes, G. L., Mckee, K. K., & Howard, I. (2014). Vibration of a curved subsea pipeline due to internal slug flow.
- Robert, D., Ao, Y., Senthilkumar, M., Kodikara, J., & Rajeev, P. (2020). Cyclic loading response of offshore pipelines using simple shear tests. *Soil Dynamics and Earthquake Engineering*.
- SAIPEM Group. (2020). *Private communication*. Fano.
- Seo, J. K., Kim, D. W., & Bae, S. Y. (2015). Design Parameter Characteristics in a Subsea Rigid Jumper. *Journal of Applied Mechanical Engineering*.
- Shoham, O., Dukler, A. E., & TaHel, Y. (1982). Heat Transfer during Intermittent Slug Flow in Horizontal Tubes.
- Some Details of Developing Slugs in Horizontal two-Phase Flow. (1985). *AIChE Journal*.
- Storkaas, E., & Skogestad, S. (2007). Controllability analysis of two-phase pipeline-riser systems at riser slugging conditions. *Control Engineering Practice*.
- Sultan, I. A., Reda, A. M., & Forbes, G. L. (2013). Evaluation of Slug Flow-Induced Flexural Loading in Pipelines Using a Surrogate Model. *Journal of Offshore Mechanics and Arctic Engineering*.
- Sun, B. (2016). *Multiphase Flow in Oil and Gas Well Drilling*.
- Sun, L., & Kang, Y. (2015). Installation Strength Analysis of Subsea Flowline Jumpers. *Journal of Marine Science and Application*.
- Tada, S., Oshima, S., & Yamane, R. (1996). Classification of Pulsating Flow Patterns in Curved Pipes. *Journal of Biomechanical Engineering*.
- Taha, T., & Cui, Z. (2005). CFD modelling of slug flow in vertical tubes.
- Taitel, Y., & Barnea, D. (1983). Counter Current Gas-Liquid Vertical Flow, Model For Flow Pattern and Pressure Drop. *International Journal of Multiphase Flow*.

- Taitel, Y., & Duckler, A. E. (1976). A Model for Predicting Flow Regime Transitions in Horizontal and Near Horizontal Gas-Liquid Flow. *A.I.Ch.E. Journal*.
- Taitel, Y., Barnea, D., & Duckler, A. (1980). Modelling flow pattern transitions for steady upward gas-liquid flow in vertical tubes. *A.I.Ch.E. Journal*.
- Taitel, Y., Sarica, C., & Brill, J. (2000). Slug Flow modeling for downward inclined pipe flow: theoretical consideration. *International Journal of Multiphase Flow*.
- Trippit, D. B., Chee, K. Y., & Aizad, S. (2012). Pipeline Dynamics with Flowing Contents in Abaqus/Standard. *SIMULIA Community Conference*.
- Tronconi, E. (1990). Prediction of Slug Frequency in Horizontal Two-Phase Slug Flow. *AICHE Journal*.
- Ujang, P. M., Lawrence, C. J., Hale, C. P., & Hewitt, G. F. (2005). Slug initiation and evolution in two-phase horizontal flow. *International Journal of Multiphase Flow*.
- Urthaler, Y., Breaux, L. E., McNeill, S. I., Luther, E. M., Austin, J., & Tognarelli, M. (2011). A methodology for assessment of internal flow-induced vibration (FIV) in subsea piping systems.
- Vásquez, J. A., & Avila, J. P. (2019). A parametric analysis of the influence of the internal slug flow on the dynamic response of flexible marine risers. *Ocean Engineering*.
- Wang, L., Yang, Y., Li, Y., & Wang, Y. (2018). Resonance analyses of a pipeline-riser system conveying gas-liquid two-phase flow with flow-pattern evolution. *International Journal of Pressure Vessels and Piping*.
- Wang, L., Yang, Y., Liu, C., Li, Y., & Hu, Q. (2018). Numerical investigation of dynamic response of a pipeline-riser system caused by severe slugging flow. *International Journal of Pressure Vessels and Piping*.
- Xiaoming, L., Limin, H., & Huawei, M. (2011). Flow Pattern and Pressure Fluctuation of Severe Slugging in Pipeline-riser System. *Chinese Journal of Chemical Engineering*.
- Xie, C., Guo, L., Li, W., Zhou, H., & Zou, S. (2017). The influence of backpressure on severe slugging in multiphase flow pipeline-riser systems. *Chemical Engineering Science*.
- Xing, L., Yeung, H., Shen, J., & Cao, Y. (2013). Numerical study on mitigating severe slugging in pipeline/riser system with wavy pipe. *International Journal of Multiphase Flow*.
- Xu, Q., Li, W., Liu, W., Zhang, X., Yang, C., & Guo, L. (2020). Intelligent recognition of severe slugging in a long-distance pipeline-riser system. *Experimental Thermal and Fluid Science*.
- Yadigaroglu, G., & Hewitt, G. F. (2018). *Introduction to multiphase flow: basic concepts, applications and modelling*.



- Yanga, Y., Lia, J., Wanga, S., & Wenb, C. (2017). Understanding the formation process of the liquid slug in a hilly-terrain wet natural gas pipeline. *Journal of Environmental Chemical Engineering*.
- Yao, T., Wu, Q., Liu, Z., Zou, S., Xu, Q., & Guo, L. (2019). Experimental investigation on mitigation of severe slugging in pipeline-riser system by quasi-plane helical pipe device. *Experimental Thermal and Fluid Science*.
- Yarrarapu, S. K. (2015). Mudmat Role in Offshore Drilling Operations. *International Journal of Engineering and Management Research*.
- Zhao, T., Cooper, P., & Brugmans, J. (2010). Deepwater Rigid Spools Slugging Flow Fatigue Design. *International Conference on Ocean, Offshore and Arctic Engineering*.
- Zhou, C., Qi, X., & Wang, L. (2014). Subsea Flowline-PLET-Jumper Integrated Abaqus Model. *SIMULIA Community Conference*.
- Zhu, H., Gao, Y., & Zhao, H. (2018). Experimental investigation on the flow-induced vibration of a free-hanging flexible riser by internal unstable hydrodynamic slug flow. *Ocean Engineering*.

ACKNOWLEDGMENTS

Il primo ringraziamento va al Professor Lando Mentrasti, relatore di questo lavoro ma soprattutto persona speciale, per l'aiuto fornitomi, per la disponibilità, la pazienza e la comprensione che mi ha dimostrato nel corso di questi mesi.

Penso che un grazie sia comunque riduttivo e non basti ad esprimere tutta la mia riconoscenza e la stima che provo nei suoi confronti.

La mia gratitudine va anche a Saipem S.p.A. per avermi concesso l'opportunità di svolgere lo stage con il quale è nato questo lavoro. Ringrazio l'ufficio SESY: ricorderò sempre con piacere tutti coloro che vi lavorano; da ognuno di essi ho avuto modo di imparare qualcosa, non solo a livello didattico ma anche a livello umano.

In particolare desidero ringraziare Mauro Pigliapoco e Francesco Tattoli sempre cortesi e disponibili, per la pazienza dimostrata nei miei confronti e per l'importante supporto che mi hanno fornito.

Grazie a Pierluigi, Tommaso, Francesco, Alessio, Ezio, compagni di corso con i quali ho affrontato questa avventura. Mi avete sempre strappato un sorriso e aiutato a dimenticare (almeno per un po') le difficoltà, rendendo migliori questi anni. Un ringraziamento speciale va a Maria, una vera amica che non ha mai smesso di essermi vicina e che ha sempre creduto in me: grazie di cuore perché senza di te tutto questo non sarebbe stato possibile!

Grazie a tutti i miei amici che in un modo o nell'altro hanno condiviso con me anni di gioie, delusioni e sacrifici, che non mi hanno mai fatto mancare il loro affetto e che non hanno mai dubitato di me nemmeno per un secondo. Grazie soprattutto a Giorgia che mi ha sempre ascoltata e non ha mai smesso di essere, in tutti questi anni, un porto sicuro. Grazie a Marco, fratello acquisito, sempre al mio fianco e senza il quale non saprei veramente come fare.

Infine vorrei ringraziare la mia famiglia per aver sempre creduto in me e per avermi supportata (e sopportata) nei momenti più difficili. Un grazie speciale va a mia sorella Martina che, seppur distante, non mi ha mai fatto sentire sola con i suoi preziosi consigli e che mi ha dato spesso la forza di non mollare. Grazie a mia zia Luisa che prima di ogni esame mi faceva sentire la sua vicinanza e che ha sempre dato per scontato i miei successi.